The effect of changing tidal energy over the spring-neap cycle on net sediment deposition in a hypertidal Bay of Fundy salt marsh creek

by Casey O'Laughlin

A Thesis Submitted to Saint Mary's University, Halifax, Nova Scotia,

in Partial Fulfillment of the Requirements for the

Degree of Master of Science in Applied Science

August 23rd, 2012, Halifax, Nova Scotia

Approved:	Dr. Danika van Proosdij
	Supervisor
	Department of Geography
Approved:	Dr. Dwight Keane Muschenheim
	External Examiner
	Department of Biology
	Acadia University
Approved:	Dr. Timothy Milligan
	Supervisory Committee Member
	Bedford Institute of Oceanography
Approved:	Dr. Andrew MacRae
	Supervisory Committee Member
	Department of Geology
Approved:	Dr. Kevin Vessey
	Dean of Graduate Studies
Date:	August 23rd, 2012

Library and Archives
Canada

Published Heritage
Branch

395 Wellington Street
Ottawa ON K1A 0N4
Canada

Bibliothèque et
Archives Canada

Direction du
Patrimoine de l'édition

395, rue Wellington
Ottawa ON K1A 0N4
Canada

Canada

The effect of changing tidal energy over the spring-neap cycle on net sediment deposition in a hypertidal Bay of Fundy salt marsh creek

ABSTRACT

Removal of tidal energy by proposed commercial-scale tidal power installations in the Minas Passage has raised concern for a non-linear response of fine sediments in far-field environments, including salt marshes. To investigate the effects of changing tidal amplitude and energy on tidal creek processes, measurements of current velocity and suspended sediment concentration, and samples of deposited and suspended sediment, were collected in a hypertidal (tide range > 6 m) creek in the Upper Bay of Fundy over 15 tidal cycles. Current velocity and turbulence in the creek showed: (1) marked variability associated with increasing tidal amplitude, and (2) the influence of flood and ebb pulses with flooding and drainage of the marsh surface. Parameterization of disaggregated inorganic grain size (DIGS) spectra with a non-liner, least-squares fit model suggest that fluctuating net deposition over the study period ($55 - 328$ $g \cdot m^{-2}$) is not directly related to changes in the flocculated nature of suspended materials, despite variation in mean floc fraction ($0.67 - 0.89$) and floc limit ($12 - 26$ μm).

Acknowledgements

I would like to thank first and foremost my Supervisor, Danika van Proosdij, for her ideas and support as well as her optimistic, yet realistic view of the world and the work she does. I also extend sincere gratitude to the rest of my Supervisory Committee, Tim Milligan and Andrew MacRae, for their assistance, guidance and patience throughout this epic process. Extensive thanks are owed to our collaborators at Dalhousie University (Paul Hill, Jessica Carrière-Garwood, Laura deGelleke and John Newgard) and the Bedford Institute of Oceanography (Brent Law and Vanessa Page). Special thanks to Greg Baker (Maritime Provinces Spatial Analysis Research Center) for crucial geomatics and surveying support, Jeremy Lundholm (Saint Mary's University) for statistical advice, and Ken Carroll (Nova Scotia Department of Agriculture, retired) for assistance with site access, providing workspace and carting around truckloads of muddy lumber. Many thanks to the suite of field and lab assistants who worked tirelessly with me, either in field data collection (Amber Silver, Ben Lemieux, Sara Lowe) or processing samples in the lab (Emma Poirier, Christa Skinner, Carly Wrathall and Brenden Blotnicky). Finally, thanks to my family (Brian, Lisanne and Keighan) for their continued support in everything I do. And last, but certainly not least, special thanks to my grandparents, Ken and Marguerite, and their car 'Bessie', who made so many trips to the field possible.

TABLE OF CONTENTS

LIST OF FIGURES

LIST OF TABLES

LIST OF SYMBOLS

τ_0	Bed shear stress $(N \cdot m^{-2})$
w_s	Settling velocity $(mm \cdot s^{-1})$
d_f	Floc limit (μm)
$\hat{d}$	Roll-off diameter (μm)
f	Floc fraction (0-1)
m	Source slope (0-1)
μ	Dynamic viscosity of seawater $(kg \cdot m^{-1} \cdot s^{-1})$
ρ_s	Sediment density $(kg \cdot m^{-3})$
ρ	Density of sea water $(kg \cdot m^{-3})$
g	Acceleration due to gravity $(m \cdot s^{-2})$
γ	Tidal asymmetry factor (0-1)
ρ	Density of seawater at 20°C $(1025\ kg \cdot m^{-3})$
u_*	Friction velocity $(m\ s^{-2})$
u_{b*}^2	Bed shear velocity $(m \cdot s^{-1})$
ε	TKE dissipation rate $(m^{-2} \cdot s^{-3})$
η	Kolmogorov microscale $(\mu m \cdot 10^{3})$
G	Dissipation parameter (s^{-1})

CHAPTER 1: INTRODUCTION

1.0   Introduction

With the recent recognition of tidal salt marshes as sites of coastal defense and ecological significance, interest in intertidal sedimentation processes has increased significantly (Reed et al., 1999). The capacity of salt marshes to function as critical habitat in biological production, and as energy-absorbing features that shield coastal infrastructure from storm surges and rising seas, is entirely dependent on their ability to import and retain sedimentary material (Donnelly and Bertness, 2001). Marshes are dominant estuarine features, occupying a large portion of high intertidal zones in temperate and high-latitude regions, where energy conditions are sufficiently low for sediment deposition and establishment of salt-tolerant grasses (Allen and Pye, 1992; Friedrichs and Perry, 2001). Due to the inherent controls of tidal range and energy, and in response to modern rising sea levels, tidal marshes are always adjusting toward a new equilibrium (Morris *et al.*, 2002).

Potential links between anthropogenic fossil fuel consumption and climate change, along with rising sea level and the dwindling global supply of fossil fuels, has driven an increased desire for the development and implementation of renewable energy technologies (Dincer, 1999; Omer, 2008). Initiatives designed to develop tidal production in the Bay of Fundy are currently underway, and testing of tidal in-stream energy conversion (TISEC) devices in the area began in 2009 (DFO, 2009; OEER, 2008a). Potential modification of local tidal characteristics (e.g. reduced tidal amplitude) associated with the extraction of

2

tidal energy for electrical generation may result in changes to intertidal sedimentation patterns that are beyond the natural range (Sanders and Baddour, 2008; OEER, 2008a). Based on the impacts of previous engineering projects in Bay of Fundy estuaries (e.g. Petitcodiac and Avon causeways), such as disruption of natural hydrodynamics and associated large-scale deposition, there is concern for a non-linear response of fine sediments in intertidal zones following energy extraction (e.g. van Proosdij et al., 2009; Amos and Mosher, 1985; Turk et al., 1980). An overall reduction in tidal amplitude in the inner Bay of Fundy (predicted by Karsten et al. (2008) in response to moderate energy extraction) would ultimately reduce the inundation time of salt marsh surfaces. This may reduce deposition in salt marshes due to decreased sediment supply, or alternatively act to increase sediment deposition in intertidal zones. Either circumstance will impact the morphology and survival of salt marsh environments. Without salt marshes acting as buffer zones to absorb and dissipate energy, vulnerability of coastal areas will increase. Changes to or loss of salt marsh functionality will also impact ecosystem services, such as organic material and nutrient supply (Craft et al., 2009; Boorman, 1999).

The extraction of tidal energy for generation of electricity is a viable source of renewable energy in many locations around the world (Charlier, 2003). With the possibility of adverse impacts of tidal power generation, the general recommendation for TISEC technology in the Bay of Fundy region has been to adopt a conservative approach to development, and to conduct thorough

investigations into far and near-field effects (Karsten *et al.*, 2008; Sanders and Baddour, 2008; OEER 2008a). Sedimentary and hydrodynamic models of the Bay of Fundy region are currently in development (e.g. Wu *et al.*, 2011; Greenberg *et al.*, 2005), along with existing models of far-field effects of tidal power extraction (e.g. Polagye and Malte, 2010; Pethick *et al.*, 2009). However, due to the extensive intertidal zone and complex sediment dynamics, modelling Bay of Fundy dynamics has proven to be challenging. As a result, regional models produced to date do not consider relatively shallow portions of the intertidal zone, such as extensive salt marshes and tidal creeks. To increase model resolution and accuracy, validation by hydrodynamic and sediment transport data from the intertidal zone is essential, including site-specific baseline information on sedimentary and hydrodynamic processes (DFO, 2009; OEER, 2008b), such as that presented in the following chapters. The purpose of this thesis is identification of the processes which control sediment dynamics in a sheltered tidal creek, through analysis of in-channel hydrodynamics and inorganic grain size, to determine the effects of changing tidal amplitude and energy on sediment deposition. This research is designed to develop a better understanding of processes that may be linked to a non-linear response of fine sediment to energy extraction, such as the influence of tidal amplitude on the flocculated nature of suspended and deposited sediment.

Data presented in this study were collected in the Upper Bay of Fundy region during the summer of 2009. Subsequent analyses presented within this document are aimed at identification of processes controlling sediment dynamics

4

in a sheltered, hypertidal creek (tide range < 6 m). A full range of tidal conditions have been sampled for current velocity, suspended sediment concentration and sediment deposition over the spring-neap cycle.

1.2 Tides

Astronomical tides are driven by orbital variation in the positioning, rotation and relative inclination angles of the Earth, Moon and Sun. The principal component of global tidal circulation is the semi-diurnal M_2 tidal constituent, driven by the rotation of the Moon around Earth (Wells, 1986). In addition, spring-neap tidal cycles are generated by changing lunar phases, and the variable positioning of the Moon, Sun and Earth relative to each other. The spring portion of the cycle occurs during Full and New Moon phases, when the Earth, Moon and Sun are lined up, generating tides that are typically higher and stronger than average. Neap tides are generally lower and weaker than average, and occur during the First or Last Quarter. Thus there are two sets of spring-neap tides during the synodical month, or the period of time from New Moon to New Moon (Desplanque and Mossman, 2001; Kvale, 2006).

Flow magnitude in tidal creeks is directly linked to the amplitude of individual tidal cycles, as the resulting flow velocity corresponds with the volume of water being moved through a system. This volume, known as the tidal prism, is a determining factor for inundation time, maximum depth, and drainage patterns in the intertidal zone. The relationship between tidal prism and inundation time shows variation within the same environment in response to the

5

spring-neap tidal cycle (Voulgaris and Meyers, 2004; Manning and Dyer, 2002; Murphy and Voulgaris, 2006; Manning and Bass, 2006). Increased tidal amplitude is generally associated with spring tides, and implies longer inundation time, faster and more turbulent currents, and higher suspended sediment concentration, due to a greater carrying capacity relative to lower tidal amplitude (Allen 2000; Friedrichs and Perry, 2001).

Evidence has been presented to support the existence of energy variability between spring and neap tidal cycles, through analysis of various parameters associated with tidal energy exchange. Evidence includes variations in biomass and water content, tidal currents, suspended sediment concentration (SSC), flocculation processes, nutrient fluxes and tidal dissipation (e.g. Manning *et al.*, 2006; Murphy and Voulgaris, 2006; Friend *et al.*, 2005; Manning and Dyer, 2002; O`Brien *et al.*, 2000; Voulgaris and Meyers, 2004; Cartwright, 1997; Peters, 1997; Vörösmarty and Loder, 1994; Middleton, 1972). Spring tides show greater mean current velocity and suspended sediment concentration compared with neap tides, along with higher rates of inter-particle collision and optimal conditions for formation of fast-settling flocs (Manning *et al.*, 2006). Neap tides have reportedly weaker than average current velocities and kinetic energy, and comparatively lower rates of floc formation and depositional capabilities than spring tides (Manning and Dyer, 2002; Voulgaris and Murphy, 2006).

1.3 Salt marshes

Minerogenic salt marshes and mudflats require sufficient amounts of sediment input to keep pace with rising sea level, meaning that marshes are typically areas of net sediment accumulation (Craft *et al.*, 2009; Voulgaris and Meyers, 2004; Reed, 1988). Marshes are generally composed of a flat, gently sloping platform dissected by tidal creeks (Lawrence *et al.*, 2004; Voulgaris and Meyers, 2004). The characteristic morphology of these systems (which includes salt marsh, tidal channels and adjacent intertidal flats) consists of both vegetative growth and sedimentary features. Minerogenic marshes have platforms dominated by tidally introduced mineral matter, with a smaller component of locally sourced organics, such as plant litter and below-ground root biomass (Allen, 2000; Allen and Pye, 1992). The occurrence of salt marsh vegetation is generally limited to the zone between mid-neap tide level and the high water level during spring tides, while non-vegetated mudflats and creek banks occupy the space below (Allen and Pye, 1992). High marsh is known to develop above the mean high water line, while low marsh extends from this line in the seaward direction. Salt marsh vegetation communities adhere to strict boundaries imposed by tolerance to stressors, such as saline tidal waters (Bertness, 1991). Vegetation has been shown to reduce velocity and turbulence of tidal flow moving through salt marsh canopies (Leonard and Croft, 2006; Leonard and Luther, 1995); however, it remains uncertain whether this action actually increases deposition or simply protects against erosion (Silva *et al.*, 2009).

7

Marsh morphology is closely linked with tidal cycles, through platform accretion and the development and maintenance of creek networks. Local tide range limits the altitudinal growth of a marsh surface within the tidal frame (Allen, 2000; French and Stoddart, 1992; Davidson-Arnott et al., 2002). The composition and linkages of salt marsh systems has been well illustrated by Allen (2000), where surface sedimentation is dictated by the relative elevation of the marsh surface and tidal inundation. Typically less than one third of tides are high enough to overfill tidal creeks and fully inundate high marsh surfaces. These flooding events, known as the hydroperiod or inundation period, range in duration from a few minutes to two or three hours. The remaining tides pass without surpassing the limits of potentially deeply incised channels (Lawrence et al., 2004). The relationship between tidal range, inundation time and sedimentation controls the ability of a marsh to import sediment (Voulgaris and Meyers, 2004, Christiansen et al., 2000).

An increase in inundation time is related to greater maximum water depth over the marsh surface, which is associated with faster current velocity and the capacity for more sediment transport, increasing the availability of sediment for deposition (Friedrichs and Perry, 2001; Christiansen et al., 2000). It follows that any process acting to increase concentration in adjacent source areas will also increase the accretion rate of the marsh surface. With higher tides, and in macrotidal environments, a proportion of the total marsh tidal prism is not restricted to creeks, and flow moves across the marsh margin (Davidson-Arnott et

8

al., 2002). The percentage of total input from marsh margins is greater with increasing high water level (Temmerman *et al.*, 2005). Therefore, potential controls of salt marsh and tidal creek processes include those intrinsic to the marsh (e.g. topography, vegetation height and density), and others which are externally-driven (e.g. suspended sediment concentration, wave height, atmospheric effects, tidal amplitude and current velocity) (van Proosdij *et al.*, 2006a; Davidson-Arnott *et al.*, 2002; Friedrichs and Perry, 2001; French and Stoddart, 1992). The resulting deposition of sedimentary material on mudflats, creek banks and the marsh surface is a complex function of variables controlling sediment availability and the opportunity for deposition (van Proosdij *et al.*, 2006a).

Tidal creeks are essential components of inorganic salt marsh systems, providing conduits for the import and export of sediment and organic material (Craft et al., 2009; Davidson-Arnott *et al.*, 2002). In hypertidal salt marshes (e.g. the Bay of Fundy), generally straight, shore-normal channels with steep banks characterize the typical creek network arrangement, while micro- and meso-tidal marshes show more complex patterns (Davidson-Arnott et al., 2002). The sediment supply available to the marsh surface has been shown as proportional to the suspended sediment concentration of adjacent source areas, such as creeks and mudflats (Friedrichs and Perry, 2001). Deposition decreases with increasing distance from creeks (Christiansen *et al.*, 2000; Allen, 2000; Friedrichs and Perry, 2001; Reed et al., 1999), implying that creeks are the dominant

9

supplier of sediment to much of the marsh surface. Grain size of bed sediments has also been shown to decrease with increasing distance from the sediment source (Christiansen *et al.*, 2000; French and Stoddart, 1992). Resuspension of newly introduced material from creek banks has also been identified as a source of sediment for accretion on the marsh surface, especially with the occurrence of waves during flood tide stages (Reed, 1988).

The efficiency of sediment delivery to the marsh surface impacts the vertical development in the tidal frame, especially for restoration sites and managed marshes (Reed et al., 1999). Tidal creek morphology is dictated by topographic boundaries, such as the marsh platform itself, which influences general marsh morphology by controlling hydrodynamics and acting as a topographic threshold separating two relatively different flow regimes (French and Stoddart, 1992; Allen 2000; Friedrichs and Perry, 2001). Flood- and ebb-phase velocity and discharge asymmetries have been identified, and are impacted by channel geometry and marsh morphology (Dronkers, 1986; Bayliss-Smith, *et al.*, 1979; Boon, 1975). As high marsh areas flood and drain in close proximity to high water, peak flood and ebb currents develop, typically shortly before or after slack tide (Blanton *et al.*, 2002; Dronkers, 1986). Marshes with a high equilibrium surface that is relatively flat promote a rapid transition from zero surface submergence to complete surface submergence with increasing tidal height (Friedrichs and Perry, 2001).

Flow within tidal creeks has been identified as fully turbulent (Christiansen et al., 2000). Current velocity in tidal creeks during over-marsh tides velocity has been shown not to exceed 1 m·s^{-1}, compared with channel-restricted tides which typically demonstrate slower velocity (10 - 20 cm·s^{-1}) (Christiansen et al., 2000, Voulgaris and Meyers, 2004; Lawrence et al., 2004). Tidal currents flowing across a marsh surface are known to be strongly influenced by the presence of vegetation, and are generally an order of magnitude lower (< 2 cm·s^{-1}) than flow over unvegetated areas (Leonard and Croft, 2006; Murphy and Voulgaris, 2006; Davidson-Arnott et al., 2002; Leonard and Luther, 1995; Friedrichs and Perry, 2001). The turbulence structure and wave mechanics of marsh surface flow is modified by vegetation (Leonard and Croft, 2006; Möller, 2006; Lawrence et al., 2004; Neumier and Ciavola, 2004; Christiansen et al., 2000; Leonard and Luther, 1995). Reduction of turbulence and resulting low shear stress on the marsh surface encourages rapid settling of suspended material, and discourages sediment resuspension (Leonard and Luther, 1995; Friedrichs and Perry, 2001). The absolute relationship between salt marsh vegetation and sedimentation patterns is not immediately clear, and it has been proposed that the characteristics of individual marshes must be considered to fully understand the role of vegetation in the stabilization of those areas (Silva et al., 2009).

1.4   The Bay of Fundy

Development of the Fundy Basin began during the Appalachian Orogeny, approximately 286-360 million years before present, which established a system

of faults across the region during the mountain building process. The modern Bay of Fundy is within an aulacogen (failed rift valley), formed by reactivation of these faults during the spreading of the supercontinent Pangea, which began about 220 million years ago (AGS, 2001). Seafloor spreading at the Mid-Atlantic Ridge dominated the extensional process, and eventually separated North America from Europe and Africa, leaving the failed Fundy Basin rift valley as a landlocked sedimentary graben. The infilling of this basin with sediments and volcanics which began more than 200 million years ago, and in more recent times has been affected by erosion and deposition related to Pleistocene glaciation, which established the modern Bay (Desplanque and Mossman, 2001; AGS, 2001).

Bay of Fundy tides are dominated by the M_2 (lunar semi-diurnal) tidal constituent and to a lesser extent the S_2 (solar semi-diurnal) and N_2 (lunar elliptic) components (Garrett, 1972; Scott and Greenberg, 1983). Fundy tides are strongly semi-diurnal and show an extreme range (up to 16 metres), which is described as hypertidal (> 6m) (van Proosdij et al., 2010). This is caused by near resonance of the Bay of Fundy - Gulf of Maine system with the oceanic semi-diurnal tide, coupled with influences of basin geometry and bottom friction (Shaw et al., 2010). Changes in relative sea level are largely responsible for the development of the modern tidal regime in the Bay of Fundy, particularly the water depth over George's Bank; Scott and Greenberg (1983) report a 1-2% increase in tidal amplitude for every 1 metre of rising sea level. The system is transgressive, and with changing basin geometry, tidal amplification has

increased over the past 6000 years, with the greatest rate of tidal amplification between 7000 and 4000 BP (Scott and Greenberg, 1983; Amos, 1987).

Bay of Fundy estuaries are routinely exposed to a high suspended sediment concentration and the aforementioned tidal range, as well as snow and ice for up to three months of the year (van Proosdij *et al.*, 2001). The modern 1400 km Bay of Fundy coastline is bound by sandstone and conglomerate cliffs which experience high rates of erosion, up to 1 $m \cdot a^{-1}$ in some areas (Desplanque and Mossman, 2001). Fine sediments are also entrained from bed scours in the Minas Basin, introducing laminated silts and clays to suspension (Amos, 1987). Sections of coastline (e.g. Chignecto Bay) that show a dominance of Paleozoic siltstone and shale also contribute fine-grained materials, which maintain suspension through wave action and tidal cycling (Desplanque and Mossman, 2001).

The movement of estuarine mud is governed by hydrodynamic forcing agents, such as tidal currents and waves, which can be driven by gravity or pressure gradients. Waves generally have a lesser influence on sediment dynamics in an estuary than on an open coast, and thus energy exchange in estuaries is dominated by tidal processes (Whitehouse et al., 2000). The inner Fundy bays show considerable accumulations of fine sediments throughout the Minas and Cumberland Basins, a supply that has encouraged extensive salt marsh development in those areas. The lower portion of the Bay of Fundy is characterized by primarily sandy material (Davidson-Amott *et al.*, 2002). It has been suggested that the Bay of Fundy in undergoing a period of modern change,

13

evidenced by changing grain size distributions on tidal mudflats, increasing water depths in some areas and changing benthic communities (Desplanque and Mossman, 2004).

1.5 Tidal power

The extraction of tidal energy for electrical generation is a viable source of renewable energy in many locations around the world (Karsten *et al.*, 2008; Garrett and Cummins, 2005; Bryden *et al.*, 2004; Charlier, 2003). Recent initiatives to harness this resource in the Bay of Fundy began with testing of in-stream energy conversion devices in 2009 (DFO, 2009; OEER, 2008a, b). Since the 1970s, studies have been undertaken at various sites in the Bay of Fundy to test suitability and feasibility of tidal power installations (e.g. Gordon, 1994; Seoni, 1979; Karas, 1978; Lee and Dechamps, 1978). These evaluations considered barrage construction and did not yield promising results, primarily due to the unknown effects of damming major components of the system, and construction within the upper Bay was never attempted. The modern approach involves tidal in-stream energy conversion (TISEC) devices, which are stationary, independent structures that are fully or partially submerged and do not completely disrupt tidal flow. Similar to wind turbines, these devices convert kinetic energy from flowing water into electricity, and do not require a dam or barrage-type structure. The naturally large tidal range of the Bay of Fundy creates a unique opportunity to employ TISEC technology for electrical generation (DFO, 2009; Sanders and Baddour, 2008; OEER, 2008a, b).

14

Energy extraction from tidal flows is understood to alter hydrodynamics in the near-field environment (Sun *et al.*, 2008; Garrett and Cummins, 2005). However, the response of far-field environments to changes in tidal energy remains uncertain (Sanders and Baddour, 2008; Bryden *et al.*, 2004). Numerical modeling has shown that the environmental significance of change in response to energy removal may be site-specific and non-linear (Polagye and Malte, 2010). A large amount of power can be harvested from the Bay of Fundy system, and extraction of the maximum amount of power available (up to 7 gigawatts) would generate significant regional impacts. Even moderate extraction would result in a reduction of local tidal amplitude by approximately 5% per 2.5 gigawatts of power extracted (Karsten *et al.*, 2008). The effect of energy extraction on sediment dynamics in salt marshes and tidal creeks is largely unknown, which is the main motivation for this study.

1.6 Mud and Flocculation

Suspended particles fall through a fluid with different settling rates that are directly dependant on their physical properties. Stokes' Law describes the frictional force exerted on spherical objects held in a continuous viscous fluid. Settling rates of fine-grained spherical particles of constant size and density suspended in still water of constant density and viscosity can be defined by Stokes' law:

$$w_s = \frac{(\rho_p - \rho_f) g d^2}{18\mu}$$

Equation 1

15

where w_s is the settling velocity, ρ_p is particle density, ρ_f is fluid density, g is gravitational acceleration, d is the particle diameter, and μ is the dynamic viscosity of the fluid (Smith and Friedrichs, 2011; Voulgaris and Meyers, 2004; Christiansen *et al.*, 2000). Stokes' Law applies well to silt grains, whose nearly equidimensional shapes result in settling velocities that are relatively similar to spheres of similar volumes. Smaller clay particles are more commonly non-spherical in shape, and settling velocities of these particles are not as closely tied to Stokes' Law, although correction factors are available (Winterwerp, 2002; Eisma 1986).

Mud is defined as the fraction of any sediment distribution that is less than 63 μm in diameter, and generally consists of a large proportion of very small silt and clay particles (Whitehouse et al., 2000). The main mode of transport for particles in this size range is in suspension, and suspended muds span a variety of densities and critical shear-stresses that influence particle cohesion and deposition (Whitehouse et al., 2000; Kranck, 1980). Particles less than 63 μm in diameter tend to flocculate, which strongly influences depositional processes by enhancing the flux of muds to the bed (Kranck and Milligan, 1991; Law et al., in press). Flocculation is the process whereby suspended sediment and organic particles aggregate as the cumulative result of collision and cohesion processes to form loose associations of particles called flocs (Eisma, 1986; Kranck, 1980). The tendency of fine sediments to settle as aggregates or flocs rather than as single grains reduces Stokes' law applicability to fine sediments, as aggregates

demonstrate settling velocities greater than that of individual constituent grains (Whitehouse et al., 2000; Kranck, 1980). It has been shown that the settling velocity of silt- and clay-sized particles can be increased by several orders of magnitude, as flocculation enhances the flux of muds to the bed (Kranck and Milligan, 1991; Law et al., in press). Increased settling velocity of suspended particles can lead to increased water column clearance when flow conditions are calm (Kranck and Milligan, 1992).

Particle collisions can occur through three mechanisms: Brownian motion of suspended particles, turbulent shear in the water column, and differential settling velocities of particles and flocs (Winterwerp, 1998, 2002; Whitehouse *et al.*, 2000). Brownian motion describes the seemingly random motion of particles suspended in a fluid, while turbulent and shear forces in the water column simultaneously create opportunities for particle collisions, and limit the maximum size flocs can achieve (Winterwerp, 2002). Differential settling velocities can effectively cause particle collisions as faster settling particles overtake and collide with slower settling grains (Kranck, 1980).

Three dominant factors influence flocculation processes: (1) the concentration of particles in suspension which will control the frequency of particle collisions, (2) the efficiency of individual particles for adhesion upon collision, and (3) the level of turbulent shear in the water column (Milligan and Hill, 1998; Manning and Dyer, 2002; Winterwerp, 1998; van Leussen, 1999). Turbulent shear can enhance floc formation due to increased contact between

particles, but at some level will limit maximal floc size due to floc break-up (Winterwerp, 1998; Milligan and Hill, 1998). This is well described by Winterwerp's (1998) model of floc evolution, which demonstrates that particle residence time in a turbulent environment constrains floc growth. The rate at which flocculation occurs is primarily a function of sediment concentration (Milligan et al., 2007; Kranck, 1980). This can result in rapid deposition in episodic events, such as floods (Milligan *et al.*, 2007), but other factors such as sedimentary characteristics (including composition, particle size, organic content, and the nature of structures) play significant roles in determining floc density and maximum floc size (Milligan and Hill, 1998; Whitehouse et al., 2000). As flocs grow larger, more water is incorporated into the total volume, leading to a decrease in density with growth (Hill *et al.*, in press). Increased particle size is also known to reduce floc density due to increased interstitial space between particles (Curran *et al.*, 2007). On seasonal time scales, floc sizes are dependent on binding properties related to biological activity, while settling velocities show minor variations resulting from a counterbalance of increased floc size by a decrease in floc density (Van der Lee, 2000).

Floc cohesion is maintained through a combination of molecular attractive and electrostatic forces between neighbouring clay grains and organic complexes on particle surfaces (Whitehouse *et al.*, 2000; Dyer and Manning, 1999; Eisma, 1986; Kranck, 1981). This latter category includes the production of adhesive organic matter (mucopolysaccharides) by bacterial, algae and higher plants (van

Der Lee, 2000; Eisma, 1986; Kranck, 1980). The significance of biological factors in flocculation is related to the cohesive properties of these organic compounds, which potentially enhance particle aggregation via organic coatings on individual mineral grains (Eisma, 1986; van der Lee, 2000). For example, enhanced flocculation on spring tides has been linked to a high total carbohydrate concentration (Manning *et al.*, 2006). Also, laboratory experiments by Kranck and Milligan (1985) demonstrated that a 1:1 mixture of organic matter and mineral particles settles at a much higher rate than the organic matter or mineral particles alone. A strengthening effect of salinity on flocs has also been identified, which is considered to be an important contributing factor in estuarine processes (Pejrup and Mikkelsen, 2010; Milligan *et al.*, 2001; Kranck, 1981). In estuarine environments, flocculation processes are subject to variations related to the spring-neap cycle, due to increased current velocity (and associated shear stresses) associated with spring tides. This results in typically higher suspended sediment concentration, which increases flocculation efficiency. This in turn encourages the retention of fine particles that would otherwise be swept out to sea (Manning and Bass, 2006; Bartholomä *et al.*, 2009; Kranck, 1981).

Limited knowledge of suspension rates and particle characteristics, coupled with variation on spring-neap and seasonal scales, make time-variant flocculation processes challenging yet essential components of sediment transport models (Friedrichs and Perry, 2001; Manning *et al.*, 2006; Milligan and Hill, 1998). Flocculation processes are especially important for proper

19

assessment of environmental impacts of development in the coastal zone (Milligan and Hill, 1998; Milligan and Law, 2005; van Proosdij *et al.*, 2009). The transport and deposition of mud is therefore complex and widely varied, and is linked to the concentration of particulates in suspension, turbulence and shear in the water column, and biological processes which impact particle cohesion and flocculation (Milligan and Hill 1998; Manning et al., 2006; van Der Lee, 2000; Kranck, 1981).

Eisma (1986) differentiated suspended flocs by diameter and the origin of constituent particles. He assigned the term microflocs to flocs that measure up to 125 µm, are composed of tightly-packed organic and inorganic particles, and are typically smaller mineral grains held together by organic matter. Macroflocs by comparison are porous and loosely-bound, and are a combination of microflocs as well as individual particles (Mikkelson *et al.*, 2006). Macroflocs are fragile agglomerations that form under viscous flow conditions, and those found in estuaries can measure up to sizes of 3-4 mm and are easily destroyed during sampling (Eisma, 1986; Curran *et al.*, 2007). Larger macroflocs (up to 12 mm diameter), such as those which occur in coastal waters or farther offshore where the supply of mineral particles is limited, show lower density and demonstrate high organic content, much more than those found in estuarine environments (Eisma, 1986).

1.7   Inverse floc model

Work by Kranck (1980) has shown that flocs are unbiased samplers of the parent suspension, and they remove material from the water column in the same proportions that are found in suspension. The size distribution of that suspension provides a record of sedimentary origin and insight into the conditions of the depositional environment (Kranch and Milligan, 1985; Milligan and Loring, 1997). A bottom deposit is therefore a proportional mixture of single-grain and floc-deposited material, relative to the environmental conditions at the time of deposition (Curran *et al.*, 2004; Kranck and Milligan, 1991). Results of disaggregated inorganic grain size (DIGS) analysis of bed sediment can be applied to estimate the ratio of material deposited as flocs, under the assumption that suspended material can either be deposited within flocs or as single grains (Kranck and Milligan, 1985; Kranck, 1980). Several studies have employed this principle to study sediments in estuarine and marine environments (e.g. Kranck *et al.*, 1996a & 1996b; Milligan and Loring, 1997; Hill *et al.*, 2000; Mikkelsen *et al.*, 2004; Milligan *et al.*, 2001; Fox *et al.*, 2004; van der Lee, 2000; van der Lee *et al.*, 2009; Manning *et al.*, 2010) and the method is widely accepted. This research applies the inverse floc model to marsh sediment to investigate its usefulness in this environment, which has not been extensively studied using this method (e.g. Voulgaris and Meyers, 2004; Christiansen *et al.*, 2000). Recently, the inverse floc model has been applied to investigate particle size characteristics on intertidal flats (e.g. Hill *et al.*, in press; Law *et al.*, in press).

A conceptual model modified from Curran *et al.* (2004) demonstrates the relationship between suspended fine sediment and bottom deposits (Figure 1.1). The texture of bed sediment is largely dependent on the relative effectiveness of the two modes of arriving at the bed (either as single grains or as flocs), and the proportional mixture is relative to the environmental conditions (e.g. concentration, energy and particle adhesion) at the time of deposition. This is the basis of the bottom sediment DIGS parameterization, and for the 'inverse floc model' developed by Curran *et al.*, (2004) and based on work by Kranck and Milligan (1991) and Kranck *et al.* (1996a, 1996b). The model assumes that sediment of a particular component grain size may exist in one of three unique reservoirs: suspended as single grains, suspended as part of flocs, or within the bed deposit (Figure 1.1). Aggregation and disaggregation processes transfer grains to and from suspended single grain and floc reservoirs, and deposition to the bed occurs as both single-grain and flocs.

Parameterization of DIGS distributions can be completed using the inverse floc model (Figure 1.2). As mineral grains are the first principle of flocculation, the material that remains after organics are removed from a sample is the focus of this study due to the relationship between particle size and deposition, and the mode with which particles arrive at the bed (either within a floc or as a single grain). Model parameters include source slope (m), which indicates the relative amounts of fine versus coarse particles, is a property of the parent material, and is generally similar among different samples from a common source (Kranck *et*

al., 1996a). Roll-off diameter ($d^\wedge$) describes the diameter (in μm) of particles whose concentration has fallen to 1/e of its initial concentration. Floc limit (d_f) describes the grain size at which the flux of mass to the seabed via floc or single-grain deposition is equal (Curran *et al.*, 2004); this value conceptually represents the upper size limit of particles held in flocs, and the lower size limit of single grains held in suspension (Christiansen *et al.*, 2000). The flocculated component of a bottom deposit is represented by floc fraction (f), or the proportion of suspended mass held in flocs at the time of deposition (Curran *et al.*, 2004). The model uses a non-linear fit of observed bottom sediment DIGS distributions to the modeled equation, and is capable of separation of floc and single-grain settled components, and estimation of source slope (m) and roll-off diameter ($d^\wedge$) (Figure 1.2). Changes in these characteristics can indicate fluctuation in depositional conditions (e.g. turbulence), and represent the dynamic influence of flocculation on estuarine sediment transport. A detailed description of the analytical processes and routines discussed here, including model assumptions and limitations, can be found in Milligan and Kranck (1991), Curran *et al.* (2004) and Mikkelsen *et al.* (2007).
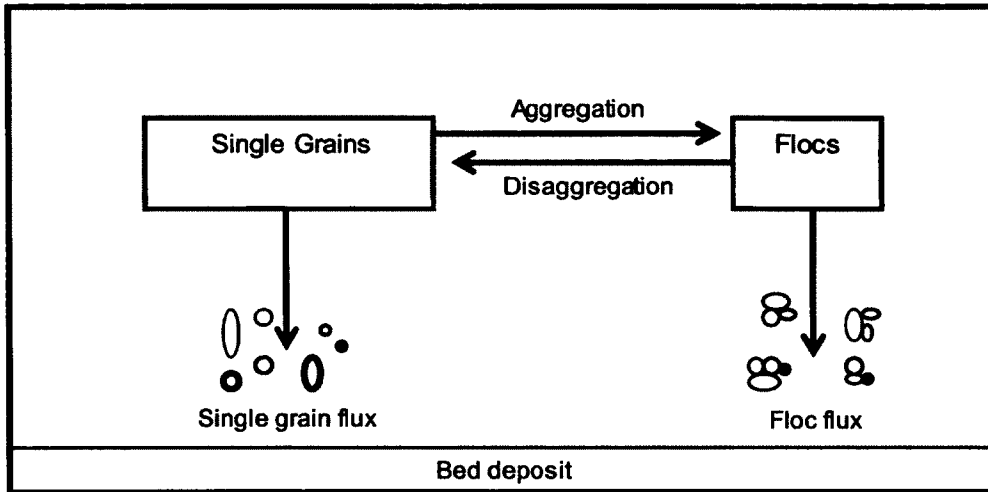
Figure 1.1: Conceptual basis for the inverse-floc model (modified from Curran et al., 2004).
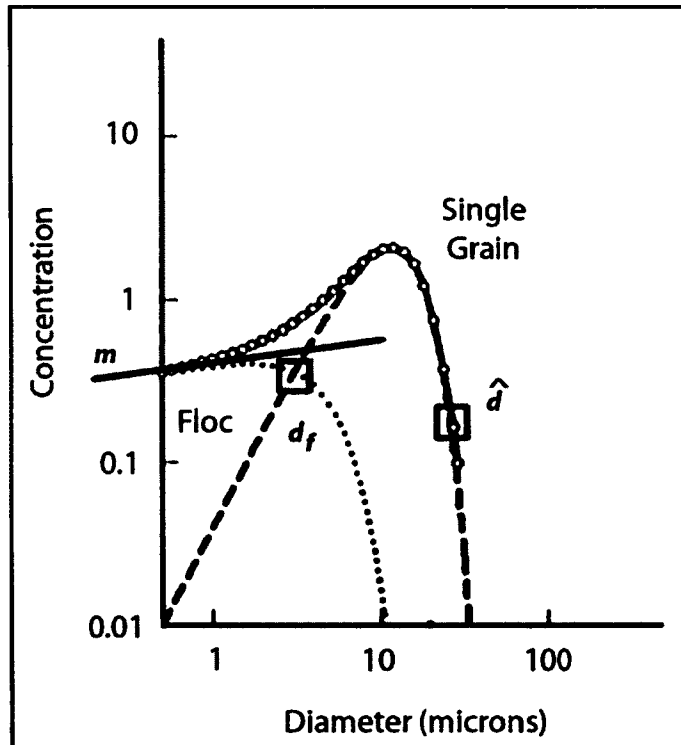
Figure 1.2: Idealized DIGS distribution (solid line) showing concentration versus diameter on log-log axes. The floc-settled (dotted line) and single-grain (dashed line) components are determined by the inverse floc model. Graphical locations of model parameters (d_f, $\hat{d}$, m) are shown. Modified from deGelleke (2011).

1.8   Additional Analyses

1.8.1   Entropy analysis

Entropy analysis can be applied to group DIGS distributions into categories based on similarity, minimizing information loss that is typical of traditional descriptors by taking the entire size spectrum into consideration, and enabling analysis of multi-modal size distributions (Mikkelsen et al., 2007). The concept of entropy was first discussed by Shannon (1948) in relation to information theory, as a measure of information, choice and uncertainty. In reference to particle size distributions, entropy is greatest (and randomness is maximized) when particles are evenly distributed between all size classes. Conversely, if all particles fit into one size class, then entropy and randomness are minimized. The use of entropy analysis for grouping data has long been recognized, but applications to geological and sedimentological problems was initially limited (Woolfe and Michibayashi, 1995). Johnson and Semple (1983) originally applied this approach to sediment size, and subsequent work by Forrest and Clark (1989) and Woolfe and Michibayashi (1995) demonstrated that entropy analysis of bottom sediment size distributions generated groupings that could be correlated to depositional environment. This method has recently been applied to classify in-situ particle size spectra of suspended and bottom sediments, reflecting variations in forcing conditions (e.g. turbulence variability) (Mikkelsen et al., 2007). Bottom sediment textures have also been successfully interpreted using entropy analysis, for definition of ecological habitats on continental shelves (Orpin and Kostylev, 2006).

1.8.2 Acoustic backscatter

The use of acoustic backscatter intensity (e.g. amplitude, or signal strength) as a surrogate estimation of suspended sediment concentration (SSC) has been successfully evaluated and employed in laboratory and field settings for measuring size and fall velocity of suspended particles (e.g. Voulgaris and Meyers, 2004; Thorne and Hanes, 2002; Fugate and Friedrichs, 2002). Several calibration routines are available, and frequently involve co-location of optical backscatter and/or laser in-situ scattering and transmissometery instrumentation (e.g. Hoitink and Hoekstra, 2005; Hill *et al.*, 2003; Holdaway *et al.*, 1999; Lynch *et al.*, 1991). While it has been demonstrated that acoustic backscatter can be converted to valuable estimates of SSC, Hoitink and Hoekstra (2005) describe complications related to unknown influences of flocculation, as well as anomalous scatterers in the water column (e.g. phytoplankton). Kim and Voulgaris (2003) found calibration methods to be most accurate for fine sands, whereas silt and finer materials generate bias in acoustic measurement. Additionally, high SSC is generally understood to generate measurement inaccuracies due to significant signal attenuation in the water column (Thorne *et al.*, 1991). Consequently, acoustic Doppler current profiler (ADCP) amplitude data presented in the following chapters is not quantified, but has been applied as a relative indicator of changing suspended sediment concentration in the absence of calibration. Rates of changing signal strength in the water column can be applied to characterize suspended sediment dynamics and link with periods of deposition (e.g. Hill *et al.*, in press).

1.9   Summary and thesis goals

Salt marshes play a crucial role in sediment exchange by occupying zones of transition between terrestrial and marine ecosystems, and also provide valuable ecosystem and storm-protection services, such as nutrient supply and enhancing coastal stability (Craft *et al.*, 2009; Davidson-Arnott *et al.*, 2002; Donnelly and Bertness, 2001; Reed *et al.*, 1999). Primary and secondary productivity in the intertidal zone is strongly linked to salt marsh environments, which makes the presently uncertain practice of predicting the fate of estuarine sediments a high priority (Smith and Friedrichs, 2011; OEER, 2008a). In response to modification of local tidal characteristics (e.g. reduced tidal amplitude), changes in intertidal sedimentation patterns can be expected due to the high sensitivity of intertidal zones to sediment supply, which is inherently linked to hydrodynamics (Ralston and Stacy, 2007; Boorman, 2003). Such environmental effects of tidal power development in the Bay of Fundy have been previously considered (e.g. Yeo and Risk, 1979; Gordon 1994), but the magnitude of potential change still remains to be fully understood (Polagye *et al.*, 2011). It is hypothesized that intertidal sedimentation rates in the Minas Basin will demonstrate a non-linear response to modification of the tidal energy regime, due to a naturally high suspended sediment concentration (Polagye *et al.*, 2011; Polagye and Malte, 2010; OEER, 2008a). This notion is well-supported by previous work assessing the response of estuarine systems on the Bay of Fundy

to anthropogenic alterations of natural hydrodynamics (e.g. van Proosdij *et al.*, 2009; Amos and Mosher, 1985; Turk *et al.*, 1980).

As stated, the goal of this thesis is to identify processes controlling sediment dynamics in a sheltered tidal creek environment and determine the effects on inorganic grain size. This research has been undertaken to better understand processes that may be linked to a potentially non-linear response of fine sediment to energy extraction, such as the influence of tidal amplitude on the flocculated nature of suspended and deposited sediment. Data were collected in the Upper Bay of Fundy region during the summer of 2009 over a range of tidal conditions associated with the spring-neap cycle. Individual tidal cycles were sampled for current velocity, suspended sediment concentration and sediment deposition. Chapters in this document have been organized manuscript-style; chapters 2 and 3 are focussed companion papers for submission to academic journals. Chapter 2 focuses on the variability of creek hydrodynamics and suspended sediment concentration, while Chapter 3 discusses the sedimentary characteristics of associated suspended and deposited sediments. Finally, Chapter 4 provides a synthesis of information collected and discussed throughout this document.

References

AGS, 2001. The Last Billion Years: A Geological History of the Maritime Provinces of Canada. Fensome RA, Williams GL [eds], Atlantic Geoscience Society, Nimbus Publishing: 212 pp.

Allen JRL. 2000. Morphodynamics of Holocene salt marshes: a review sketch from the Atlantic and Southern North Sea Coasts of Europe. *Quartemary Science Reviews* 19: 1155-1231.g

Allen JRL, Pye K. 1992. Coastal saltmarshes: Their nature and importance. In: *Saltmarshes: Morphodynamics, conservation and engineering significance.* Cambridge University Press: Cambridge; 1-19.

Amos C. 1987. Fine-grained sediment transport in Chignecto Bay, Bay of Fundy, Canada. *Continental Shelf Research* 7 (11/12): 1295-1300.

Amos CL, Mosher DC. 1985. Erosion and deposition of fine-grained sediments from the Bay of Fundy. *Sedimentology* 32: 815-832.

Bayliss-Smith TP, Healey R, Lailey R, Spencer T, Stoddart DR. 1979. Tidal flows in salt marsh creeks. *Estuarine and Coastal Marine Science* 9 (3): 235-255. DOI: 10.1016/0302-3524(79)90038-0.

Bartholomä A, Kubicki A, Badewien TH, Flemming BW. 2009. Suspended sediment transport in the German Wadden Sea – seasonal variations and extreme events. *Ocean Dynamics* 59: 213-255.

Bertness MD. 1991. Zonation of Spartina Patens and Spartina Alterniflora in a New England salt marsh. *Ecology* 72 (1): 138-148.

Biron PM, Robson C, Lapointe MF, Gaskin SJ. 2004. Comparing different methods of bed shear stress estimates in simple and complex flow fields. *Earth Surface Processes and Landforms* 29: 1403-1415. DOI: 10.1002/esp.1111

Blanton JO, Lin G, Elston SA. 2002. Tidal current asymmetry in shallow estuaries and tidal creeks. *Continental Shelf Research* 22: 1731-1743.

Boon, JD III. 1975. Tidal Discharge Asymmetry in a salt marsh drainage system. *Limnology and Oceanography* 20 (1): 71-80.

Boorman LA. 1999. Salt marshes - present functioning and future change. *Mangroves and Salt Marshes* 3: 227-241.

Boorman LA. 2003. Saltmarsh Review. An overview of coastal saltmarshes, their dynamic and sensitivity characteristics for conservation and management. *JNCC Report*, No. **334**. 98 pp.

Bryden IG, Grinsted T, Melville GT. 2004. Assessing the potential of a simple channel to deliver useful energy. *Applied Ocean Research* **26**: 198-204. doi:10.1016/j.apor. 2005.04.001

Cartwright DE. 1997. Some thoughts on the spring-neap cycle of tidal dissipation. *Progress in Oceanography* **40**: 125-133.

Charlier, RH. 2003. A "sleeper" awakes: tidal current power. *Renewable and Sustainable Energy Reviews* **7**: 515-529.

Christiansen T, Wilberg PL, Milligan TG. 2000. Flow and sediment transport on a tidal salt marsh surface. *Estuarine, Coastal and Shelf Science* **50**: 315-331. DOI: 10.1006/ecss.2000.0548

Craft C, Clough J, Ehman J, Joye S, Park R, Pennsings S, Guo H, Machmuller M. 2009. Forecasting the effects of accelerated sea-level rise on tidal marsh ecosystem services. *Frontiers in Ecology and the Environment* **7(2)**: 73-78. DOI: 10.1890/070219

Curran KJ, Hill PS, Schnell TM, Milligan TG, Piper DJW. 2004. Inferring the mass fraction of floc-deposited mud: application to fine-grained turbidites. *Sedimentology* **51**: 927-944. DOI: 10.1111/j.1365-3091.2004.00647.x

Curran KJ, Hill PS, Milligan TG, Mikkelsen OA, Law BA, Durrieu de Madron X, Bourrin F. 2007. Settling velocity, effective density, and mass composition of suspended sediment in a coastal bottom boundary layer, Gulf of Lions, France. *Continental Shelf Research* **27**: 1408-1421.

Davidson-Arnott RGD, van Proosdij D, Ollerhead J, Schostak L. 2002. Hydrodynamics and sedimentation in salt marshes: examples from a macrotidal marsh, Bay of Fundy. *Geomorphology* **48**: 209-231.

Desplanque C, Mossman DJ. 2001. Bay of Fundy tides. *Geoscience Canada* **28 (1)**: 1-11.

Desplanque C, Mossman DJ. 2004. Tides and their seminal impacts on the geology, geography, history and socio-economics of the Bay of Fundy, eastern Canada. *Atlantic Geology Special Publication*.

DFO. 2009. Department of Fisheries and Oceans Assessment of Tidal and Wave Energy Conversion Technologies in Canada. *DFO Canadian Science Advisory Secretariat Science Advisory Report*, 2009/064.

Dincer I. 1999. Environmental impacts of energy. *Energy Policy* **27**: 845-854.

Donnelly JP, Bertness MD. 2001. Rapid shoreward encroachment of salt marsh cordgrass in response to accelerated sea-level rise. *Proceedings of the National Academy of Sciences of the United States of America* **98 (25)**:14218-14223.

Dronkers J. 1986. Tidal asymmetry and estuarine morphology. *Netherlands Journal of Sea Research* **20 (2/3)**: 117-131.

Dyer KR, Manning AJ. 1999. Observation of the size, settling velocity and effective density of flocs and their fractal dimensions. *Journal of Sea Research* **41**: 87-95.

Eisma D. 1986. Flocculation and de-flocculation of suspended matter in estuaries. *Netherlands Journal of Sea Research* 20 (2/3): 183-199.

French JR, Stoddart DR. 1992. Hydrodynamics of salt marsh creek systems: Implications for marsh morphological development and material exchange. *Earth Surface Processes and Landforms* **17**: 235-252.

Friedrichs CT, Perry JE. 2001. Tidal salt marsh morphodynamics: a synthesis. *Journal of Coastal Research* **27**: 7-37.

Friend PL, Lucas CH, Rossington SK. 2005. Day-night variation of cohesive sediment stability. *Estuarine, Coastal and Shelf Science* **64**: 407-418.

Forrest J, Clark NR. 1989. Characterizing grain-size distributions: evaluation of a new approach using a multivariate extension of entropy analysis. *Sedimentology* **36**: 711-722.

Fox JM, Hill PS, Milligan TG, Ogston AS, Boldrin A. 2004. Floc fraction in the waters of the Po River prodelta. *Continental Shelf Research* **24**: 1699-1715.

Fugate DC, Friedrichs CT. 2002. Determining concentration and fall velocity of estuarine particle populations using ADV, OBS and LISST. *Continental Shelf Research* **22**:1867-1886.

Garrett C. 1972. Tidal resonance in the Bay of Fundy and Gulf of Maine. *Nature* **238 (5365)**: 441-443.

Garrett C, Cummins P. 2005. The power potential of tidal currents in channels. *Proceedings of the Royal Society A* **461**: 2563-2572.

Greenberg DA, Shore JA, Page FH, Dowd M. 2005. A finite element circulation model for embayments with drying intertidal areas and its application to the Quoddy region of the Bay of Fundy. *Ocean Modelling* **10**: 211-231.

Gordon DC. 1994. Intertidal ecology and potential power impacts, Bay of Fundy, Canada. *Biological Journal of the Linnean Society* **51**: 17-23.

Hill DC, Jones SE, Prandle D. 2003. Derivation of sediment resuspension rates from acoustic backscatter time-series in tidal waters. *Continental Shelf Research* **23**: 19-40.

Hill PS, Milligan TG, Geyer WR. 2000. Controls on the effective settling velocity of suspended sediment in the Eel River flood plume. *Continental Shelf Research* **20**: 2095-2111.

Hill PS, Newgard JP, Milligan TG. In press. Flocculation on a muddy intertidal flat in Willapa Bay, Washington, Part II: Observations of suspended particle size in a secondary channel and adjacent flat. *Continental Shelf Research*. 44 pp.

Hoitink AJF, Hoekstra P. 2005. Observations of suspended sediment from ADCP and OBS measurements in a mud-dominated environment. *Coastal Engineering* **52**: 103-118. DOI: 10.1016/j.coastaleng.2004.09.005

Holdaway GP, Thorne PD, Flatt D, Jones SE, Prandle D. 1999. Comparison between ADCP and transmissometer measurements of suspended sediment concentration. Continental Shelf Research **19**: 421-441.

Johnston R J, Semple RK. 1983. Classification using information statistics. Geo-Books, Norwich. 43 pp.

Karas AN. 1978. System planning for Bay of Fundy tidal power development. *IEEE Transactions on Power Apparatus and Systems* PAS-**97** **(5)**: 1600-1606.

Karsten RH, McMillan JM, Lickley MJ, Haynes RD. 2008. Assessment of tidal current energy in the Minas Passage, Bay of Fundy. *Proceedings of the Institution of Mechanical Engineers* **222** **(A-J)**: 493-507.

Kim SC, Voulgaris G. 2003. Estimation of suspended sediment concentration in estuarine environments using acoustic backscatter from an ADCP. *Proceedings of the Fifth International Conference on Coastal Sediments*, 2003. 10pp.

Kranck K. 1980. Experiments on the significance of flocculation in the settling of fine-grained sediment in still water. *Canadian Journal of Earth Sciences* **17**: 1517-1526.

Kranck K. 1981. Particulate matter grain-size characteristic and flocculation in a partially mixed estuary. *Sedimentology* **28**: 107-114.

Kranck K, Milligan TG. 1991. Grain size in oceanography. In: Syvitski, JPM [ed]. *Principles, Methods, and Applications of Particle Size Analysis.* Cambridge University Press: 368 pp.

Kranck K, Milligan TG. 1985. Origin of grain size spectra of suspension deposited sediment. *Geo-Marine Letters* **5**: 61-66.

Kranck K, Smith P, Milligan TG. 1996a. Grain-size characteristics of fine-grained unflocculated sediments I: 'one-round' distributions. *Sedimentology* **43**: 589-596.

Kranck K, Smith P, Milligan TG. 1996b. Grain-size characteristics of fine-grained unflocculated sediments II: 'multi-round' distributions. *Sedimentology* **43**: 597-606.

Kranck K, Milligan TG. 1992. Characteristics of Suspended Particles at an 11-Hour Anchor Station in San Francisco Bay, California, *J. Geophys. Res.*, **97(C7)**, 11,373-11,382, doi:10.1029/92JC00950

Kvale E. 2006. The origin of spring-neap tidal cycles. *Marine Geology* **235**: 5-18.

Law BA, Hill PS, Milligan TG, Curran KJ, Wiberg PL, Wheatcroft RA. 2008. Size sorting of fine-grained sediments during erosion: Results from the western Gulf of Lions. *Continental Shelf Research* **28**: 1935-1946.

Law BA, Milligan TG, Hill PS, Newgard JP, Wheatcroft RA, Wilberg PL. In press. Flocculation on a muddy intertidal flat in Willapa Bay, Washington, Part I: A regional survey of the grain size of surficial sediments. *Continental Shelf Research.* 44 pp.

Lawrence DSL, Allen JRL, Havelock GM. 2004. Salt marsh morphodynamics: An investigation of tidal flows and marsh channel equilibrium. *Journal of Coastal Research* **20**: 301-316.

Lee STY, Deschamps C. 1978. Mathematical model for economic evaluation of tidal power in the Bay of Fundy. *IEEE Transactions on Power Apparatus and Systems* PAS-97 (**5**): 1769-1778.

Leonard LA, Croft AL. 2006. The effect of standing biomass on flow velocity and turbulence in *Spartina alterniflora* canopies. *Estuarine, Coastal and Shelf Science* **69**: 325-336. DOI: 10.1016/j.ecss.2006.05.004

Leonard LA, Luther ME. 1995. Flow hydrodynamics in tidal marsh canopies. *Limnology and Oceanography* **40 (8)**: 1474-1484.

Lynch JF, Gross TF, Brumley BH, Filyo RA. 1991. Sediment concentration profiling in HEBBLE using a 1-Mhz acoustic backscatter system. *Marine Geology* **99**: 361-385.

Manning AJ, Bass SJ, Dyer KR. 2006. Floc properties in the turbidity maximum of a mesotidal estuary during neap and spring tidal conditions. *Marine Geology* **235**: 193-211.

Manning AJ, Dyer KR. 2002. A comparison of floc properties observed during neap and spring tidal conditions. In: Winterwerp, J.C. and Kranenburg [eds]. *Fine Sediment Dynamics in the Marine Environment.* Elsevier, Amsterdam, 713 pp.

Manning AJ, Langston WJ, Jonas PJC. 2010. A review of sediment dynamics in the Severn Estuary: Influence of flocculation. *Marine Pollution Bulletin* **61**: 37-61.

Middleton, GV. 1972. Brief field guide to intertidal sediments, Minas Basin, Nova Scotia. *Maritime Sediments* **8 (3)**: 114-122.

Mikkelsen OA, Curran KJ, Hill PS, Milligan TG. 2007. Entropy analysis of in situ particle size spectra. *Estuarine, Coastal and Shelf Science* **72**: 615-625.

Mikkelsen OA, Hill PS, and Milligan TG. 2006. Single-grain, microfloc and macrofloc volume variations observed with a LISST-100 and a digital floc camera. Journal of Sea Research **55**: 87-102.

Mikkelsen OA, Milligan TG, Hill PS, Moffatt D. 2004. INSSECT– an instrumented platform for investigating floc properties close to the seabed. *Limnology and Oceanography: Methods* **2**: 226-236.

Milligan TG, Hill PS. 1998. A laboratory assessment of the relative importance of turbulence, particle composition, and concentration in limiting maximal floc size and settling behaviour. *Journal of Sea Research* **39**: 227-241.

Milligan TG, Hill PS, Law BA. 2007. Flocculation and the loss of sediment from the Po River plume. *Continental Shelf Research* **27**: 309-321.

Milligan TG, Kineke GC, Blake AC, Alexander CR, Hill PS. 2001. Flocculation and Sedimentation in the ACE Basin, South Carolina. *Estuaries* **24 (5)** Dedicated

Issue: Processes and Products of the Estuarine Turbidity Maximum: Symposium Papers from the 15th Biennial Estuarine Research Federation Conference: 734-744.

Milligan TG, Kranck K. 1991. Electroresistance particle size analyzers. In: Syvitski, JPM. [ed]. *Principles, methods and applications of particle size analysis.* Cambridge University Press, New York, 368 pp.

Milligan TG, Law BA. 2005. The effect of marine agriculture on fine sediment dynamics in coastal inlets. In: Hargrave, B. [ed]. Environmental Effects of Marine Finfish Aquaculture. *The Handbook of Environmental Chemistry* **5**: Water Pollution. Springer, Berlin Heidelbrg, New York, 467 pp.

Milligan TG, Loring DH. 1997. The effect of flocculation on the size distributions of bottom sediment in coastal inlets: implications for contaminant transport. *Water, Air and Soil Pollution* **99**: 33-42.

Möller I. 2006. Quantifying salt marsh vegetation and its effect on wave height dissipation: Results from a UK East coast salt marsh. *Estuarine, Coastal and Shelf Science* **69**: 337-351.

Morris JT, Sundareshwar PV, Nietch CT, Kjerfve B, Cahoon DR. 2002. Responses of coastal wetlands to rising sea level. *Ecology* **83** (10): 2869-2877.

Murphy S, Voulgaris G. 2006. Identifying the role of tides, rainfall and seasonality in marsh sedimentation using long-term suspended sediment concentration data. *Marine Geology* **227**: 31-50.

Neumeier U, Amos CL. 2006. The influence of vegetation on turbulence and flow velocity in European salt-marshes. *Sedimentology* **53**: 259-277. DOI: 10.1111/j.1365-3091.2006.00772x

Neumeier U, Ciavola P. 2004. Flow resistance and associated sedimentary processes in a *Spartina maritima* salt marsh. *Journal of Coastal Research* **20** (2): 435-447.

O'Brien DJ, Whitehouse RJS, Cramp A. 2000. The cyclic development of a macro-tidal salt marsh on varying timescales. *Continental Shelf Research* **20**: 1593-1619.

OEER. 2008a. Final Report: Background Report for the Fundy Tidal Energy Strategic Environmental Assessment. Prepared by Jacques Whitford Consultants for the OEER Association. Project No. 1028476. 291 pp.

OEER. 2008b. Fundy Tidal Energy Strategic Environmental Assessment: Final Report. Prepared by the Offshore Energy Environmental Research (OEER) Association for the Nova Scotia Department of Energy (April 2008). 92 pp.

Omer AM. 2008. Energy, environment and sustainable development. *Renewable and Sustainable Energy Reviews* **12 (9)**: 2265-2300.

Orpin AR, Kostylev VE. 2006. Towards a statistically valid method of textual seafloor characterization of benthic habitats. *Marine Geology* **225**: 209-222.

Pejrup M, Mikkelsen OA. 2010. Factors controlling the field settling velocity of cohesive sediment in estuaries. *Estuarine,Coastal and Shelf Science* **87**: 177-185.

Peters H. 1997. Observations of stratified turbulent mixing in an estuary: Neap-to-spring variations during high river flow. *Estuarine, Coastal and Shelf Science* **45**: 69-88.

Pethick JS, Morris RKA, Evans DH. 2009. Nature conservation implications of a Severn tidal barrage - A preliminary assessment of geomorphological change. *Journal for Nature Conservation* **17**: 183-198.

Polagye BL, Malte PC. 2010. Far-field dynamics of tidal energy extraction in channel networks. *Renewable Energy* **36**: 222-234. DOI:10.1016/j.renene.2010.06.025

Polagye B, Van Cleve B, Copping A, Kirkendall K (eds). 2011. Environmental effects of tidal energy development. *U.S. Dept. Commerce, NOAA Tech. Memo.* 181 pp.

Pope ND, Widdows J, Brinsley MD. 2006. Estimation of bed shear stress using the turbulent kinetic energy approach - A comparison of annular flume and field data. *Continental Shelf Research* **26**: 959-970. DOI: 10.1016/j.csr.2006.02.010

Ralston DK, Stacey MT. 2007. Tidal and meteorological forcing of sediment transport in tributary mudflat channels. *Continental Shelf Research* **27**: 1510-1527.

Reed D. 1988. Sediment dynamics and deposition in a retreating coastal salt marsh. *Estuarine, Coastal and Shelf Science* **26**: 67-79.

Reed D, Spencer T, Murray AL, French JR, Leonard L. 1999. Marsh surface sediment deposition and the role of tidal creeks: implications for created and managed coastal marshes. *Journal of Coastal Conservation* **5**: 81-90.

Sanders RE, Baddour E. 2008. Engineering issues in the harvest of tidal energy in the Bay of Fundy, Canada. *Report to the Engineering Committee on Oceanic Resources Symposium.* 10 pp.

Scott DB, Greenberg DA. 1983. Relative sea-level rise and tidal development in the Bay of Fundy system. *Canadian Journal of Earth Sciences* **20**: 1554-1564.

Seoni RM. 1979. Major electrical equipment proposed for tidal power plants in the Bay of Fundy. *IEEE Transactions on Power Apparatus and Systems* PAS-**89** **(5)**: 1750-1760.

Shannon CE. 1948. A mathematical theory of communication. *The Bell System Technical Journal* **27**: 379-423.

Shaw J, Amos CL, Greenberg DA, O'Reilly CT, Parrott DR, Patton, E. 2010. Catastrophic tidal expansion in the Bay of Fundy, Canada. *Canadian Journal of Earth Sciences* **47**: 1079-1091.

Silva H, Dias JM, Caçador I. 2009. Is the salt marsh vegetation a determining factor in the sedimentation process? *Hydrobiologia* **621**: 33-47. DOI 10.1007/s10750-008-9630-7

Smith SJ, Friedrichs CT. 2011. Size and settling velocities of cohesive flocs and suspended aggregates in a trailing suction hopper dredge plume. *Continental Shelf Research* **31**: 550-563.

Sun X, Chick JP, Bryden IG. 2008. Laboratory-scale simulation of energy extraction from tidal currents. *Renewable Energy* **23**: 1267-1274.

Temmerman S, Bouma TJ, Govers G, Lauwaet D. 2005. Flow paths of water and sediment in a tidal marsh: relations with marsh development stage and tidal inundation height. *Estuaries* **28** **(3)**: 338-352.

Thorne PD, Hardcastle PJ, Soulsby RL. 1993. Analysis of acoustic measurements of suspended sediment. *Journal of Geophysical Research* **98** **(C1)**: 899- 910.

Thorne PD, Hanes DM. 2002. A review of acoustic measurements of small-scale sediment processes. *Continental Shelf Research* **22**: 603-632

Turk TR, Risk MJ, Hirtle RWM, Yeo RK. 1980. Sedimentological and biological changes in the Windsor mudflat, and area of induced siltation. *Canadian Journal of Fisheries and Aquatic Sciences* **37**: 1387-1397.

Van der Lee WTB. 2000. Temporal variation of floc size and settling velocity in the Dollard estuary. *Continental Shelf Research* **20**: 1495-1511.

van der Lee EM, Bowers DG, Kyte, E. 2009. Remote sensing of temporal and spatial patterns of suspended particle size in the Irish sea in relation to the Kolmogorov microscale. *Continental Shelf Research* **29**: 1213-1225.

van Leussen W. 1999. The variability of settling velocities of suspended fine-grained sediment in the Ems estuary. *Journal of Sea Research* **41**: 109-118.

van Proosdij D. 2001. Spatial and temporal controls on the sediment budget of a macro-tidal saltmarsh. Ph.D. Diss., University of Guelph, 2001.

van Proosdij D, Davidson-Arnott RGD, Ollerhead J. 2006a. Controls on spatial patterns of sediment deposition across a macro-tidal salt marsh surface over single tidal cycles. *Estuarine, Coastal and Shelf Science* **69**: 64-86. DOI: 10.1016/j.ecss.2006.04.022

van Proosdij D, Lundholm J, Neatt N, Bowron T, Graham J. 2010. Ecological re-engineering of a freshwater impoundment for salt marsh restoration in a hypertidal system. *Ecological Engineering* **36**: 1314-1332.

van Proosdij D, Ollerhead J, Davidson-Arnott RGD. 2006b. Seasonal and annual variations in the volumetric sediment balance of a macro-tidal salt marsh. *Marine Geology* **225**: 103-127. DOI: 10.1016/j.margeo.2005.07.009

van Proosdij D, Milligan T, Bugden G, Butler K. 2009. A tale of two macro-tidal estuaries: Differential morphodynamic response of the intertidal zone to causeway construction. *Journal of Coastal Research*, Special Issue **56**: 772-776.

Vörösmarty CJ, Loder TC III. 1994. Spring-neap tidal contrasts and nutrient dynamics in a marsh-dominated estuary. *Estuaries* **17** (3): 537-551.

Voulgaris G, Meyers ST. 2004. Temporal variability of hydrodynamics, sediment concentration and sediment settling velocity in a tidal creek. *Continental Shelf Research* **24**: 1659-1683. DOI: 10.1016/j.csr.2004.05.006

Wells N. 1986. *The Atmosphere and Ocean: A Physical Introduction*. Taylor & Francis Ltd., London, 346pp.

Whitehouse, R., Soulsby, R., Roberts, W. and Mitchener, H. (2000). *Dynamics of estuarine muds*. Thomas Telford Publishing, London, 210 pp.

Winterwerp JC. 1998. A simple model for turbulence induced flocculation of cohesive sediments. *Journal of Hydraulic Research* **36** (3): 309-326.

Winterwerp JC. 2002. On the flocculation and settling velocity of estuarine mud. *Continental Shelf Research* **22**: 1339-1360.

Winterwerp JC, van Kesteren WGM. 2004. Introduction to the physics of cohesive sediment in the marine environment. *Developments in Sedimentology* **56**: 466 pp.

Williams ND, Walling DE, Leeks GTL. 2006. High temporal resolution in situ measurement of the effective particle size characteristics of fluvial suspended sediment. *Water Research* **41** (5): 1081-1093.

Woolfe KJ, Michibayashi K. 1995. "Basic" entropy grouping of laser-derived grain-size data: An example from the Great Barrier Reef. *Computers and Geosciences* **21** (4): 447-462.

Wu Y, Chaffey J, Greenberg DA, Colbo K, Smith PC. 2011. Tidally-induced sediment transport patterns in the upper Bay of Fundy: A numerical study. *Continental Shelf Research* **31**: 2041-2053.

Yeo RK, Risk MJ. 1979. Fundy tidal power: Environmental sedimentology. *Geoscience Canada* **6** (3): 115-121.

CHAPTER 2: INFLUENCE OF VARYING TIDAL PRISM ON HYDRODYNAMICS AND SEDIMENTARY PROCESSES IN A HYPERTIDAL SALT MARSH CREEK

2.1 Abstract

Recent initiatives directing tidal power development in the Bay of Fundy have raised questions about far-field environmental impacts related to energy extraction. It has been proposed that commercial scale tidal power installations in the Minas Passage will result in an overall decrease in tidal amplitude in the Minas Basin. Corresponding changes in sedimentation patterns may or may not be within the natural range of variability, and it is hypothesized that intertidal sedimentation rates will demonstrate a non-linear response to modification of the tidal energy regime. This research considers current velocity and suspended sediment concentration data from a sheltered tidal creek in the Minas Basin, for analysis of tidal characteristics in a hypertidal creek environment over spring and neap tidal cycles. Sediment deposition in the creek was also measured. Results show a first-order control of topography on flow magnitude in the tidal creek, which impacts net sediment deposition through resuspension and removal of newly introduced material. This study demonstrates that tides which peak around the bankfull level show reduced early ebb stage turbulence and flow velocity and encourage an extended depositional period.

2.2 Introduction

Interest in intertidal sedimentation processes has increased over the past decade, along with recognition that tidal salt marshes provide valuable ecological and storm-protection services (Craft *et al.*, 2009; Boorman, 1999). The capacity of salt marshes to function as critical habitat, in biological production, and as a coastal defense is entirely dependent on their ability to import and retain sedimentary material (Donnelly and Bertness, 2001; Reed *et al.*, 1999). Intertidal systems in eastern Canada, where concentrations of suspended fine-grained sediments are high (up to 30,000 mg/L), have shown marked decadal-scale changes in sedimentation patterns in response to anthropogenic alterations of the natural hydrodynamics (van Proosdij *et al.*, 2009; van Proosdij *et al.*, 2006b; Amos and Mosher, 1985; Turk *et al.*, 1980). However, current knowledge regarding the distribution and dynamics of sediments in shallow, muddy and vegetated environments such as the Bay of Fundy is limited (Whitford, 2008; DFO, 2009; Sanders and Baddour, 2008).

Tidal creeks are essential components of inorganic salt marsh systems, providing conduits for the import and export of sedimentary material, material that is required to maintain a positive balance and mitigate regional changes in sea level (van Proosdij 2006b; Voulgaris and Meyers 2004a). Deposition and particle grain size have been shown to decrease with increasing distance from creek margins (Christiansen *et al.*, 2000; Allen, 2000; Friedrichs and Perry, 2001), implying that creeks are the dominant supplier of sediment to the marsh surface. With higher tides and in macrotidal environments, a proportion of the total marsh

tidal prism is not restricted to creeks and flow moves across the marsh margin (Davidson-Arnott et al., 2002). The percentage of total input from marsh margins is greater with increasing high water level (Temmerman et al., 2005). Flow magnitude in tidal creeks is linked to the amplitude of individual tidal cycles, which is also a determining factor for inundation time, as the resulting flow velocity corresponds with the volume of water being moved through a system. This relationship shows variation within the same environment in response to the spring-neap tidal cycle (Voulgaris and Meyers, 2004a; Manning and Dyer, 2002; Murphy and Voulgaris, 2006; Manning and Bass, 2006). In general, increased tidal amplitude is associated with spring tides, and implies longer inundation time, faster and more turbulent currents, and higher suspended sediment concentration due to a greater carrying capacity, relative to lower tidal amplitude (Allen 2000; Friedrichs and Perry, 2001). Evidence has been presented to support the existence of an energy variation over the spring-neap cycle, which affects suspended concentration and flocculation processes (e.g. Voulgaris and Meyers, 2004a), depositional capabilities (e.g. O`Brien et al., 2000), variations in sedimentary, biomass and water content (e.g. Friend et al., 2005), as well as tidal dissipation, currents and depth (e.g. Desplanque and Mossman, 2001; Cartwright, 1997; Peters, 1997; Middleton, 1972).

Tides which inundate the marsh surface show very different velocity patterns from those that remain restricted to channels (Torres and Styles, 2007; Lawrence et al., 2004; French and Stoddart, 1992). In general, greater flow

43

velocity in tidal creeks (up to 1 m·s^{-1}) has been reported during over-marsh tides, compared with channel-restricted tides (10 – 20 cm·s^{-1}) (Christiansen et al., 2000, Voulgaris and Meyers, 2004a). Tidal creek morphology is dictated by topographic boundaries, such as the marsh platform itself, which influences marsh structure through hydrodynamics and acts as a topographic threshold separating two relatively different flow regimes (French and Stoddart, 1992; Allen 2000; Friedrichs and Perry, 2001). Torres and Styles (2007) present results that imply a first-order control of salt marsh topographic structure on over-marsh flow complexities, including current reversal in tidal creeks associated with high tide. Velocity and discharge asymmetries have been identified between flood and ebb phases of individual tidal cycles, impacted by channel geometry and marsh morphology (Dronkers, 1986; Bayliss-Smith, et al., 1979; Boon, 1975). As intertidal areas (e.g. high marsh) flood and drain in close proximity to high water, peak flood and ebb currents develop shortly before or after slack tide at high water (Blanton et al., 2002; Dronkers, 1986). Marshes with a high equilibrium surface that is relatively flat promote a rapid transition from zero surface submergence to complete surface submergence with increasing tidal height, evidenced by sudden changes in velocity patterns with submergence of marsh topography (Friedrichs and Perry, 2001; Torres and Styles, 2007).

Potential controls that influence salt marsh and tidal creek processes include those intrinsic to the marsh (e.g. topography, tidal prism, vegetation height), and others which are externally-driven (e.g. suspended sediment

concentration, wave height, tidal amplitude and current velocity). The resulting deposition of sedimentary material on mudflats, creek banks and the marsh surface is therefore a complex function of variables controlling sediment availability and the opportunity for deposition (van Proosdij *et al.*, 2006a). Vegetation has been shown to reduce velocity and turbulence of tidal flow moving through salt marsh canopies (Leonard and Croft, 2006; Leonard and Luther, 1995); however, it remains uncertain whether this action actually increases deposition or simply protects against erosion (Silva *et al.*, 2009). The occurrence of salt marsh vegetation is generally limited to the zone between mid-neap tide level and the high water level during spring tides, while non-vegetated mudflats and creek banks occupy the space below (Allen and Pye, 2002). Marsh vegetation communities adhere to sharp boundaries defined by tolerance to stressors, such as saline tidal waters (Bertness, 1991).

As part of a provincial renewable energy initiative, the Minas Passage has been selected as a test site for tidal in-stream energy conversion (TISEC) devices, which commenced in 2009. Numerical modelling of regional hydrodynamics (e.g. (Karsten *et al.*, 2008) demonstrates that a significant decrease in tidal energy will lead to reduced tidal amplitude in the Minas Basin, related to modification of the resonant period in the Bay of Fundy-Gulf of Maine system, in response to alteration of flow through the Minas Passage. The purpose of this project is to investigate natural variations in tidal characteristics (e.g. tidal prism, velocity, suspended and deposited sediment) and determine the

variability of controls on sedimentation processes in a tidal creek over the spring-neap cycle. Recent initiatives driving tidal power development in the Bay of Fundy have raised questions about far-field environmental impacts. Simple numerical models of energy extraction from various channel networks show a general decrease in kinetic power density of tidal flows with increasing dissipation by turbines (Polagye and Malte, 2010; Sun *et al.*, 2008; Bryden *et al.*, 2004). According to Karsten *et al.* (2008), proposed tidal power installations in the Minas Passage will result in an overall lowering of tidal amplitude in the Minas Basin; a 5% reduction in tidal amplitude has been associated with moderate levels (e.g. 2.5 gigawatts) of energy extraction from the Minas Passage. Environmental effects of tidal power development in the Bay of Fundy have been previously considered (e.g. Yeo and Risk, 1979; Gordon 1994), but the magnitude of potential change still remains to be fully understood (Polagye *et al.*, 2011) and may or may not occur within a range of natural variability. It is hypothesized that intertidal sedimentation rates in the Minas Basin will demonstrate a non-linear response to modification of the tidal energy regime, due to a naturally high suspended sediment concentration (Polagye *et al.*, 2011; Polagye and Malte, 2010; Whitford, 2008), and based on previous work assessing estuarine response to anthropogenic alterations of hydrodynamics (e.g. van Proosdij *et al.*, 2009; Amos and Mosher, 1985; Turk *et al.*, 1980). The present research will investigate the hypothesis that sedimentation rates in the tidal creek will decrease in response to a reduced frequency of over-marsh tides, associated

with an overall lowering of tidal amplitude. This may reduce deposition in tidal creeks, and by extension, salt marshes, due to a decreased sediment supply. Alternatively, a reduction in tidal amplitude may increase sediment deposition in intertidal zones, including increased sedimentation in tidal creeks. Either circumstance will impact the form and function of salt marshes, as changes to balanced sediment budgets will show the greatest impact in accretion rates on low marsh surfaces (Chmura et al., 2001). It is anticipated that tidal prism and depth of inundation on the marsh surface will play a key role in intertidal hydrodynamics, and resulting sediment mobility in the tidal creek.

2.3 Study Area

The Bay of Fundy is a funnel-shaped, macrotidal embayment on Canada's east coast. It forms the north-eastern extension of the Gulf of Maine, and splits into two inner-bay systems: Chignecto Bay and the Minas Basin (Davidson-Arnott et al., 2002; van Proosdij et al., 2000). The intertidal zone is extensive, and salt marshes and mudflats dominate a large portion of the coastal zone. The Bay is famous for its tidal range (up to 16 meters), and was the subject of tidal barrage research in the 1970s (Desplanque and Mossman, 2004; Charlier, 2003; Yeo and Risk, 1979). Relative sea level rise is largely responsible for the development of the modern tidal regime in the Bay of Fundy, particularly the
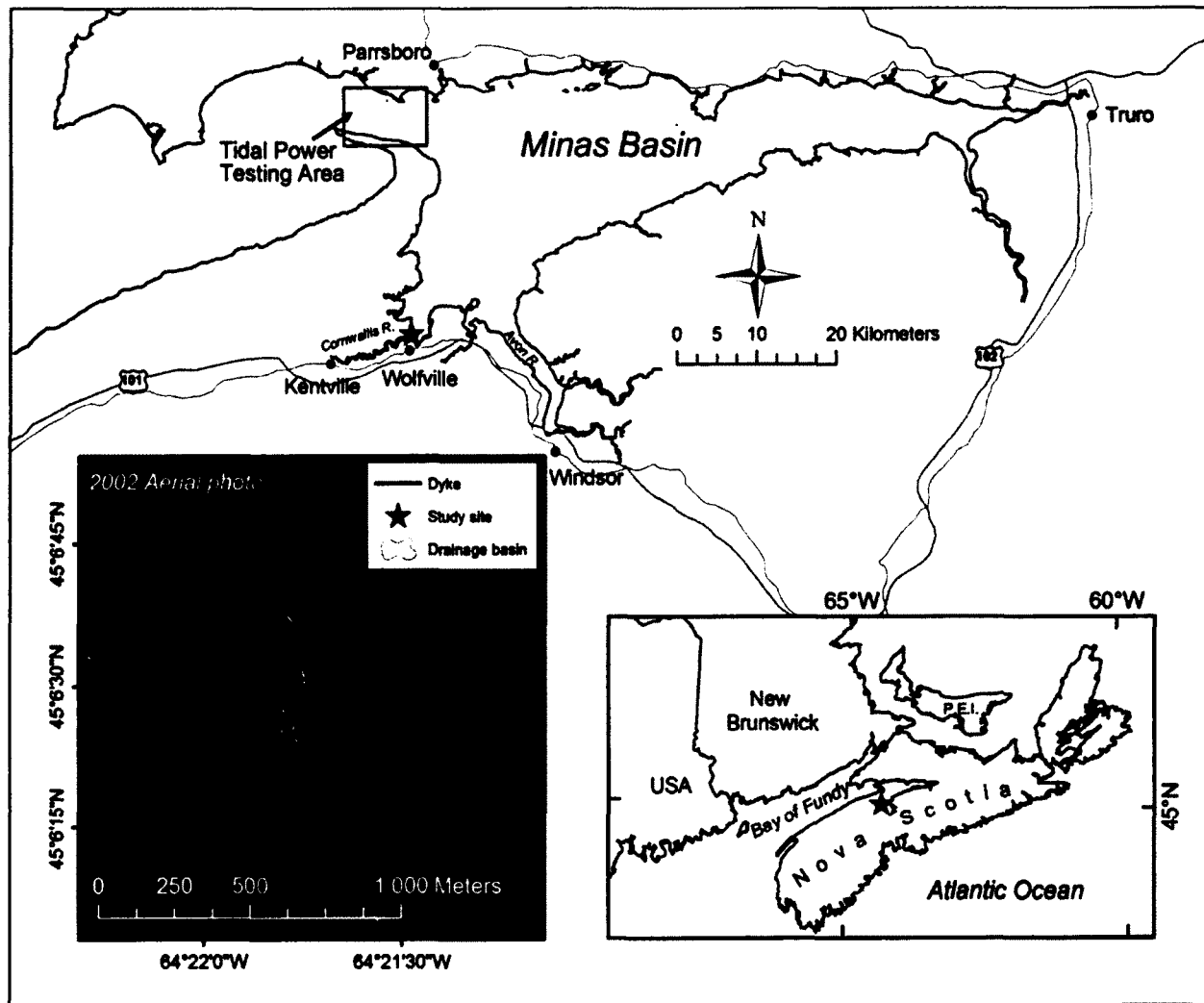
Figure 2.1: Study Area: Maritime Provinces (bottom right), the Minas Basin (large view, top), and Starrs Point marsh on the Cornwallis River (2002 air photo, bottom left). The study site is indicated by a star in each instance. The tidal power testing area in the Minas Passage is also indicated on the top layout (rectangle).

water depth over George's Bank. Scott and Greenberg (1983) report a 1-2% increase in tidal amplitude for every 1 meter of rising sea level. The Bay's 1400 km coastline is bound by sandstone and conglomerate cliffs which experience high rates of erosion, up to 1 $m \cdot a^{-1}$ in some areas. Bed scours of fine sediment introduce laminated silts and clays to suspension (Desplanque and Mossman, 2001; Amos 1987). High erosion rates correspond with typically high suspended sediment concentration (SSC) in the intertidal zone (van Proosdij *et al.*, 2000). Salt marshes in the region are minerogenic, and are typically dominated by *Spartina alterniflora* and *S. patens*.

The study site is a sheltered terminal creek at Starrs Point marsh, near the upper limit of the Minas Basin, at the mouth of the Cornwallis River (Figure 2.1). A headwater location was selected for investigation of subtle variations in tidal parameters that occur in a low-energy segment of the tidal environment, where high rates of sediment deposition are anticipated as channel banks receive sediment for eventual distribution over the marsh surface. Accessibility also played a considerable role in site selection. Mean grain size and the diameter of the 50th percentile (d50) of deposited sediment samples collected from the tidal creek are 6.2 and 6.1 μm, respectively. Salinity is relatively constant (~30 practical salinity units). The marsh surface is characterized by a mix of high marsh platforms (dominated by *Spartina patens*) and deeply incised creeks, with a dominance of *Spartina alterniflora* on the upper creek banks and in low marsh areas.

Elevations are reported relative to the Canadian Geographic Vertical Datum of 1928 (CGVD28), which is referenced from Mean Water Level (MWL) measurements made in 1928 at tide gauges across Canada. This is the most current standard for vertical datums in Canada. Bankfull elevations are variable from the east to west creek banks, ranging from ~4.2 - 4.8 meters above datum, respectively. Creek banks are gently sloping and partially vegetated (Figure 2.2). Tidal flows navigate more than one kilometer of main channel before reaching the study location. A deep, incised ditch (~1 meter width, > 1 meter depth) continues for several hundred meters beyond the creek head and through an area of densely-vegetated low marsh, parallel to an agricultural dike (most recent construction in 1955). The ditch is a former burrow pit that has been incorporated into the drainage network, as is common on Fundy marshes (MacDonald et al., 2010; Bowron et al., 2009; van Proosdij et al., 2010).

2.4 Methods

Current velocity and suspended sediment concentration data were collected with two instrument arrays mounted at different elevations in the tidal creek. Each array includes an acoustic Doppler velocimeter (ADV) (Vector, Nortek) and co-located optical backscatter sensor (OBS) (OBS3+, Campbell-Scientific) (Figure 2.3 and 2.4). Two measurement locations in the tidal creek where chosen to allow full characterization of creek flows, and to facilitate comparison between thalweg and above-bank locations. Instruments were positioned for measurement at 10 centimeters above the bed. Each
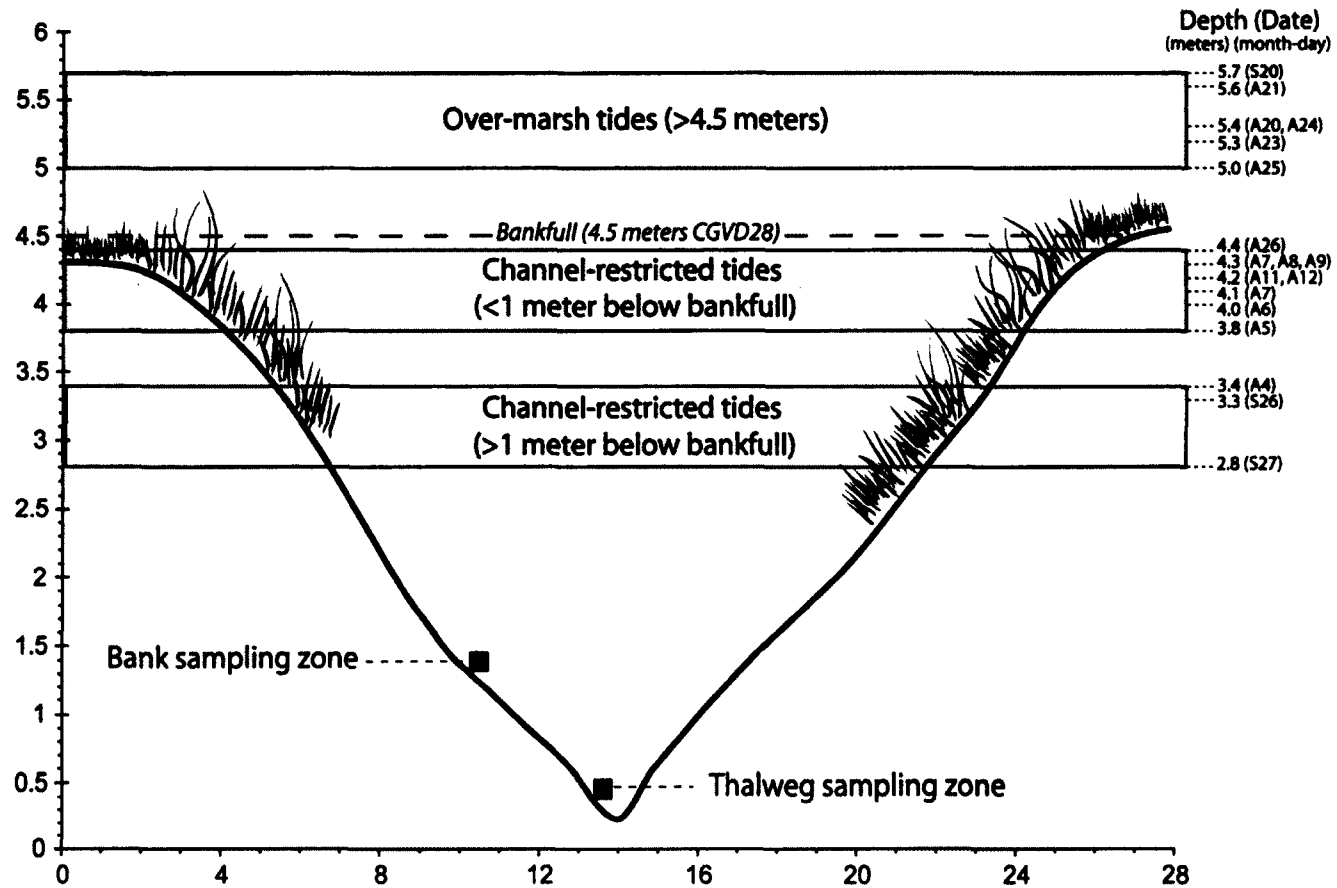
Figure 2.2: Tides were separated into two main groups: over-marsh and channel-restricted. Channel-restricted tides can also be separated into two categories, defined by their proximity to the bankfull level.
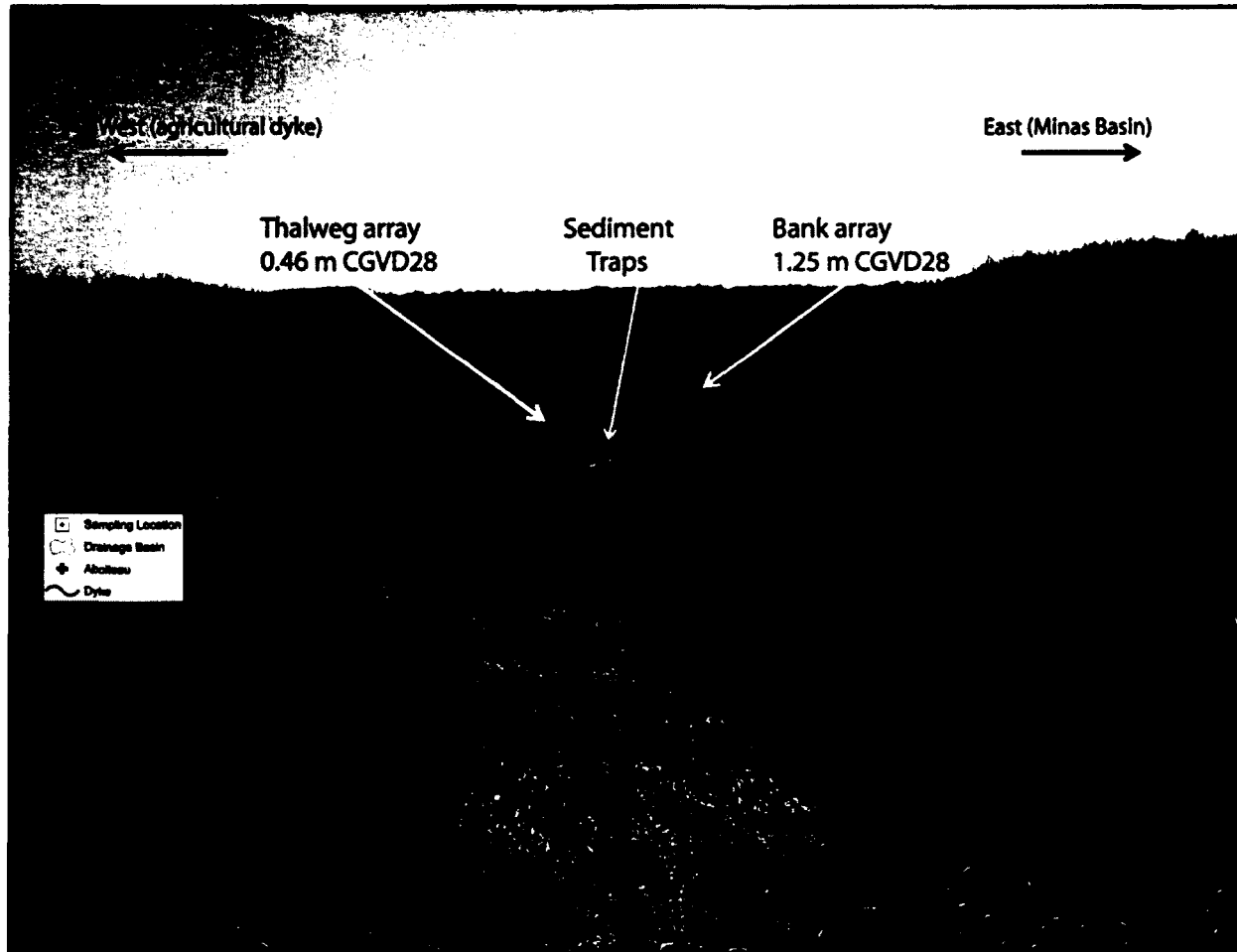
Figure 2.3: View looking down the tidal creek, from the creek head. The general instrument configuration in the creek is shown, along with elevations of thalweg (0.47 m) and bank (1.25 m) ADV/OBS arrays, in local datum (CGVD28). The location of sediment traps on the creek bank is also indicated. Note the person for vertical scale. Red arrows indicate flood tide direction.

OBS sensor was individually calibrated in the field (Puleo *et al.*, 2007; Hoitink and Hoekstra, 2005; Voulgaris and Meyers, 2004a). The thalweg array was placed above the creek thalweg (sampling volume at 0.47 m CGVD28), and sampled continuously at a rate of 16Hz. The bank array was located approximately 3 meters away from the thalweg on the eastern creek bank, sampling at an elevation of 1.25 m (CGVD28). This array sampled continuously at a lower rate (4Hz) to allow data collection over extended periods, and limit disturbance of the creek bank associated with repeated access to the sampling location by personnel. The hard thalweg was used to access the lower array to download data daily and make available memory space for further data collection.

Samples of deposited sediment were collected with surface-mounted sediment traps and pre-weighed filter papers (Whatman 5, 90 mm paper filters), based on the design by van Proosdij *et al.* (2006a, 2006b) (Figure 2.4). This trap design allows for resuspension of deposited materials within a tidal cycle and can be used to characterize net sediment deposition on non-vegetated creek banks and tidal flats. Four traps were deployed within an approximately 2 m^2 plot on the creek bank, with three filter papers in each trap, and were leveled using a spirit level. This study focuses on in-creek deposited sediment to enable full characterization of tides that remain confined to channels and do not flood the marsh surface. Traps were not deployed in rainy weather. Deposited samples were air dried for 24-48 hours before weighing to determine the total amount of sediment deposited on each paper, on each trap, and at each trap location over

Figure 2.4: Sediment traps are shown before (left) and following (right) inundation, in early August, 2009. Each tide was sampled using 4 traps, with three filters in each. Filter papers were recovered after individual tidal cycles.

the course of the study. The traps were not rinsed prior to analysis since minimal salt accumulated over individual tidal cycles. Salinity was measured with a RBR XR-420 logger positioned at the mouth of the study creek, and remained relatively constant over the experimental period. Statistical analyses on deposited sediment samples were completed using a nested ANOVA and standard two-sample t-tests (SYSTAT 13).

A detailed total station survey of the creek and surrounding marsh area was conducted in June 2009 with a Lecia TCR705 reflectorless total station. This was applied to create a high-resolution (0.25 meter) digital elevation model (DEM) of the creek and adjacent marsh surface. A profile located near the instrumentation arrays was interpolated to characterize the creek and develop cross-sectional areas at 10-centimeter increments. A regional, LiDAR-generated DEM (2 meter resolution) was applied for analysis and quantification of drainage basin geometry. Channel morphology can be quantified by the tidal asymmetry factor (γ), which considers changes in surface area as a function of water level to determine if a given channel has stronger flood or ebb currents, given by:

$$\gamma = \delta \frac{\Delta h}{\bar{h}} - \frac{\Delta b}{\bar{b}}$$

Equation (1)

where $\bar{h}$ and $\bar{b}$ represent average channel depth and embayment width, and Δh and Δb describe the amplitude of depth and width variation over a tidal cycle.

Flood or ebb dominance is demonstrated when $\gamma \geq$ or $\leq$ 0, respectively (Friedrichs and Perry, 2001; Blanton *et al.*, 2002).

A portable weather station (Campbell-Scientific) was installed at the study site to record meteorological parameters, including wind speed and direction, rainfall, temperature and atmospheric pressure. Hourly averaged records were collected for the duration of the study period. 'Webtide' (Dupont *et al.*, 2005) was used to develop a one-year record (15 minute intervals) of predicted tide elevations at Starr's Point. These were found to vary consistently by 0.5 – 1.0 metres less, compared with observed water levels, possibly representative of hydraulic friction in the channel. A correction was applied to reduce modeled tidal elevations by the mean variation between observed and predicted tidal elevations (0.92 meters).

Wave conditions during the sampling periods were investigated using raw pressure signals from the bank ADV, where consistently identified centimeter-scale ripples on the water surface reflect field observations. Instantaneous horizontal flow components (x, y) from ADV records were rotated into down-stream (u) and cross-stream (v) velocities following methods outlined by Roy *et al.* (1996) and Lane *et al.* (1998).

Mean current velocity and subsequent derived parameters were estimated through time-averaging over each measurement burst (5 minutes). Resolved horizontal velocity was computed as $\sqrt{u^2 + v^2}$. Instantaneous turbulent

components (u_t, v_t, w_t) were derived using the relationship $u = U + u_t$, and turbulence intensities (i_u, i_v, i_w) were calculated as the root mean square of turbulent components. Turbulent kinetic energy (TKE) $(J \cdot m^{-3})$ was calculated using:

$$TKE = \frac{1}{2} \rho \ (u_t{}^2 + v_t{}^2 + w_t{}^2)$$

<div align="right">Equation (2)</div>

where ρ is water density at 20°C $(\rho = 1025 \ kg \cdot m^{-3})$ (Neumier and Amos, 2006; Voulgaris and Meyers, 2004a). Mean kinetic energy $(\overline{KE})$ (J) in the tidal creek was estimated with:

$$\overline{KE} = a \ (\ ^1\!/_2 \ \rho \ u^2 \ )$$

<div align="right">Equation (3)</div>

where a is the channel cross-sectional area and u is upstream current velocity (Karsten et al., 2008). Friction velocity (u_*) was computed using the Reynolds stress method (Soulsby, 1983; Kim and Friedrichs, 2000):

$$u_* = (-\overline{u_t \, w_t})^{1/2}$$

<div align="right">Equation (4)</div>

where u_t and w_t are instantaneous components of down-stream and vertical velocity, respectively. Friction velocity can then be applied to calculate bed shear stress (τ_0) $(N \cdot m^{-2})$:

$$\tau_0 = \rho \ u_*{}^2$$

<div align="right">Equation (5)</div>

and bed shear velocity $(u_b \cdot)$ $(m \cdot s^{-1})$:

$$u_{b^*} = \frac{u_*(z)^2}{1-z/h}$$

<div align="right">Equation (6)</div>

where z is the measurement elevation above the sea bed, and h is the total local water depth in the channel (Barnes et al., 2009; Kim and Friedrichs, 2000; Biron et al., 2004; Voulgaris and Meyers, 2004a).

2.5   Results

A total of 17 tides were measured over 4 separate experiments during August and September of 2009 (Table 2.1). Time series of all data including mean water depth, current velocity, suspended sediment concentration, sediment deposition and environmental parameters are shown in Figure 2.5. Elevations of marsh topography and tidal amplitude are relative to CGVD28. The drainage basin of the studied creek has a total volume of approximately 9,800 m³ and a submerged area over 13,800 m² at the mean bankfull level (4.5 m). Equation (1) describes the study creek as flood dominant, which is typical for macrotidal channels with relatively high equilibrium marsh (Friedrichs and Perry, 2001). However, tides that exceeded the bankfull level showed notable ebb-dominance during initial ebb phases and as water depth in the creek fell below bankfull. A broad range of maximum tidal amplitudes (2.7 to 5.7 m) were considered for this study. Tides were categorized by water depth, into two groups: over-marsh tides (amplitude > 4.5 m & tidal prism > 9800 m³) and channel-restricted tides (amplitude < 4.5 meters & tidal prism < 9800 m³) (Figure 2.2). This division was based primarily on the visual appearance of these data when plotted as stage

curves Figure 2.6 (Allen, 2000). Over-marsh tides are therefore defined as those which fully inundate the high marsh surface, while channel-restricted tides do not surpass the general bankfull level and remain confined to the creek network.

A series of morphological stages controls flow as it enters the creek. The tidal bore at this location is slight, and initial flood velocities are low $(0.5 - 3 \text{ cm·s}^{-1})$. Tidal flow moves into the creek gradually and is detained at the creek head, while filling continues until water depth reaches ~2.0 meters above datum. Above this elevation, tidal flow is allowed access to the incised ditch which extends into the high marsh beyond the creek head, and a slight increase in flow velocity (up to 5 cm·s^{-1}) was found to occur at this stage. Above the bankfull level, over-marsh flows develop marked increases in velocity $(5 - 12 \text{ cm·s}^{-1})$ (Figure 2.6). Wave development during the sampling period was minor, where storm and non-storm conditions failed to produce waves greater than a few centimeters in height. Minor increases in flow velocity are seen during final ebb stages, associated with gravity-driven drainage of the marsh surface. Velocity measurements demonstrate that over-marsh tides (> 4.5 m) typically generate higher current velocities and greater estimates of TKE. The highest mean flow velocities (10 - 12 cm·s^{-1}) occurred during the early ebb stages of two over-marsh tides, while the marsh surface was well submerged (Figure 2.6). These enhanced flows may be linked to wind alignment with the channel at high tide. Other tides of comparable depth showed notably lower flow velocity during this stage.
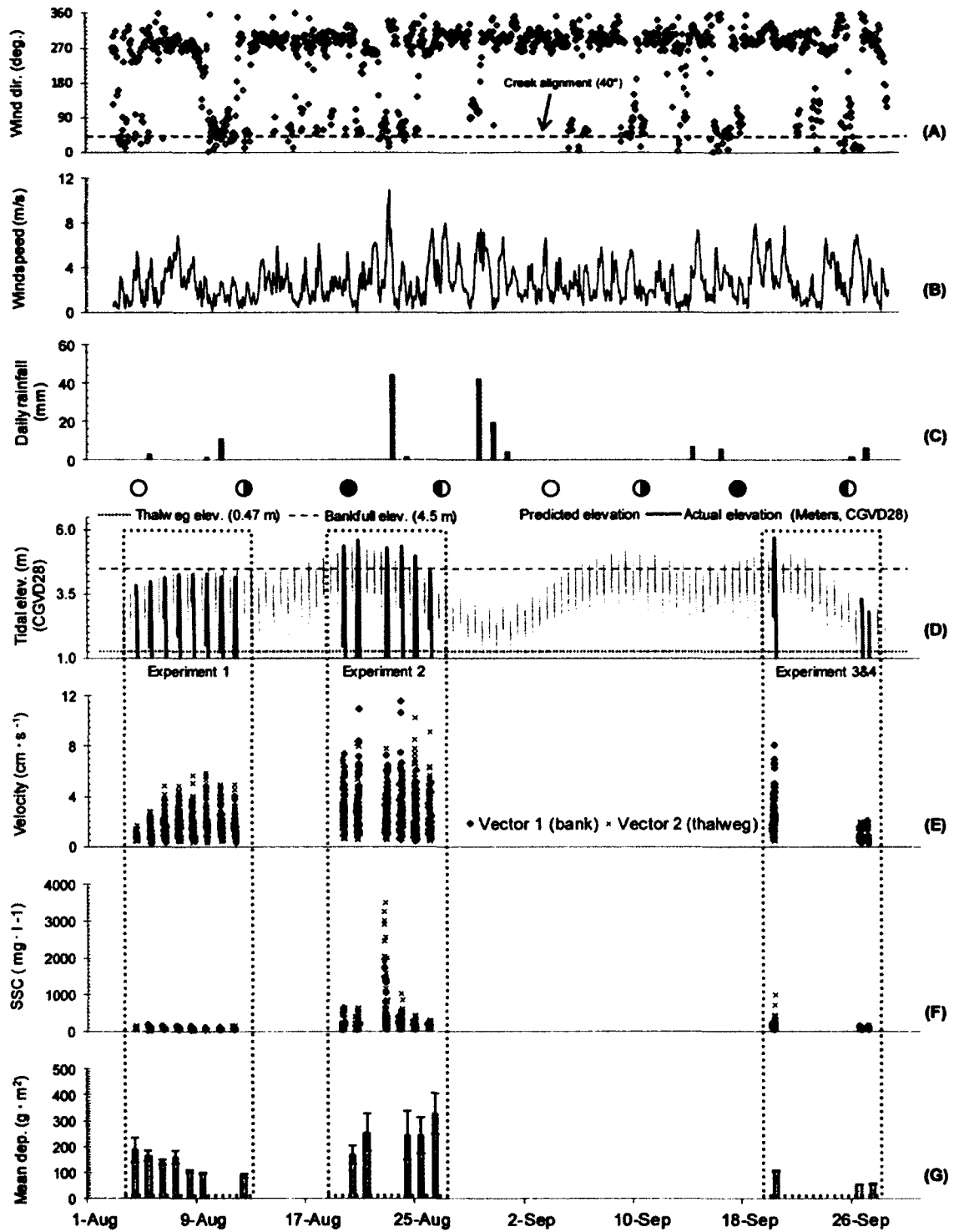
Figure 2.5: Full deployment time-series, showing weather conditions as measured on-site (A - C); predicted and corrected (WebTide, DFO) and actual water heights (ADV records) (D); measurements of current velocity (E) and suspended sediment concentration (F) from bank and thalweg measurement locations; finally, deposited sediment is shown (G), with standard error bars.

60

Tidal Conditions – Starr's Point 2009				Data Collected			
Date	Elevation (CGVD28) (m)		Over-marsh vs. Channel-restricted	Bank array ADV/OBS1	Thalweg array ADV/OBS2	Traps	Comments
	Predicted	Observed					
04-Aug-09	3.3	3.6	Channel-Restricted			✓	
05-Aug-09	3.5	3.8	Channel-Restricted		✓	✓	Thalweg array start (V2)
06-Aug-09	3.8	3.9	Channel-Restricted	✓	✓	✓	Bank array start (V1)
07-Aug-09	4.1	4.1	Channel-Restricted	✓	✓	✓	
08-Aug-09	4.3	4.2	Channel-Restricted	✓	✓	✓	
09-Aug-09	4.4	4.2	Channel-Restricted	✓	✓	✓	V2 error (late start)
10-Aug-09	4.5	4.2	Channel-Restricted	✓	✓		Rain: No traps.
11-Aug-09	4.3	4.1	Channel-Restricted	✓	✓		Rain: No traps.
12-Aug-09	4.5	4.1	Channel-Restricted	✓	✓	✓	
20-Aug-09	5.1	5.3	Over-Marsh	✓	✓	✓	
21-Aug-09	5.2	5.5	Over-Marsh	✓	✓	✓	
23-Aug-09	5.2	5.2	Over-Marsh	✓	✓		Hurricane Bill
24-Aug-09	5	5.3	Over-Marsh	✓	✓	✓	
25-Aug-09	4.7	4.9	Over-Marsh	✓	✓	✓	
26-Aug-09	4.3	4.4	Channel-Restricted	✓	✓	✓	
20-Sep-09	5.2	5.7	Over-Marsh	✓	✓	✓	
26-Sep-09	3.3	3.3	Channel-Restricted	✓	✓	✓	
27-Sep-09	2.7	2.7	Channel-Restricted	✓	✓	✓	

Table 2.1: Summary of tidal conditions and data collection at Starr's Point (2009). Predicted (Webtide, corrected) and observed (ADV records) high tide elevation is shown in meters (converted to CGVD28). Successful data collection is indicated by ✓.

Peak flood tide velocity (9 – 10 $cm \cdot s^{-1}$) on over-marsh tides occurred between 3.5 and 4.1 meters, just below the bankfull level, while the channel was full and at its widest and before flow spread over the marsh surface. Flow velocity decreased markedly above the bankfull level, and slack tide velocities (2 – 5 $cm \cdot s^{-1}$) persist until early ebb stages. Velocity typically increased as water depth fell below bankfull and flow became channelized, and reached typical peak ebb flows of 5 – 8 $cm \cdot s^{-1}$. The remainder of over-marsh tidal cycles was consistently characterized by velocity decreasing to low values (0.5 – 1.5 $cm \cdot s^{-1}$) and late ebb drainage, which was regularly measured at the thalweg position (Figure 2.6).

Channel-restricted tides displayed a strong tendency towards flood dominant velocity at both measurement locations. Velocity consistently increased with depth during flood stages, typically reaching peak velocities of 5 – 7 $cm \cdot s^{-1}$ just prior to high tide (Figure 2.6). The highest velocity associated with channel-restricted tides (9.1 $cm \cdot s^{-1}$) occurred at the thalweg position on August 26, associated with a peak water depth in the tidal creek of ~4.4 meters, which is near the bankfull level. Ebb stages of channel-restricted tides consistently generated the lowest velocities (0.1 - 2 $cm \cdot s^{-1}$) measured at this site, which remained nearly constant except for gravity-driven acceleration during final ebb. These slowly flowing ebb stages showed very low values (< 1) of velocity ($cm \cdot s^{-1}$), TKE ($J \cdot m^{-3}$), and KE (J), compared with the preceding flood stages.

A)

6.0

Bankfull region

Ebb tide

Flood tide

Bank sampling location (1.25 m CGVD28)

○ Over-Marsh

× Channel-Restricted

-12 -10 -8 -6 -4 -2 0 2 4 6 8 10 12

B)

6.0

Bankfull region

Ebb tide

Flood tide

Thalweg sampling location (0.47 m CGVD28)

-12 -10 -8 -6 -4 -2 0 2 4 6 8 10 12

Velocity (cm·s⁻¹)

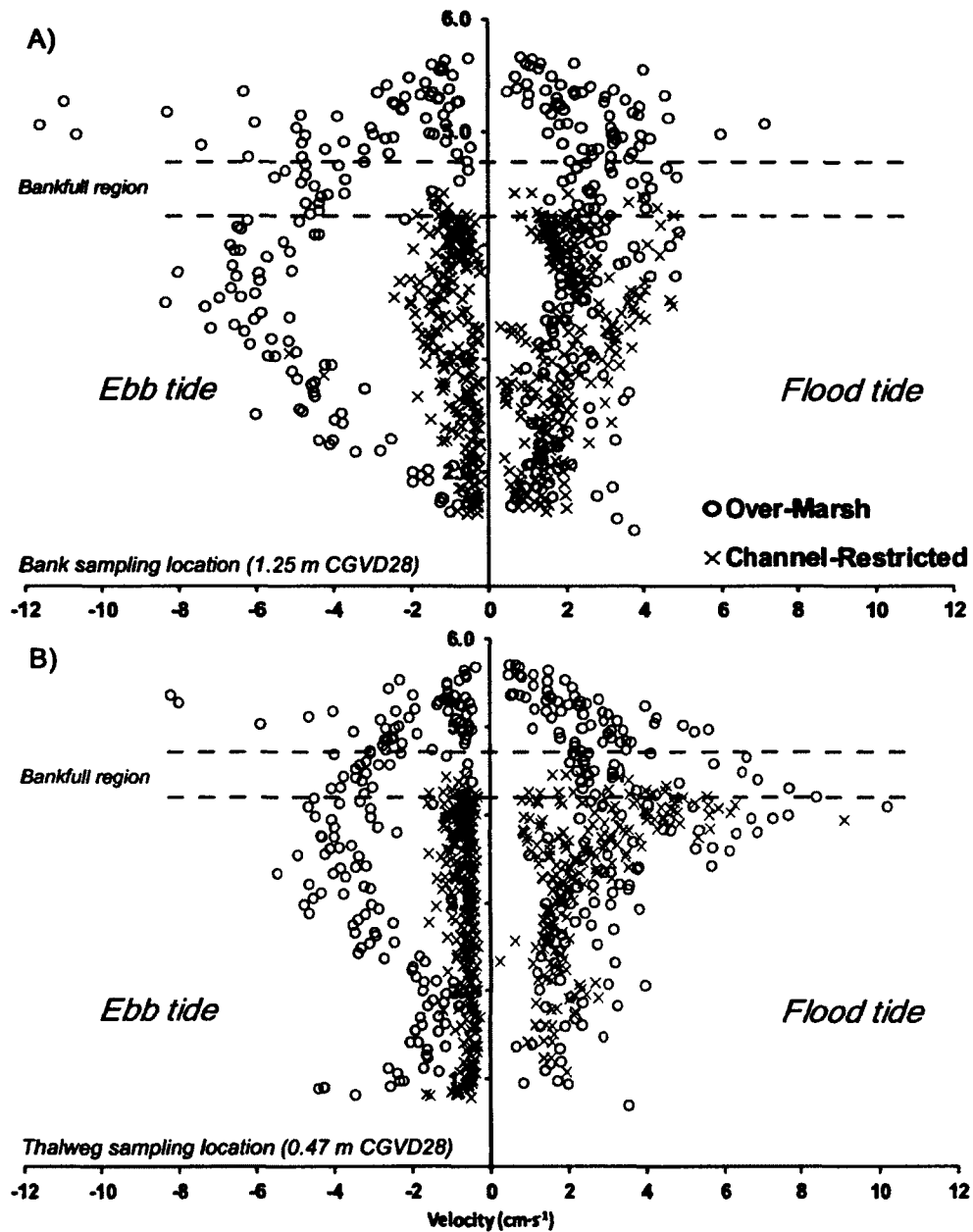*Figure 2.6: Stage-height relationships of current velocity in the tidal creek (5-minute mean ADV data). Over-marsh (black circles) and channel-restricted (red x's) tides are shown, as measured at both thalweg and bank positions: plot (a) show datas from the creek bank (1.25 m) while plot (b) shows thalweg data (0.47 m). Elevation of bankfull level and the thalweg are shown. All elevations are referenced in CGVD28.*

63

As with velocity, higher estimates of TKE are associated with greater tidal prism, resulting in generally ebb-dominant TKE during over-marsh tides. Increase in TKE around the bankfull level with rising flood tide is consistently observed, although peak values of TKE (up to 1.5 $j \cdot m^{-3}$) occurred during ebb stages of over-marsh tides, as flow is re-channelized and the marsh surface is emptied (Figure 2.7). Thalweg values of TKE are near-zero (0.01 – 0.1 $j \cdot m^{-3}$) for the majority of ebb-stage flow during channel-restricted tides, compared with slightly greater flood values (0.1 – 0.8 $j \cdot m^{-3}$). Kinetic energy (KE) in the tidal creek was slightly higher during flood stages of over-marsh tides, compared with similar stages of channel-restricted tides. Over-marsh ebb stages showed KE up to a magnitude greater than that noted during channel-restricted ebbs (Figure 2.11). Peak values of KE (90 – 118 J) are associated with tides that peaked near the bankfull level (e.g. Aug 25 & 26); maximum values occurred prior to high tide in these cases, and was seen to reduce dramatically with the onset of ebb tide. Early ebb phases of some over-marsh tides (e.g. Aug 21 & 24) showed high KE with water depth above bankfull (4.8 – 5.1 m). Estimates of bed shear stress (τ_0) (Figure 2.8) were higher for over-marsh tides (up to 0.4 $N \cdot m^{-2}$), and achieved maximum with water depth near the bankfull level before and after slack tide, and during ebb drainage below bankfull. Channel-restricted tides show low bed shear stresses (< 0.1 $N \cdot m^{-2}$) for the duration of tidal stages, although a marginal flood dominance can be identified, most notably during the August 26th tide, which peaked near the bankfull level (Figure 2.8).
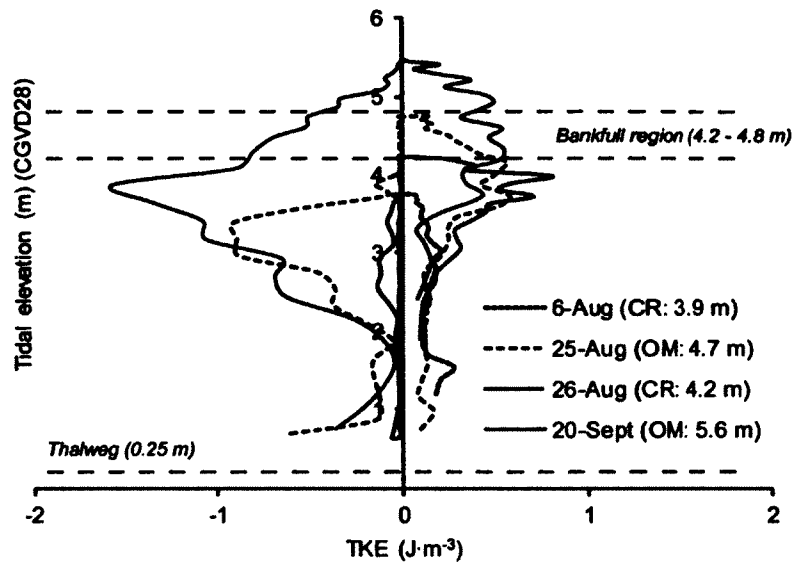
Figure 2.7: Select stage curves of 5 minute mean turbulent kinetic energy (TKE) values from the thalweg measurement location in the tidal creek.
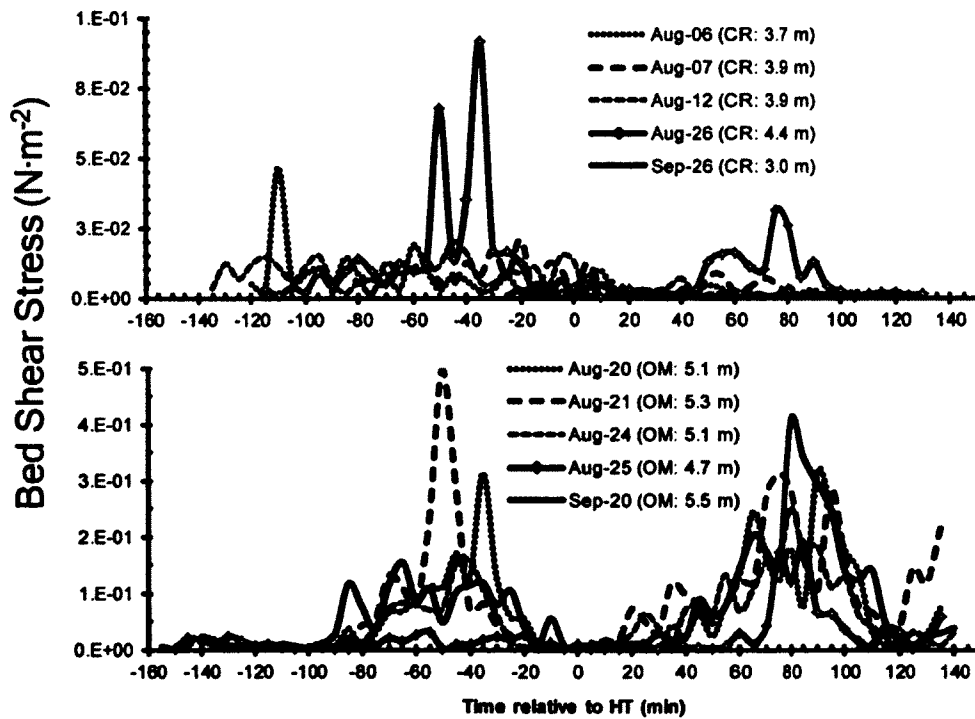

Figure 2.8: Estimates of bed shear stress from the thalweg ADV sampling location (0.47 m CGVD28). Channel-restricted tides are shown to have lower bed shear stress than over-marsh tides. Note the variation in Y-axis values.

65

Over-marsh tides were generally found to demonstrate similar incoming suspended sediment concentration (SSC) compared with channel-restricted tides (Figure 2.10). A broad range of concentration values were reported by OBS sensors (1 - 1000 mg·l^{-1}) in the tidal creek under non-storm conditions. Maximum initial suspended concentrations (2000 - 3000 mg·l^{-1}) were measured ahead of Hurricane Bill (Aug 23rd), in response to periods of rain that occurred prior to flood tide, increasing the potential for mobilization of exposed sediments on mudflats and creek banks. Regardless of varying maximum water depth, suspended concentration during flood phases of both channel-restricted and over-marsh tides is similar, showing a gradual reduction from moderate initial values (100 – 300 mg·l^{-1}) to a stabilized low concentration (~50 mg·l^{-1}). Stable concentrations around this level were noted at both thalweg and bank sampling locations, and persisted through high water and ebb stages on channel-restricted tides. Final ebbs of all tides were characterized by increasing concentration (up to 700 mg·l^{-1}); in many cases this is when peak per-tide concentrations occurred, associated with increased flow velocity via gravity-driven drainage. In addition, ebb phases of over-marsh tides brought about episodic, rapid increases to high concentration (600 – 1000 mg·l^{-1}) at only the thalweg location. Such increases occurred much earlier during ebbs than the final stages, and are linked to brief periods of flow acceleration with depth near the bankfull level. These rapid increases in concentration were not measured by the
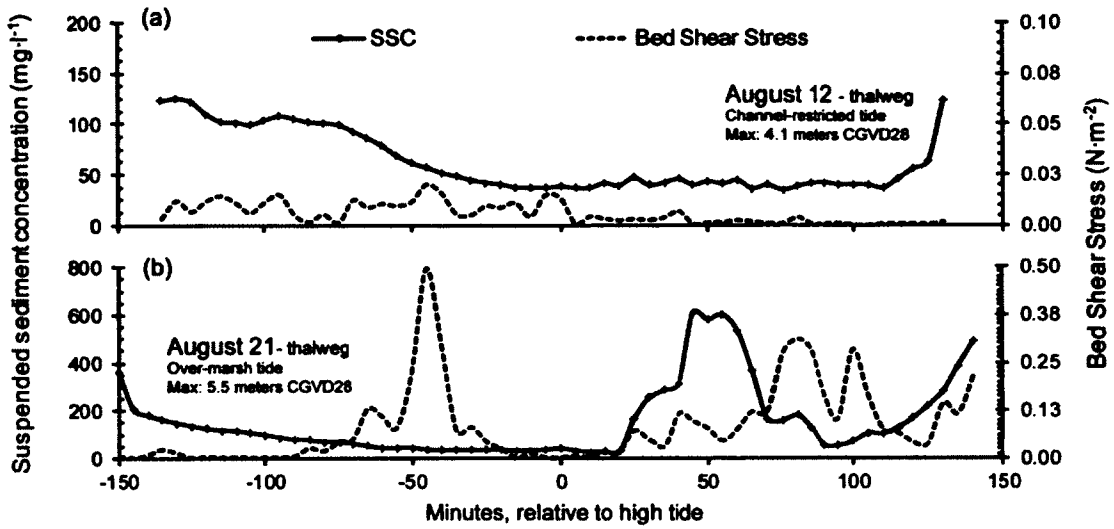
Figure 2.9: Representative time-series of channel-restricted (August 12) and over-marsh (August 21) tides. Note variability in Y-axis values.
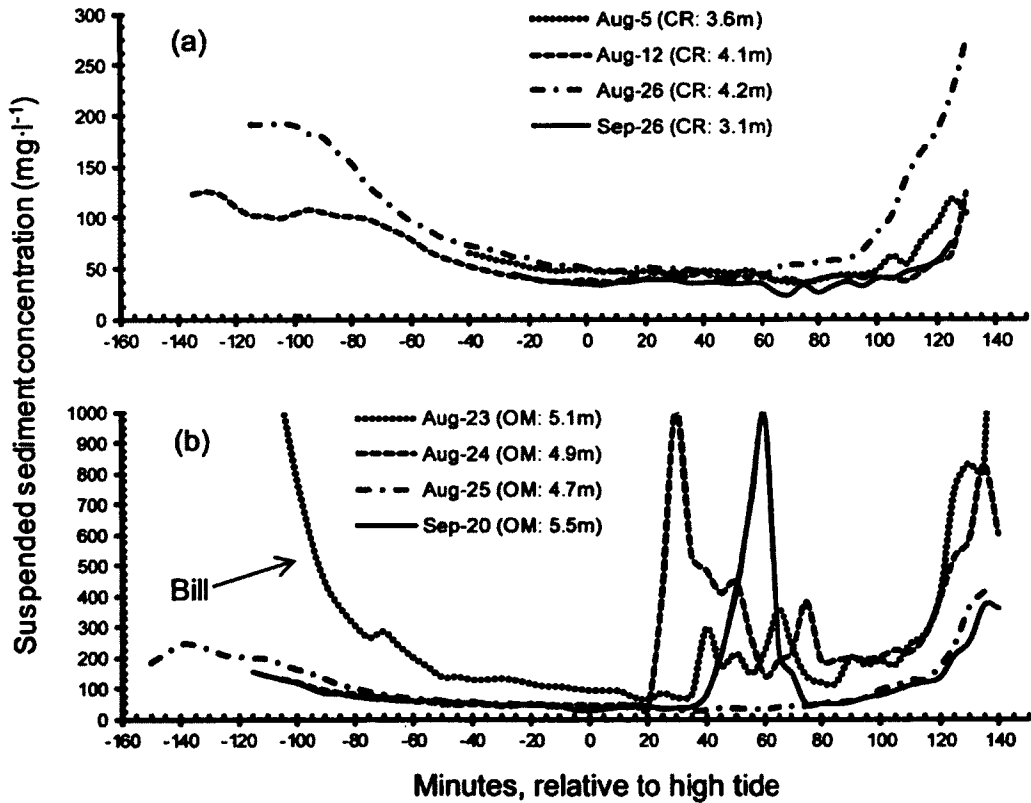
Figure 2.10: Time-series of thalweg SSC for (a) a series of channel-restricted tides and (b) a series of over-marsh tides. Impacts on the August 23 flood tide are credited to the passage of Hurricane Bill.

67

bank array. The maximum suspended sediment concentration measured during the study period occurred in close proximity to the passing of Hurricane Bill on August 23. At the thalweg, initial SSC was ~3500 mg·l^{-1}, and reached 2000 mg·l^{-1} during late ebb stages. Along with these high flood and ebb values, the stabilized, high water concentration (~100 mg·l^{-1}) was twice that of tides with similar depth and under non-storm conditions (~50 mg·l^{-1}). Moderate storm conditions were measured at the study site associated with Bill, including an average wind speed of 15 m/s, and 40 millimeters of rain over a 5 hour period, ending just before high tide.

The general relationship interpreted from samples of deposited sediment is that over-marsh tides introduce more material to the creek banks through deposition (Figure 2.11). However, a wide range of variability exists here. The lowest deposition (55.02 g·m^{-2}) was measured on a channel-restricted tide (Sept 26), and the highest (328.19 g·m^{-2}) on another channel-restricted tide (August 26). However, statistical analysis using nested ANOVA and standard two-sample t-test showed that the difference in deposition for over-marsh versus channel-restricted tides was not statistically significant. However, the result is different with inclusion of the August 26th tide (which peaked near the bankfull level and partially flooded low-marsh areas) in the over-marsh category: the result of this analysis yields a statistically significant difference (p-value of 0.05, 95% confidence) between deposition resulting from over-marsh and channel-restricted groups. Variability across the sampling zone (between the 4 traps) was
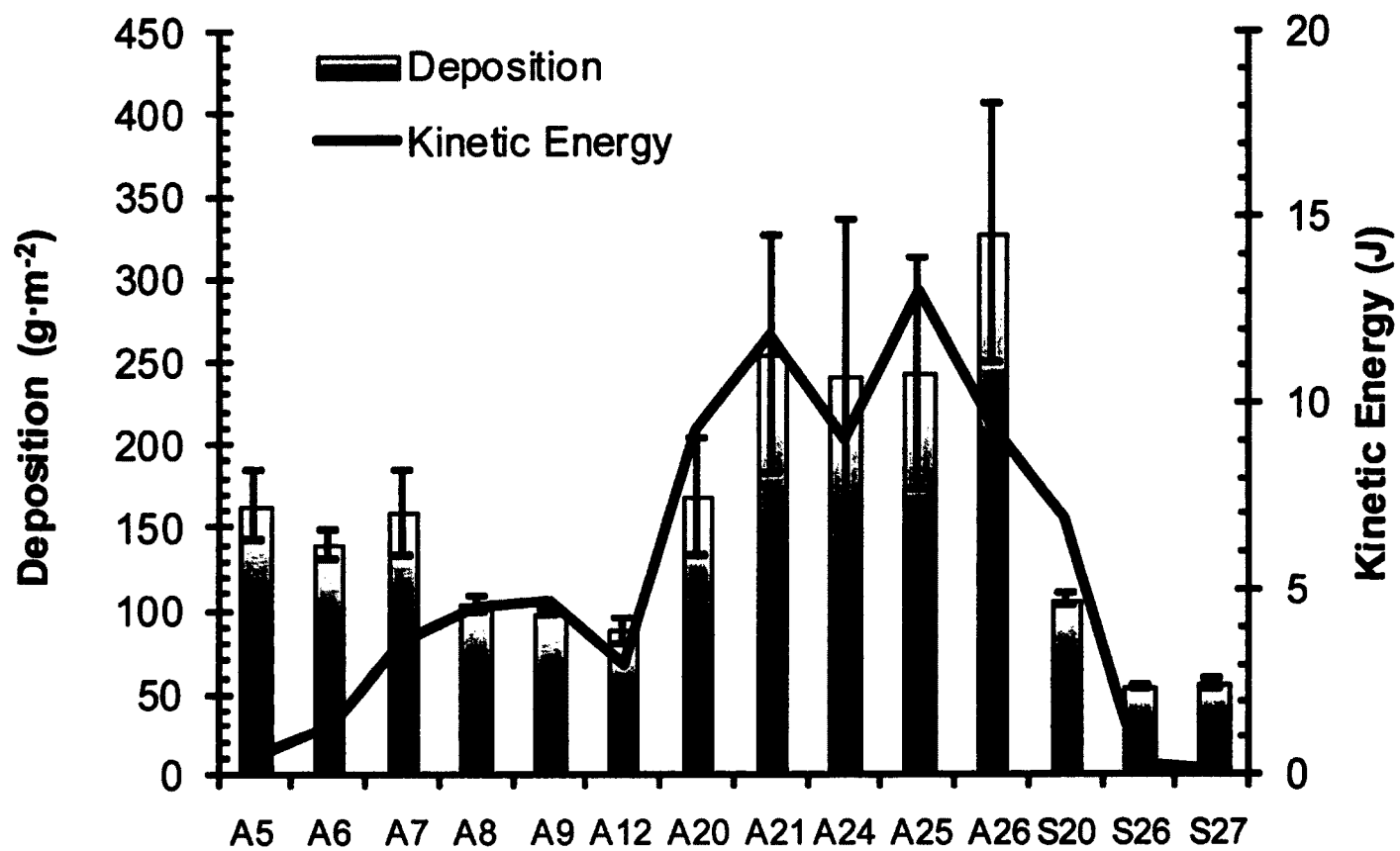
Figure 2.11: Mean deposition, with standard error bars, and kinetic energy per tide. Increased variability in deposited samples across the sampling zone is accompanied by an increase in kinetic energy.

maximized on over-marsh tides (e.g. with increasing kinetic energy), and variability was notably lower following channel-restricted tidal cycles. This suggests that with decreased tidal energy, net sediment deposition is more consistent over the sampling location, contrasting the large variability following over-marsh tides, which show increased energy (Figure 2.11).

2.6 Discussion

Intertidal sedimentation is a complex balance of variables controlling sediment availability and the opportunity for deposition (van Proosdij et al., 2006a). Macrotidal embayments tend to have high equilibrium marsh and flood-dominant channels, and generally transport more sediment landward through deep tidal creeks compared with smaller tidal ranges (Friedrichs and Perry, 2001). At the studied location, deposition shows high variability linked to incoming SSC and topographic influences on local flow dynamics. This reflects the results of Torres and Styles (2007), which identifies topography as a first-order control on in-channel currents. Due to the large tidal range in the Bay of Fundy, complete submergence of high marsh surfaces (e.g. beyond the limits of the drainage basin) can promote marginal ebb-dominance of currents in tidal creeks, due to rapid drainage and basin-scale influences. Equation (1) describes the study creek as flood dominant, although over-marsh tides showed marked phases of ebb-dominance following high water and with gravity-driven drainage of the marsh surface during mid-ebb stages. Blanton et al. (2002) point out that this equation was developed for lagoonal systems where there is no influence of

freshwater discharge on tidal currents. As this does not apply to the studied system, the results of Equation (1) were used only as a preliminary indicator of flood versus ebb dominance for channel-restricted flows. Atmospheric pressure measured at the study site remained relatively constant during sampling (1010 – 1025 millibars). Variations in atmospheric pressure are not thought to impact flow and sediment dynamics discussed here.

With inundation of the marsh surface, a component of incoming suspended sediment that passes through the creek can be expected to deposit on the marsh (Reed, 1988). Deposition in tidal creeks cannot be extrapolated to deduce marsh sedimentation; however, the relative availability of sediment in the tidal creek can be viewed as a controlling factor for deposition on the marsh surface. In this way, sediment dynamics in the tidal creek can be applied to infer the relative depositional capacity of both channel-restricted and over-marsh tides.

Over-marsh tides appear distinctly different compared with channel-restricted tides on stage-curve plots, due to the utilization and drainage of storage space on the marsh surface that is associated with tides of sufficient depth (>4.5 meters). Peak flood and ebb currents at this site were found to develop shortly before or after slack tide, where high marsh flooded and drained in close proximity to high water; this reflects the results of other studies (e.g. Blanton *et al.*, 2002; Friedrichs and Perry, 2001; Dronkers, 1986). Over-marsh tides generally show greater suspended sediment concentration and deposition in the tidal creek, demonstrating increased sediment availability compared with

71

tides that are restricted to channels. Currents associated with over-marsh tides were primarily ebb-dominant, due to topographic forcing through drainage of the marsh surface, influencing net deposition on creek banks.

Tides which inundate the marsh surface have been found to generate faster and more turbulent ebb phases, in response to a greater tidal prism (Friedrichs and Perry, 2001; Allen, 2000; French and Stoddart, 1992). This is consistent with results presented here, where channel-restricted tides are distinctly flood-dominant and show ebb phases that are calm (< 2 cm·s⁻¹), compared with those of over-marsh tides (3 - 6 cm·s⁻¹). Enhanced ebb stage velocity of over-marsh tides is linked to drainage of the marsh surface; the magnitude of enhanced ebb currents is in turn linked to the maximum depth on the marsh. With submergence of the marsh surface beyond the limits of individual drainage basins, flow becomes unconfined and the potential for higher ebb-stage flow is increased. There is also the potential for basin-scale or wind influence on flow velocity, with sufficient depth (up to 1 meter) above the marsh surface (Davidson-Arnott *et al.*, 2002). Over-marsh tides on Aug 21ˢᵗ and 24ᵗʰ showed increased flow velocity during early ebb stages, with water depths above the bankfull level (Figures 2.6 & 2.7). Wind conditions were moderate (~3 m·s⁻¹) near high tide on both days. Wind directions (50 - 60° relative to magnetic North) were well-aligned with the general direction of the flood tide. This pushed water to the back of the marsh at high tide, which resulted in more water being moved

back through the creek, and generated enhanced flow velocity with the onset of ebb tides.

A unique flow situation was found to develop with tides that peaked close to the bankfull level (e.g. Aug 25th, 5 m; Aug 26th, 4.5 m). These tides showed the highest flood velocities (9 – 10 $cm \cdot s^{-1}$); had relatively high incoming suspended sediment concentration at the thalweg (> 200 $mg \cdot l^{-1}$); and were associated with high deposition in the tidal creek (> 200 $g \cdot m^{-3}$). While both tides had typical flood and slack tide velocities, the ebb phase of Aug 25th is unique. The early ebb acceleration noted on other over-marsh tides as water depth approached the bankfull level is absent, while the typical secondary increase in flow velocity just below bankfull is maintained. According to Boon (1975), such tidal discharge asymmetries develop as a consequence of drainage basin morphology and storage characteristics, in conjunction with prevailing tidal range and stage. This suggests that only partial submergence of the marsh surface (~ 20 cm depth) results in a flow situation in the tidal creek that differs from deeper tides, most notably during early ebb phases. In contrast, Aug 26th was channel-restricted and showed distinct flood-dominant velocity (up to 9 $cm \cdot s^{-1}$), 50% faster than flood stages of other channel-restricted tides. However, with no drainage input from the marsh surface, the corresponding ebb flows were of low magnitude, and were comparable with other channel-restricted tides.

The flow conditions on Aug 25th demonstrate the influence of marsh surface storage, and subsequent drainage, on flow magnitude deep in the tidal

creek. This also implies an approximate threshold for development of early ebb-stage flow acceleration. Submergence of the marsh surface must be complete (e.g. beyond the limits of drainage basins) to generate consistently increasing velocity with decreasing depth during ebb stages. Variability in ebb stage flow magnitude may impact net deposition on creek banks, through differential resuspension or erosion of bank material associated with varying levels of bed shear stress (Figures 2.6 & 2.7). Given that incoming tidal conditions (e.g. concentration) for tidal cycles on Aug 25th and 26th were very similar, the absence of increased flow velocity during ebb stages on the lower tide may have encouraged the notably higher net deposition (328.19 g·m^3), compared with Aug 25th (254.36 g·m^3). The distribution of bed shear stress (τ_0) seems to support this, where Aug 26th shows relatively low τ_0 (0.002 – 0.9 N·m^{-2}) and general flood-ebb symmetry. This compares with higher τ_0 (> 0.4 N·m^{-2}) on over-marsh tides (e.g. Aug 25th), which show dominant ebb currents that are more capable of resuspension and transport of material back out of the creek (Figures 2.7 & 2.8). Alternatively, variation in deposition between Aug 25th and 26th could represent the component of incoming material that settled on the marsh surface on Aug 25th, but was confined to the channel on the bankfull Aug 26th tide.

Initial suspended sediment concentration in the tidal creek, under storm and non-storm conditions, represents sediment laden water moving up the channel with the onset of tidal cycles. Material may be brought from offshore or sourced from tidal flats and imported to the marsh system. Maximum initial

74

suspended concentrations (2000 - 3000 mg·l⁻¹) were measured ahead of Hurricane Bill (Aug 23rd) at both sampling locations in the creek. Periods of rain occurred in the region prior to the rising tide, which impacted exposed sediments on mudflats and creek banks. The resulting high concentrations measured in the tidal creek demonstrate well the response to intense rainfall on exposed tidal flats and creek banks, as noted by others, where sediment mobilization is significantly increased (Schostak et al., 2000; Murphy and Voulgaris, 2006; Mwamba and Torres, 2002 Voulgaris and Meyers, 2004b).

Suspended sediment dynamics during flood phases under non-storm conditions consistently showed a gradual reduction from initial concentrations (100 – 300 mg·l⁻¹) and achieved stabilized levels (20 – 50 mg·l⁻¹) that persisted until high tide. This suggests continuous deposition during this portion of all tidal cycles (van Proosdij et al., 2006a; 2006b). Final ebb phases saw concentrations increase back to levels typically comparable with initial floods, in response to gravity-driven drainage and ebb stage transport of fine particles which maintained suspension throughout tidal cycles (Reed, 1988). Results from both thalweg and bank sampling locations reflect this pattern. However, over-marsh tides which exceeded the limits of drainage basins repeatedly generated early ebb-phase peaks to high concentrations (up to 1000 mg·l⁻¹), at the thalweg location only. These peaks are timed with brief periods of increased velocity and TKE following high tide, with depth near or above the bankfull level, and are thought to represent remobilized material being transported at the thalweg. It should be

75

noted that this pattern is observed on all but one of the over-marsh tides measured (e.g. Aug 25th), which was the lowest tide of the over-marsh group. This agrees with the aforementioned depth threshold above the marsh surface for generation of early ebb velocity increases, which impacts suspended concentration in the creek.

Scatter plots relating suspended concentration to tidal elevation and ebb-stage velocity (Figure 2.12) show that increasing concentration in the tidal creek is associated with greater tide height and stronger ebb flows. Over-marsh tides are generally more energetic (Figure 2.11) and have more turbulent ebb phases (Figure 2.8). However, the maximum deposition was associated with a tidal cycle that peaked at the bankfull level and showed pronounced flood-dominance (Aug 26th, Figure 2.6). Due to the distinct velocity asymmetry in favour of flood-dominance, it would appear that the large amount of material deposited on Aug 26th was not subject to any resuspension or erosion by enhanced ebb flows. This tide showed a capacity for a high sediment load, similar to over-marsh tides, and encouraged high net sediment deposition with calm ebb stages that allowed deposition to persist over an extended period. Although it is not clear where the deposited materials originated from, high initial SSC values indicate that the majority of material was imported to the study portion of the creek during flood stages, rather than being sourced from the immediate surroundings, in the form of bank erosion, slumping or sediment-rich flow down creek banks. The range of deposition measured at this site is up to 4 times greater than estimates of marsh
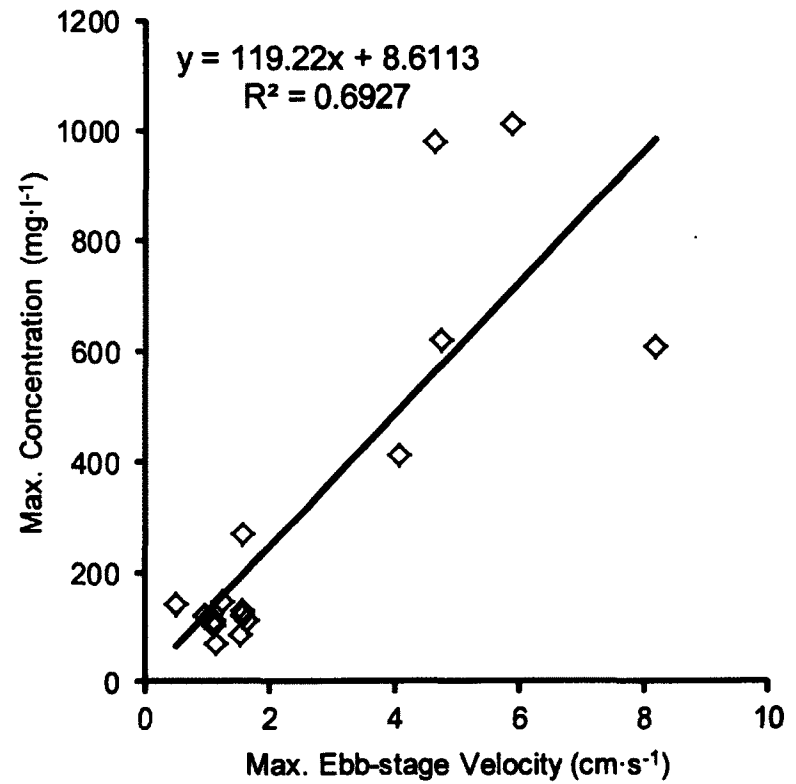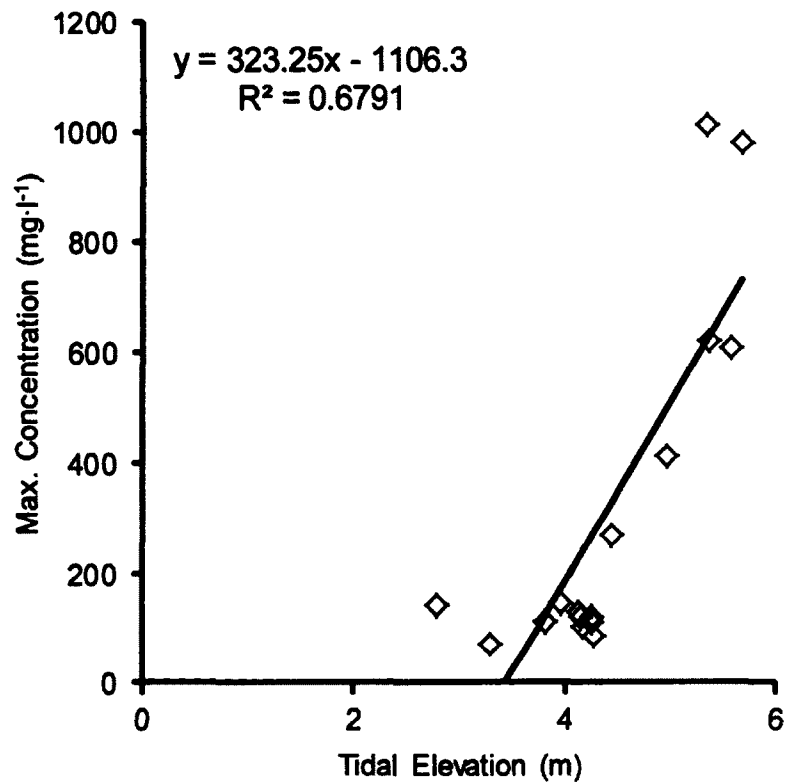
Figure 2.12: Scatterplots relating maximum tidal elevation (m) and maximum ebb-stage velocity (cm·s⁻¹) to maximum suspended sediment concentration (mg·l⁻¹)

surface deposition developed for other Bay of Fundy sites (e.g. van Proosdij *et al.*, 2006a; Davidson-Arnott *et al.*, 2002), which used a similar sediment trapping method and reported values up to 75 g·m^{-2}.

The 3-way inundation classification of tides cycles originally proposed by Bayliss-Smith (1979) included a group of tides termed 'marshfull', which peaked near or at the bankfull level and showed velocity peaks shortly before or after high tide. This division was later simplified into a two-way division to differentiate between tides that are confined to creeks and show little to no velocity asymmetry, and those that inundate the marsh surface and generate flow asymmetry (French and Stoddart, 1992). The results of this study suggest that tides which would represent the marshfull category may behave differently than either channel-restricted or over-marsh tides. Results from Reed (1988), which also describe macrotidal conditions, show peak net sediment flux associated with a bankfull tide; as waves break on the marsh edge, sediment is mobilized, but is not moved from the creek system to the marsh. The marsh edge contributes to suspended concentration in the creek in this way, and is most effective when slack tide depth is at the bankfull level. The significance of tides that peak at the marsh edge is reinforced by the lower limit threshold (depth ~0.6 m above levees) proposed by Torres and Styles (2007) for development of flow reversals in tidal creeks. The current study suggests that tides which peak around the bankfull level show reduced early ebb stage turbulence and flow velocity, and encourage an extended depositional period. In essence, strong flood

dominance, maximum depth near the bankfull level, and the associated mobility of suspended material promotes sediment availability, while enhanced slack tide duration associated with calm ebb stages provides ample opportunity for particle settling. The result is maximum potential deposition in the tidal creek. While this explanation is limited in scope as it is based on only one tidal cycle, this response to bankfull tides may be of high importance in hypertidal regions like the Bay of Fundy, where the tide range is high and marshes have a relatively high equilibrium surface.

At the studied location, a 5% reduction in tidal amplitude would reduce the number of over-marsh tides by a similar figure, and cause an increase in the occurrence of channel-restricted tides. The frequency of marshfull tides can potentially increase as well, in which case amplified erosion of marsh edges may create an additional sediment source. Decreased inundation frequency of high marsh surfaces may impose a sediment deficit in marsh systems, as less material is distributed to the marsh surface from tidal creeks. This can show impacts in marsh sedimentation and resulting elevation, channel equilibrium, vegetation community structure, and ecological productivity (Smith and Friedrichs, 2011; Craft et al., 2009; Bertness, 1991).

Decreased ebb-flow magnitude is likely to be associated with decreased tidal amplitude, due to less water being put into storage on the marsh surface, as well as less frequent inundation events. Lower magnitude ebb flows may show

less capacity for sedimentary work, reducing sediment mobility during ebb phases. The result may be creek infilling and a reduction in bank steepness, which would most likely have continued impacts on creek hydrodynamics and sediment transport. Reduced bank steepness may further accelerate creek infilling, through reduction of in-channel currents, such as ebb-phase, gravity-driven drainage of marsh surfaces, which mediate bank elevations through ebb-stage resuspension of newly introduced materials (Reed, 1988). A continuation and exacerbation of this cycle would constitute a non-linear response of fine-grained materials in tidal creeks, and would impact the movement of water in and out of the estuary through changes in deposition and erosion patterns, and the resulting basin geometry. Either a circumstance of decreased sediment supply to the marsh surface, or an increase in in-channel sedimentation, may impact the form and function of salt marshes. It has been shown that changes to balanced sediment budgets will show the greatest impact in accretion rates on low marsh surfaces (Chmura *et al.*, 2001).

2.7 Conclusions

Variability of current velocity, kinetic energy and bed shear stress in the tidal creek during flood stages of all tides was limited below the bankfull level. This suggests that the measured variation in these parameters over the studied tides is primarily linked to local topographic forcing, rather than notable variations in incoming tidal energy. Deposition in the creek generally increased with depth, along with the strength of ebb stage currents, which impacts net deposition

through resuspension of newly introduced material. The results presented here demonstrate a wide range of variability in net sediment deposition, which can be understood through links to suspended sediment concentration and topographic influences on flow dynamics in the tidal creek. The relative availability of sediment in the creek can be viewed as a controlling factor for deposition on the marsh surface, which can be applied to infer the relative depositional capacity of both channel-restricted and over-marsh tides. Over-marsh tides utilize and drain large amounts of storage space on the marsh surface, and associated currents are primarily ebb-dominant, in spite of flood-dominant channel geometry. Failure to occupy the marsh surface storage volume, as in the case of channel-restricted tides, results in calm ebb stages and prolonged periods suitable for deposition. Our results show that tides which peak near the bankfull level show reduced early ebb stage turbulence and flow velocity, and encourage such an extended depositional period. When this situation is combined with a high incoming suspended concentration, high levels of deposition occur.

The dynamics of marshfull tides (which peak at or near the bankfull level) in a hypertidal environment such as the Bay of Fundy may be responsible for the maximum sediment deposition in tidal creeks, providing large amounts of material that is eventually distributed to and deposited on marsh surfaces. High over-marsh tides (beyond limit of drainage basin) remove newly introduced material through bank erosion and resuspension during enhanced ebb flows, while channel-restricted tides typically import lesser amounts of material. The

81

resulting geomorphic workload is generally skewed towards marshfull tides for

net sediment import, and over-marsh tides for distribution of materials sourced

from creek banks onto the marsh surface. Further work to investigate the

sedimentary response to changing energy in salt marshes should consider

variation in flocculation processes, and expand to include exposed marsh

margins, where the potential for dissipation of tidal energy is high.

References

Allen JRL. 2000. Morphodynamics of Holocene salt marshes: a review sketch from the Atlantic and Southern North Sea Coasts of Europe. *Quarternary Science Reviews* **19**: 1155-1231.

Allen JRL, Pye K. 1992. Coastal saltmarshes: Their nature and importance. In *Saltmarshes: Morphodynamics, conservation and engineering significance*. Cambridge University Press: Cambridge; 1-19.

Amos C. 1987. Fine-grained sediment transport in Chignecto Bay, Bay of Fundy, Canada. *Continental Shelf Research* **7** (11/12): 1295-1300.

Amos CL, Mosher DC. 1985. Erosion and deposition of fine-grained sediments from the Bay of Fundy. *Sedimentology* **32**: 815-832.

Barnes, MP, O'Donoghue T, Alsina JM, Baldock TE. 2009. Direct bed shear stress measurements in a bore-driven swash. *Coastal Engineering* **56**: 853-867. DOI: 10.1016/j.coastaleng.2009.04.004

Bayliss-Smith TP, Healey R, Lailey R, Spencer T, Stoddart DR. 1979. Tidal flows in salt marsh creeks. *Estuarine and Coastal Marine Science* **9** (3): 235-255. DOI: 10.1016/0302-3524(79)90038-0.

Bertness MD. 1991. Zonation of Spartina Patens and Spartina Alterniflora in a New England salt marsh. *Ecology* **72** (1): 138-148.

Biron PM, Robson C, Lapointe MF, Gaskin SJ. 2004. Comparing different methods of bed shear stress estimates in simple and complex flow fields. *Earth Surface Processes and Landforms* **29**: 1403-1415. DOI: 10.1002/esp.1111

Blanton JO, Lin G, Elston SA. 2002. Tidal current asymmetry in shallow estuaries and tidal creeks. *Continental Shelf Research* **22**: 1731-1743.

Boon, JD III. 1975. Tidal Discharge Asymmetry in a salt marsh drainage system. *Limnology and Oceanography* **20** (1): 71-80.

Boorman, 1999. Salt marshes – present functioning and future change. *Mangroves and Salt Marshes* **3**: 227-241.

Bowron T, Neatt N, van Proosdij D, Lundholm J, Graham J. 2009. Macro-tidal salt marsh ecosystem response to culvert expansion. *Restoration Ecology* **19** (3): 307-322. DOI: 10.1111/j.1526-100X.2009.00602.x

Bryden IG, Grinsted T, Melville GT. 2004. Assessing the potential of a simple channel to deliver useful energy. *Applied Ocean Research* **26**: 198-204. doi:10.1016/j.apor. 2005.04.001
Christiansen T, Wilberg PL, Milligan TG. 2000. Flow and sediment transport on a tidal salt marsh surface. *Estuarine, Coastal and Shelf Science* **50**: 315-331. DOI: 10.1006/ecss.2000.0548

Cartwright, DE. 1997. Some thoughts on the spring-neap cycle of tidal dissipation. *Progress in Oceanography* **40**: 125-133.

Charlier, RH. 2003. A "sleeper" awakes: tidal current power. *Renewable and Sustainable Energy Reviews* **7**: 515-529.

Chmura G, Coffey A, Crago, R. 2001. Variation in surface sediment deposition on salt marshes in the Bay of Fundy. *Journal of Coastal Research* **17** (1): 221-227.

Craft C, Clough J, Ehman J, Joye S, Park R, Pennsings S, Guo H, Machmuller M. 2009. Forecasting the effects of accelerated sea-level rise on tidal marsh ecosystem services. *Frontiers in Ecology and the Environment* **7**(2): 73-78. DOI: 10.1890/070219

Davidson-Arnott RGD, van Proosdij D, Ollerhead J, Schostak L. 2002. Hydrodynamics and sedimentation in salt marshes: examples from a macrotidal marsh, Bay of Fundy. *Geomorphology* **48**: 209-231.

Desplanque C, Mossman DJ. 2004. Tides and their seminal impacts on the geology, geography, history and socio-economics of the Bay of Fundy, eastern Canada. *Atlantic Geology Special Publication.*

Desplanque C, Mossman DJ. 2001. Bay of Fundy tides. *Geoscience Canada* **28** (1): 1-11.

DFO. 2009. Department of Fisheries and Oceans Assessment of Tidal and Wave Energy Conversion Technologies in Canada. DFO Canadian Science Advisory Secretariat Science Advisory Report, 2009/064.

Dronkers J. 1986. Tidal asymmetry and estuarine morphology. *Netherlands Journal of Sea Research* **20** (2/3): 117-131.

Donnelly JP, Bertness MD. 2001. Rapid shoreward encroachment of salt marsh cordgrass in response to accelerated sea-level rise. *Proceedings of the National Academy of Sciences of the United States of America* **98** (25):14218-14223.

Dupont F, Hannah C, Greenberg D. 2005. Modelling the Sea Level in the Upper Bay of Fundy. *Atmosphere-Ocean* **43** (1), 33-47.

French JR, Stoddart DR. 1992. Hydrodynamics of Salt Marsh Creek Systems: Implications for Marsh Morphological Development and Material Exchange. *Earth Surface Processes and Landforms* **17**: 235-252.

Friedrichs CT, Perry JE. 2001. Tidal salt marsh morphodynamics: a synthesis. *Journal of Coastal Research* **27**: 7-37.

Friend PL, Lucas CH, Rossington SK. 2005. Day-night variation of cohesive sediment stability. *Estuarine, Coastal and Shelf Science* **64**: 407-418.

Gordon DC. 1994. Intertidal ecology and potential power impacts, Bay of Fundy, Canada. *Biological Journal of the Linnean Society* **51**: 17-23.

Hoitink AJF, Hoekstra P. 2005. Observations of suspended sediment from ADCP and OBS measurements in a mud-dominated environment. *Coastal Engineering* **52**: 103-118. DOI: 10.1016/j.coastaleng.2004.09.005

Karsten RH, McMillan JM, Lickley MJ, Haynes RD. 2008. Assessment of tidal current energy in the Minas Passage, Bay of Fundy. *Proceedings of the Institution of Mechanical Engineers* **222** (A-J): 493-507.

Kim SC, Friedrichs CT, Maa JP-Y, Wright LD. 2000. Estimating bottom stress in tidal boundary layer from acoustic Doppler velocimeter data. *Journal of Hydraulic Engineering, ASCE* **126** (6): 399–406.

Lane SN, Biron PM, Bradbrook KF, Butler JB, Chandler JH, Crowell MD, McLelland SJ, Richards KS, Roy AG. 1998. Three dimensional measurement of

river channel flow processes using acoustic Doppler velocimetry. *Earth Surface Processes and Landforms* 23: 1247–1267.

Lawrence DSL, Allen JRL, Havelock GM. 2004. Salt marsh morphodynamics: An investigation of tidal flows and marsh channel equilibrium. *Journal of Coastal Research* 20: 301-316.

Leonard LA, Croft AL. 2006 The effect of standing biomass on flow velocity and turbulence in *Spartina alterniflora* canopies. *Estuarine, Coastal and Shelf Science* 69: 325-336. DOI: 10.1016/j.ecss.2006.05.004

Leonard LA, Luther ME. 1995. Flow hydrodynamics in tidal marsh canopies. *Limnology and Oceanography* 40 (8): 1474-1484.

Manning AJ, Bass SJ. 2006. Variability in cohesive sediment settling fluxes: Observations under different estuarine tidal conditions. *Marine Geology* 235: 177-192. DOI: 10.1016/j.margeo.2006.10.013

Manning AJ, Dyer KR. 2002. A comparison of floc properties observed during neap and spring tidal conditions. In: *Fine Sediment Dynamics in the Marine Environment*, Winterwerp JC, Kranenburg C (eds). Elsevier: Amsterdam; 233-250.

MacDonald GK, Noel EN, van Proosdij D, Chumra GL. 2010. The legacy of agricultural reclamation on channel and pool networks of Bay of Fundy salt marshes. *Estuaries and Coasts* 33: 151-160. DOI 10.1007/s12237-009-9222-4

Middleton, GV. 1972. Brief field guide to intertidal sediments, Minas Basin, Nova Scotia. *Maritime Sediments* 8 (3): 114-122.

Morris JT, Sundareshwar PV, Nietch CT, Kjerfve B, Cahoon DR. 2002. Responses of Coastal Wetlands to Rising Sea Level. *Ecology* 83 (10): 2869-2877.

Murphy S, Voulgaris G. 2006. Identifying the role of tides, rainfall and seasonality in marsh sedimentation using long-term suspended concentration data. *Marine Geology* 227: 31-50. DOI: 10.1016/j.margeo.2005.10.006

Mwamba MJ, Torres R. 2002. Rainfall effects on marsh sediment redistribution, north Inlet, South Carolina, USA. *Marine Geology* 189: 267-287.

Neumeier U, Amos CL. 2006. The influence of vegetation on turbulence and flow velocity in European salt-marshes. *Sedimentology* 53: 259-277. DOI: 10.1111/j.1365-3091.2006.00772x

O'Brien DJ, Whitehouse RJS, Cramp A. 2000. The cyclic development of a macro-tidal salt marsh on varying timescales. *Continental Shelf Research* **20**: 1593-1619.

Peters H. 1997. Observations of stratified turbulent mixing in an estuary: Neap-to-spring variations during high river flow. *Estuarine, Coastal and Shelf Science* **45**: 69-88.

Polagye BL, Malte PC. 2010. Far-field dynamics of tidal energy extraction in channel networks. *Renewable Energy* **36**: 222-234. DOI:10.1016/j.renene.2010.06.025

Polagye B, Van Cleve B, Copping A, Kirkendall K (eds). 2011. Environmental effects of tidal energy development. U.S. Dept. Commerce, NOAA Tech. Memo. 181 pp.

Puleo AJ, Johnson RV, Butt T, Kooney TN, Holland KT. 2007. The effect of air bubbles on optical backscatter sensors. *Marine Geology* **230**: 87-97. DOI:10.1016/j.margeo. 2006.04.008

Reed D. 1988. Sediment dynamics and deposition in a retreating coastal salt marsh. *Estuarine, Coastal and Shelf Science* **26**: 67-79.

Reed D, Spencer T, Murray AL, French JR, Leonard L. 1999. Marsh surface sediment deposition and the role of tidal creeks: implications for created and managed coastal marshes. *Journal of Coastal Conservation* **5**: 81-90.

Roy AG, Biron P, De Serres B. 1996. On the necessity of applying a rotation to instantaneous velocity measurements in river flows. *Earth Surface Processes and Landforms* **21**: 817-827.

Sanders RE, Baddour E. 2008. Engineering issues in the harvest of tidal energy in the Bay of Fundy, Canada. Report to the Engineering Committee on Oceanic Resources Symposium. 10 pp.

Schostak LE, Davidson-Arnott RGD, Ollerhead J, Kostaschuk RA. 2000. Patterns of flow and suspended sediment concentration in a macrotidal saltmarsh creek, Bay of Fundy, Canada. In: Coastal and Estuarine Environments, Pye K, Allen JRL (eds). *Journal of the Geological Society*, Special Publication **175**: 59-73.

Scott DB, Greenberg DA. 1983. Relative sea-level rise and tidal development in the Bay of Fundy system. *Canadian Journal of Earth Sciences* **20**: 1554-1564.

Silva H, Dias JM, Caçador I. 2009. Is the salt marsh vegetation a determining factor in the sedimentation process? *Hydrobiologia* **621**: 33-47. DOI 10.1007/s10750-008-9630-7

Soulsby RL. 1983. The bottom boundary layer of shelf seas. *Elsevier Oceanography Series* **35**: 189-266.

Sun X, Chick JP, Bryden IG. 2008. Laboratory-scale simulation of energy extraction from tidal currents. Renewable Energy **33**: 1267-1274. DOI: 10.1016/j.renene.2007. 06.018

Temmerman S, Bouma TJ, Govers G, Lauwaet D. 2005. Flow paths of water and sediment in a tidal marsh: relations with marsh development stage and tidal inundation height. *Estuaries* **28** (3): 338-352.

Torres R, Styles R. 2007. Effects of topographic structure on salt marsh currents. *Journal of Geophysical Research* **112**: 1-14. DOI: 10.1029/2006JF000508

Turk TR, Risk MJ, Hirtle RWM, Yeo RK. 1980. Sedimentological and biological changes in the Windsor mudflat, and area of induced siltation. *Canadian Journal of Fisheries and Aquatic Sciences* **37**: 1387-1397.

van Proosdij D, Davidson-Arnott RGD, Ollerhead J. 2006a. Controls on spatial patterns of sediment deposition across a macro-tidal salt marsh surface over single tidal cycles. *Estuarine, Coastal and Shelf Science* **69**: 64-86. DOI: 10.1016/j.ecss.2006.04.022

van Proosdij D, Lundholm J, Neatt N, Bowron T, Graham J. 2010. Ecological re-engineering of a freshwater impoundment for salt marsh restoration in a hypertidal system. *Ecological Engineering* **36**: 1314-1332. DOI: 10.1016/j.ecoleng.2010.06.008

van Proosdij D, Ollerhead J, Davidson-Arnott RGD. 2006b. Seasonal and annual variations in the volumetric sediment balance of a macro-tidal salt marsh. *Marine Geology* **225**: 103-127. DOI: 10.1016/j.margeo.2005.07.009

van Proosdij D, Ollerhead J, Davidson-Arnott RGD. 2000. Controls on suspended sediment deposition over single tidal cycles in a macrotidal saltmarsh, Bay of Fundy, Canada. *Journal of the Geological Society,* Special Publications **175**: 43-57.

van Proosdij D, Milligan T, Bugden G, Butler K. 2009. A tale of two macro tidal estuaries: Differential morphodynamic response of the intertidal zone to causeway construction. *Journal of Coastal Research*, Special Issue **56**: 772-776.

Voulgaris G, Meyers ST. 2004a. Temporal variability of hydrodynamics, sediment concentration and sediment settling velocity in a tidal creek. *Continental Shelf Research* **24**: 1659-1683. DOI: 10.1016/j.csr.2004.05.006

Voulgaris G, Meyers ST. 2004b. Net effect of rainfall activity on salt-marsh sediment distribution. *Marine Geology* **207**: 115-129. DOI: 10.1016/j.margeo.2004.03.009

Whitford J. 2008. Final Report: Background Report for the Fundy Tidal Energy Strategic Environmental Assessment. Prepared by Jacques Whitford Consultants for the OEER Association. Project No. 1028476. 291 pp.

Yeo RK, Risk MJ. 1979. Fundy tidal power: Environmental sedimentology. *Geoscience Canada* **6** (3): 115-121.

CHAPTER 3: INFLUENCE OF TIDAL ENERGY AND AMPLITUDE ON SEDIMENTATION AND FLOCCULATION IN A HYPERTIDAL SALT MARSH CREEK

3.1 Abstract

Removal of tidal energy in response to commercial-scale tidal power development in the Minas Passage has generated concern for a non-linear response of fine sediments in far-field environments. Disaggregated inorganic grain size (DIGS) spectra were obtained using a Coulter Multisizer III to describe samples of deposited and suspended sediment collected in a hypertidal salt marsh creek, in order to investigate the effects of changing tidal amplitude and energy on the flocculated nature of sediments. Parameterization of DIGS spectra using a non-liner, least-squares fit model suggest that amidst changes in mean floc fraction (0.67 - 0.89) and floc limit (12 - 26 µm), the fluctuation in net deposition measured over the study period (55 - 328 $g \cdot m^{-2}$) is not directly related to changes in the flocculated nature of suspended materials. Both concentration and the degree of flocculation of suspended materials are consistently high in sheltered hypertidal creeks. Net deposition is predominantly controlled by topographically-influenced flow dynamics and resuspension of newly introduced material on creek banks. This suggests that changing tidal amplitude does not have a marked effect on the flocculated nature of suspended sediments in confined and sheltered tidal creeks.

3.2 Introduction

Tidal salt marshes have gained recognition as valuable coastal areas that deliver important ecological and storm-protection services (Craft *et al.*, 2009; Boorman, 1999). The capacity of salt marshes to function as critical habitat and sites of coastal defense in an era of rising sea level is dependent on continued import and retention of sedimentary material (Donnelly and Bertness, 2001; Reed *et al.*, 1999). The hypertidal (tide range > 6 metres) nature of the Bay of Fundy has encouraged modern initiatives to develop commercial-scale tidal power production facilities in the region, beginning with device testing in 2009. These activities have raised questions about far-field environmental impacts associated with energy extraction, including the fate of fine estuarine sediments (OEER, 2008b; DFO, 2009; Sanders and Baddour, 2008). While the environmental effects of tidal power development in the Bay of Fundy have been considered in the past (e.g. Yeo and Risk, 1979; Gordon 1994), the magnitude of potential change still remains to be fully understood (Polagye et al., 2011). Due to their dependence on sediment import and retention, salt marsh environments are potentially sensitive to alterations in natural tidal energy circulation and the associated sediment transport patterns.

Fine sediment less than 63 μm in diameter (e.g. silts and clays) is known as mud. Mud commonly occurs in estuaries, where forces generated by waves and currents are relatively weak at the bed (Whitehouse et al., 2000; Williams et al., 2006; Kranck and Milligan 1992). Particles in this size range tend to flocculate, which increases the settling velocity of suspended particles and leads

to increased water column clearance when flow conditions are calm (Kranck and Milligan, 1992). Flocculation strongly influences depositional processes by enhancing the flux of muds to the bed (Kranck and Milligan, 1991; Law *et al.*, in press). Transport and deposition of mud is therefore complex and widely varied, and is linked to suspended sediment concentration, turbulence, and biological processes that influence particle cohesion (Milligan and Hill 1998; Manning *et al.*, 2006; van Der Lee, 2000; Kranck, 1981; Winterwerp and van Kesteren, 2004; Dyer and Manning, 1999; Eisma, 1986). Predicting the fate of muds in coastal and estuarine environments is complicated by the effects of flocculation, which vary over time (Milligan and Law, 2005; Hill *et al.*, 2000; Smith and Friedrichs, 2011). Sediment transport models designed to assess environmental impacts in the coastal zone must account for these time-variant effects (Milligan and Hill, 1998; Smith and Friedrichs, 2011; Winterwerp, 2002). Currently, knowledge regarding the distribution and dynamics of sediments in shallow, muddy, and vegetated environments such as the Bay of Fundy is limited (e.g. Whitford, 2008; DFO, 2009; Sanders and Baddour, 2008), although studies have shown marked decadal-scale changes in sedimentation patterns in response to anthropogenic alterations of regional hydrodynamics (e.g. van Proosdij et al., 2009; van Proosdij et al., 2006a; Amos and Mosher, 1985; Turk et al., 1980).

Tidal creeks are crucial components of minerogenic salt marsh systems, acting as conduits for import and export of sediment required to maintain a positive balance and adjust to changes in sea level (van Proosdij *et al.* 2006b;

Voulgaris and Meyers 2004). Suspended sediment concentration (SSC), deposition rates and inorganic grain size have been found to decrease with distance from tidal creeks, implying that creeks are the main source of sedimentary material for adjacent marsh surfaces (Friedrichs and Perry, 2001; Christiansen *et al.*, 2000). However, the percentage of total input via marsh margins is greater with increasing high water level (Temmerman *et al.*, 2005; Davidson-Arnott *et al.*, 2002). Tides that inundate the marsh surface show different velocity patterns compared with those that remain restricted to channels (Torres and Styles, 2007; Lawrence et al., 2004; French and Stoddart, 1992). The marsh platform acts as a topographic threshold and separates two relatively different flow regimes (French and Stoddart, 1992; Allen 2000; Friedrichs and Perry, 2001). Flow magnitude in tidal creeks is defined by the amplitude of individual tidal cycles, as the resulting flow velocity corresponds with the volume of water being moved through a system. When intertidal areas (e.g. high marsh) flood and drain in close proximity to high water, peak flood and ebb currents develop shortly before or after slack tide, at high water (Blanton *et al.*, 2002; Dronkers, 1986). Marshes with an equilibrium surface that is relatively flat and high in the tidal frame promote a rapid transition from zero surface submergence to complete surface submergence with increasing tidal height, evidenced by sudden changes in velocity patterns with submergence of marsh topography (Friedrichs and Perry, 2001; Torres and Styles, 2007).

Energy extraction from tidal flows is understood to alter hydrodynamics in the near-field environment (e.g. within close proximity to turbines) (Polagye and

Malte, 2010; Sun *et al.*, 2008; Bryden, 2004). However, the response of far-field environments (e.g. upper intertidal zones) to changes in tidal energy and the magnitude of potential alterations to estuary-scale dynamics remains relatively unknown (Polagye *et al.*, 2011; Sanders and Baddour, 2008). Numerical models have shown that a 5% reduction in tidal amplitude in the Minas Basin may occur in response to 2.5 gigawatts (GW) of energy extraction from the Minas Passage (Karsten *et al.*, 2008). Changes in estuarine sedimentation patterns can be expected in response, due to a high sensitivity of intertidal zones to sediment supply and inherent links to hydrodynamics (Ralston and Stacey, 2007; Boorman, 2003). A non-linear response of sedimentation rates in the Upper Bay of Fundy may occur in response to modification of the tidal energy regime, due to a naturally high concentration of fine sediments (Polagye *et al.*, 2011; Polagye and Malte, 2010; Whitford, 2008). A cautious approach to tidal power development in the area is supported by previous studies of coastal engineering projects in Bay of Fundy estuaries (e.g. van Proosdij *et al.*, 2009; Amos and Mosher, 1985; Turk *et al.*, 1980), which have demonstrated rapid, decadal-scale changes to intertidal sedimentation patterns in response to anthropogenic manipulation of natural hydrodynamics. A reduction of tidal amplitude in the inner Bay of Fundy will reduce the overall inundation time of salt marsh surfaces, which may result in a reduction in sedimentary input over time (Friedrichs and Perry, 2001; O'Laughlin and van Proosdij, in review).

The purpose of this research is to investigate natural variations in grain size characteristics of suspended and deposited sediment during over-marsh and channel-restricted tidal cycles in a hypertidal salt marsh creek. As shown in the previous chapter, channel-restricted and over-marsh tides show variations in current velocity and kinetic energy, associated with changing tidal amplitude (O'Laughlin and van Proosdij, in review; French and Stoddart, 1992). Grain-size variations in samples of suspended and deposited sediment may be related to changing floc dynamics over the tide range, which can potentially impact net deposition through differential flow and turbulent conditions (Curran *et al.*, 2004; Dyer and Manning, 1999; Kranck and Milligan, 1992). This research considers the hypothesis that increased deposition associated with over-marsh tides is related to a higher floc fraction (the fraction of the total suspended mass held in flocs) (Law *et al.*, in press). A limited number of studies have investigated variability in the flocculated nature of salt marsh or tidal creek sediments for characterization of controls on deposition patterns (e.g. Voulgaris and Meyers, 2004; Christiansen *et al.*, 2000). It is possible that linkages between hydrodynamics and sedimentary characteristics will demonstrate a strong influence of tidal prism on net sediment deposition in the relatively low-turbulence environment of a terminal salt marsh creek.

3.3   Study Area

The Bay of Fundy is a funnel-shaped embayment on the east coast of Canada which forms the north-eastern extension of the Gulf of Maine (Figure

3.1). The upper bay is divided into two inner-bay systems: Chignecto Bay and the Minas Basin (Davidson-Arnott *et al.*, 2002; van Proosdij *et al.*, 2000). The modern 1,400 km coastline is bound by sandstone and conglomerate cliffs which demonstrate high rates of erosion (up to 1 $m \cdot a^{-1}$ in some areas) (Desplanque and Mossman, 2001). Bed scours in the Minas Basin introduce laminated silts and clays to suspension, increasing the supply of fine sediments (Amos, 1987). This abundance of material corresponds with typically high suspended sediment concentrations (SSC) in intertidal zones (van Proosdij, 2001). The Bay of Fundy system is semidiurnal and hypertidal, with a maximum tide range of up to 16 metres in the Minas Basin. Numerous salt marsh-mudflat complexes dominate the extensive intertidal zone. Marshes are predominantly mature and minerogenic, are dominated by *Spartina alterniflora* and *S. patens*, and endure extended periods of ice and snow each winter.

Data for this research were collected during the summer of 2009, in a well-sheltered terminal creek at Starr's Point marsh, near the upper limit of the Minas Basin, at the mouth of the Cornwallis River (Figures 3.1 & 3.2). A headwater location was selected for investigation of subtle variations in tidal parameters in a low-energy segment of the tidal environment, where processes are relatively straightforward and high rates of sediment deposition are anticipated. The marsh surface is characterized by a mix of high marsh platforms (dominated by *Spartina patens)* and deeply incised creeks, with a dominance of *Spartina alterniflora* in low marsh areas, such as the upper creek banks. Elevations are reported
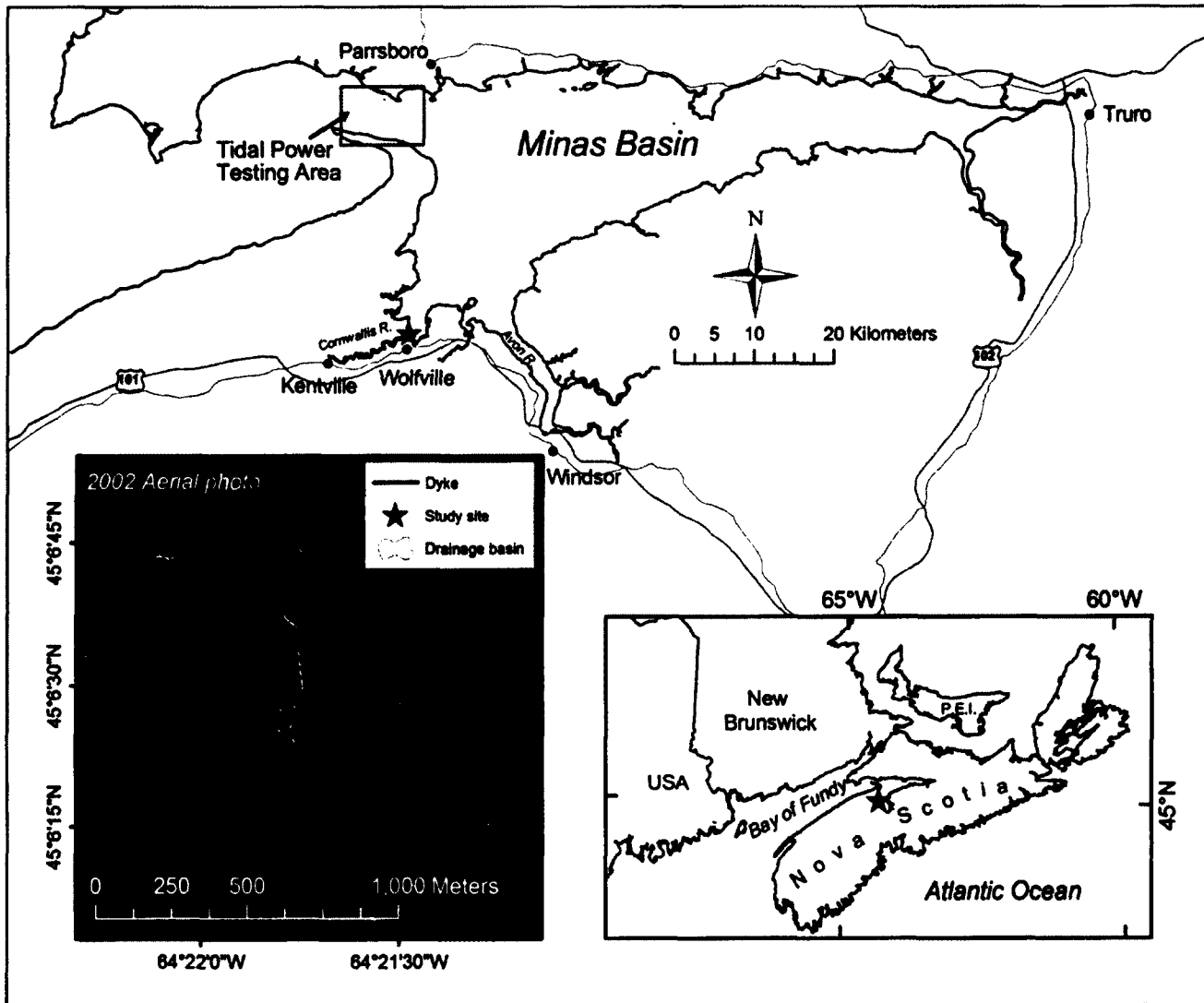
Figure 3.1: Maps of Maritime Provinces and the Minas Basin, and an aerial photo (2002) showing Starrs Point marsh. The study site is indicated in each instance with a red star in each instance.

relative to the Canadian Geographic Vertical Datum of 1928 (CGVD28), which is referenced from mean water level (MWL) measurements made in 1928 at tide gauges across Canada. This is the most current standard for vertical datums in Canada. Creek depth at the study site is 4 - 5 metres, where the banks are gently sloping and partially vegetated. Bankfull elevations vary from the east to west creek banks, ranging from 4.2 - 4.8 metres CGVD28. The drainage basin of the studied creek section has a total volume of approximately 9,800 m^3 and a submerged area of over 13,800 m^2 at the mean bankfull level (4.5 m CGVD28). Median grain size at the site is 6.7 μm, and salinity of tidal waters is relatively constant (~30). Tidal flows navigate more than one kilometer of main channel before reaching the study site. A deep, incised ditch (~1 metre width, > 1 metre depth) continues for several hundred metres beyond the creek head and through an area of densely-vegetated low marsh, parallel to an agricultural dike (most recent construction in 1955). The ditch is a former borrow pit that has been incorporated into the marsh drainage network, as is common on Fundy marshes (MacDonald *et al.*, 2010; Bowron *et al.*, 2009; van Proosdij *et al.*, 2010).

3.4 Methods

Near-bed current velocity and suspended sediment concentration were measured over 15 tides with acoustic and optical sensors at two elevations in the tidal creek: above the thalweg (0.5 meters CGVD28), and above the eastern creek bank (1.2 meters CGVD28) (Figure 3.2). Acoustic Doppler velocimeters (ADV) (Vector, Nortek) and co-located optical backscatter sensors (OBS)
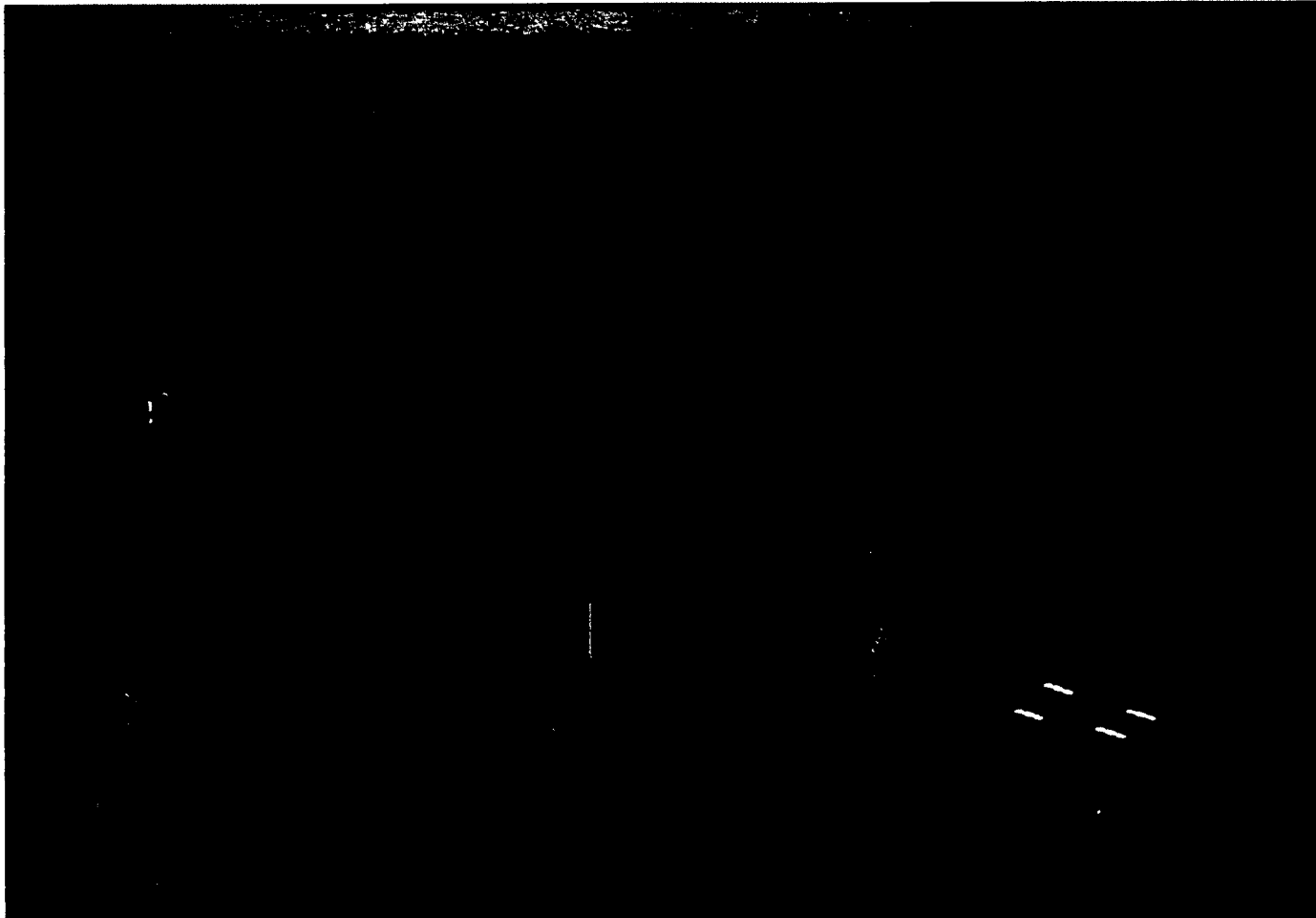
Figure 3.2: Instrument configuration in the tidal creek, including ADV/OBS arrays (2), thalweg-mounted ADCP, surface-mounted sediment traps, and RBR logger. Black arrows show flood tide direction. Photo by C. O'Laughlin, July 2009.

(OBS3+, Campbell-Scientific) were deployed at each location. All sensors were positioned for measurement at 10 centimeters above the bed. Each OBS unit was individually calibrated in the field (Puleo et al., 2007; Hoitink and Hoekstra, 2005; Voulgaris and Meyers, 2004). The thalweg array sampled continuously at 16 Hz and was accessed daily. The bank array sampled continuously at 4 Hz, to allow data collection over extended periods and limit disturbance of the creek bank. An upward-looking, thalweg-mounted acoustic Doppler current profiler (ADCP) (Aquadopp HR, Nortek) was deployed in high-resolution mode at the base of the channel. This instrument profiled up to a maximum height of 2.97 metres above the bed, in 3-centimeter bins. The pulse distance was set to approximately match the maximum profile height (3 metres), to reduce the occurrence of double pinging and signal contamination. The hard thalweg was used to access the lower ADV array and ADCP daily in order to minimize disturbance to natural surfaces, for data downloading required to make available memory space for further collection. Salinity and temperature in the creek was measured with an RBR XR-420 logger, located above the thalweg at the mouth of the study creek (Figure 3.2).

Samples of deposited sediment were collected with surface-mounted sediment traps and pre-weighed filter papers (Whatman 5, 90 mm paper filters), based on the design by van Proosdij et al. (2006) (Figure 3.3). This trap design allows for resuspension of deposited materials, and can be used to characterize net sediment deposition on non-vegetated creek banks and tidal flats. Four traps

were deployed to the sampling surface, 5 cm above the bed, spread evenly over an approximately 2 m^2 plot on the creek bank. Three filter papers were placed in each trap, which were leveled with a spirit level once placed on the bank. Sediment-laden filters were collected after single tidal cycles. Filters were air dried for ~48 hours before weighing, to determine the total amount of material on each filter. Samples were not rinsed prior to analysis, as no salt crystals were observed, and the amount of salt accumulated over individual tidal cycles was minimal relative to the amount of sediment. One sample from each trap was heated in a muffle furnace and processed for organic content, and another used in grain size analyses (discussed below).

In-situ water samples were drawn from the thalweg using an automated water sampler (Teldyne ISCO) (Figure 3.3). The intake nozzle (15 cm length) was mounted with the lowest sampling point at 10 cm above the bed. 200-millilitre samples were collected every 30 minutes during tidal cycles. A portable weather station (Campbell-Scientific) was installed at the study site to record meteorological parameters, including wind speed and direction, rainfall, temperature and atmospheric pressure. Hourly averaged records were collected for the duration of the study period. 'Webtide' (Dupont et al., 2005) was used to develop a one-year record (15 minute intervals) of predicted tide elevations at Starr's Point. These were found be consistently less (by 0.5 - 1.0 metres) compared with observed water levels, possibly due to hydraulic friction, and were corrected to reduce modeled tidal elevations by the mean variation from actual
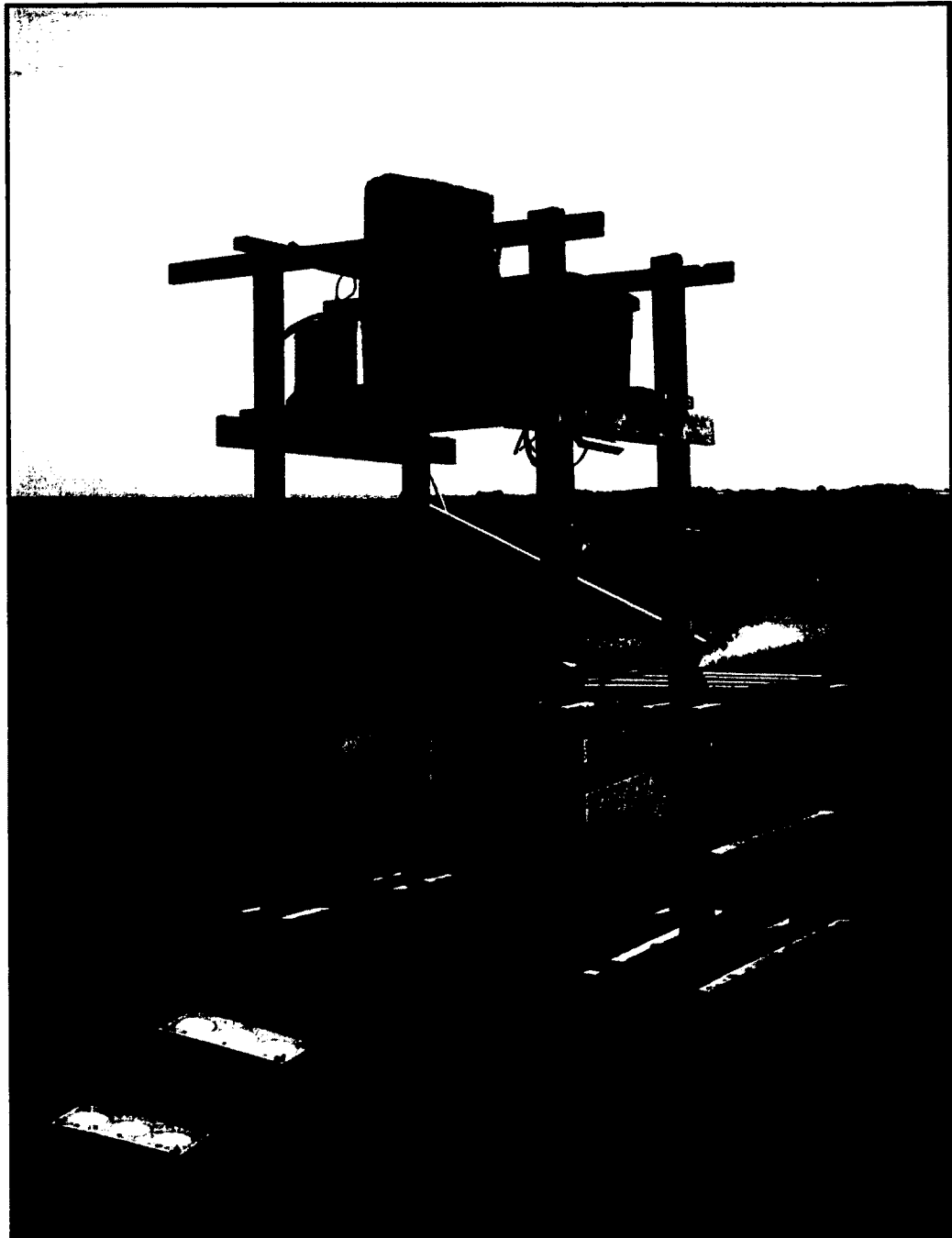
Figure 3.3: ISCO automated water sampler, mounted above the marsh surface. The intake nozzle was placed near the thalweg. Inset: Sediment traps prior to inundation. Photos by C.O'Laughlin.

water levels (0.92 m). A regional, LiDAR-generated digital elevation model (2-metre resolution) was applied for analysis and quantification of drainage basin geometry.

Acoustic data recorded by the ADCP were filtered, viewed and interpreted using the standard settings in Storm (ver. 1.08, Nortek). Flow velocity and average signal strength were considered for each deployment. Wave conditions during the sampling periods were investigated using raw pressure signals from the bank ADV, where consistently identified cm-scale ripples on the water surface reflect field observations. Mean current velocity and subsequent parameters derived from ADV records were estimated through time-averaging over 5-minute measurement bursts. Instantaneous horizontal flow components (x, y) were rotated into down-stream (u) and cross-stream (v) velocities following methods outlined in Roy *et al.* (1996) and Lane *et al.* (1998), and velocity was calculated as $\sqrt{u^2 + v^2}$. Instantaneous turbulent components (u_t, v_t, w_t) were derived using the relationship $u = U + u_t$, and turbulence intensities (i_u, i_v, i_w) were calculated as the root mean square of turbulent components. Turbulent kinetic energy (TKE) (J·m^{-2}) was calculated using:

$$TKE = \frac{1}{2} \rho \ (u_t^2 + v_t^2 + w_t^2)$$

Equation (1)

where ρ is salt water density at 20°C (ρ = 1025 kg·m^{-3}) (Neumier and Amos, 2006; Voulgaris and Meyers, 2004). Mean kinetic energy (KE) (J) in the tidal creek was estimated with:

103

$$\overline{KE} = a \left(\frac{1}{2} \rho u^2 \right),$$

where a is channel cross-sectional area and u is upstream current velocity (Karsten *et al.*, 2008). Friction velocity (u_*) was computed using the Reynolds stress method (Soulsby, 1983; Kim and Friedrichs, 2000):

$$u_* = (-\overline{u_t' w_t'})^{1/2},$$

where u_t and w_t are instantaneous components of down-stream and vertical velocity, respectively. Friction velocity can then be applied to calculate bed shear stress (τ_0) $(N \cdot m^{-2})$

$$\tau_0 = \rho u_*^2$$

and bed shear velocity (u_b*) $(m \cdot s^{-1})$:

$$u_{b}* = \frac{u_*(z)^2}{1 - z/h},$$

where z is the measurement elevation above the sea bed, and h is the total local water depth in the channel (Barnes *et al.*, 2009; Kim and Friedrichs, 2000; Biron *et al.*, 2004; Voulgaris and Meyers, 2004). The inertial dissipation (I.D.) method was also applied to develop the TKE dissipation rate (ε) $(m^{-2} \cdot s^{-3})$ from the vertical component of the current:

$$\varepsilon = \frac{u_*^3}{\kappa \cdot z},$$

where K is the von Karman constant (0.41) and z is the measurement elevation above the bed (Voulgaris and Meyers, 2004). Dissipation rate estimates (ε) were applied to calculate the Kolmogorov microscale (η) ($\mu m \cdot 10^{-3}$):

$$\eta = \left(\frac{v^3}{\varepsilon} \right)^{0.25}$$

Equation (7)

and dissipation parameter (G) (s^{-1}):

$$G = \left(\frac{\varepsilon}{v} \right)^{0.5},$$

Equation (8)

where v is the kinematic viscosity of water at 20°C (1.004 x 10^{-6} $kg \cdot m^{-1} \cdot s^{-1}$) (Milligan and Hill, 1998). The Kolmogorov microscale indicates the scale of turbulent eddies that may affect particle collision rates and therefore, floc formation. The dissipation (or shear rate) parameter (G) is a proxy measure of forces that at low values promote floc formation, and at high values break-up flocculated particles (Voulgaris and Meyers, 2004; Milligan and Hill, 1998; Dyer and Manning, 1999).

Disaggregated inorganic grain size (DIGS) analysis was performed on samples of suspended and deposited sediment, using a Beckman-Coulter Multisizer III electroresistance particle counter, following methods described by Milligan and Kranck (1991), Kranck *et al.* (1996a, 1996b), Curran *et al.* (2004), and Milligan and Law (2005). Small subsamples (0.1 - 0.5 g) for DIGS analysis were extracted from field samples of deposited sediment. Material was generally

abundant on filters, and subsamples were easily removed from filter papers after drying. Subsamples were treated with hydrogen peroxide (30%) to remove organic materials, added to ~10 ml of deionized, reverse osmosis water, and placed in a sonic bath for 10 minutes to disaggregate particles. For processing samples of suspended sediment, known volumes of sample laden-water were filtered onto Millipore 8.0 mm SCWP (cellulose acetate) pre-weighed filters using standard gravimetric methods. Millipore filters were selected based on previous studies that recommend these filters due to high retention of particles less than their nominal pore sizes (Sheldon, 1972; Sheldon and Sutcliffe, 1969). Filters were oxidized at <60° C in a low temperature oxygen/plasma asher, to prevent the fusing together of mineral grains while removing the filter. Once subsamples were isolated, they were diluted in a 1% NaCl solution and re-sonicated for 2 minutes using a sapphire-tipped ultrasonic probe, before processing with the Coulter Multisizer III.   Both 30 and 200 μm aperture tubes were used in these analyses, the size distributions measured of which were merged to create continuous grain size spectra. DIGS distributions were parameterized using a non-linear, least-squares fit 'inverse floc model', through a semi-automated MATLAB routine developed by Curran *et al.*, (2004) and based on work by Kranck and Milligan (1991) and Kranck *et al.* (1996a, 1996b). The model applies a non-linear fit of observed bottom sediment DIGS distributions to the modeled equation, and can be used for separation of floc and single-grain settled components. Additional grain size statistics were completed with GRADISTAT (Blott, 2010).

Changes in the flocculated nature of sediment can indicate fluctuation in depositional conditions, representing the dynamic influence of flocculation on estuarine sediment transport. Source slope (m) indicates the relative amounts of fine versus coarse particles, is a property of the parent material, and is generally similar among different samples from with a common source (Kranck et al., 1996a). Roll-off diameter ($d^{\wedge}$) describes the diameter (in µm) of particles whose concentration has fallen to 1/e of its initial value, and can be thought of as the largest grain held in flocs. Floc limit (d_f) describes the grain size at which the flux of mass to the seabed via floc or single-grain deposition is equal (Curran et al., 2004). The flocculated component of a bottom deposit is represented by floc fraction (f), or the proportion of suspended mass held in flocs at the time of deposition (Curran et al., 2004). Examples of merged and parameterized data are shown with model results in Figure 3.4. Deposited sediment DIGS distributions are expressed as the log of equivalent weight percent versus log of particle diameters, normalized over the size range (Kranck et al, 1996a, 1996b; Milligan and Kranck 1991). Suspended samples are expressed using log of concentration in parts per million (PPM) (Law et al., 2008).

Work by Johnson and Semple (1983) and Woolfe and Michibayashi (1995) demonstrated that entropy analysis of bottom sediment size distributions generates groupings that can be correlated to depositional environment. Entropy analysis was applied to group deposited sediment DIGS into categories based on similarity. This method has recently been applied to classify in situ particle size

107

spectra of suspended and bottom sediments into groups based on similarities in distribution characteristics, reflecting variations in forcing conditions (e.g. turbulence) (Mikkelsen *et al.*, 2007). Bottom sediment textures have also been successfully interpreted using entropy analysis, for definition of ecological habitats on continental shelves (Orpin and Kostylev, 2006).

Fluctuations in acoustic backscatter intensity (e.g. amplitude or signal strength) have been considered for investigation of sediment dynamics in both laboratory and field settings, for measurement of size and settling velocity of suspended particles (e.g. Voulgaris and Meyers, 2004; Thorne and Hanes, 2002; Fugate and Friedrichs, 2002). Kim and Voulgaris (2003) found calibration methods to be most accurate for fine sands, while silt and finer materials generated bias in acoustic measurements. High suspended sediment concentration is also understood to cause measurement inaccuracies due to significant signal attenuation in the water column (Thorne *et al.*, 1991). In consequence, ADCP amplitude data presented in this study are not quantified, but have been investigated as a relative indicator of changing suspended sediment concentration in absence of calibration. Tidal-cycle scale time-series were developed at two elevations above the bed (170 and 50 cm), where rapid changes in signal strength were observed. Rates of change over the 30-minute period following high tide were calculated at both elevations to characterize changing suspended content through the water column, in effort to link dynamics with sediment deposition (e.g. Hill *et al.*, in press).
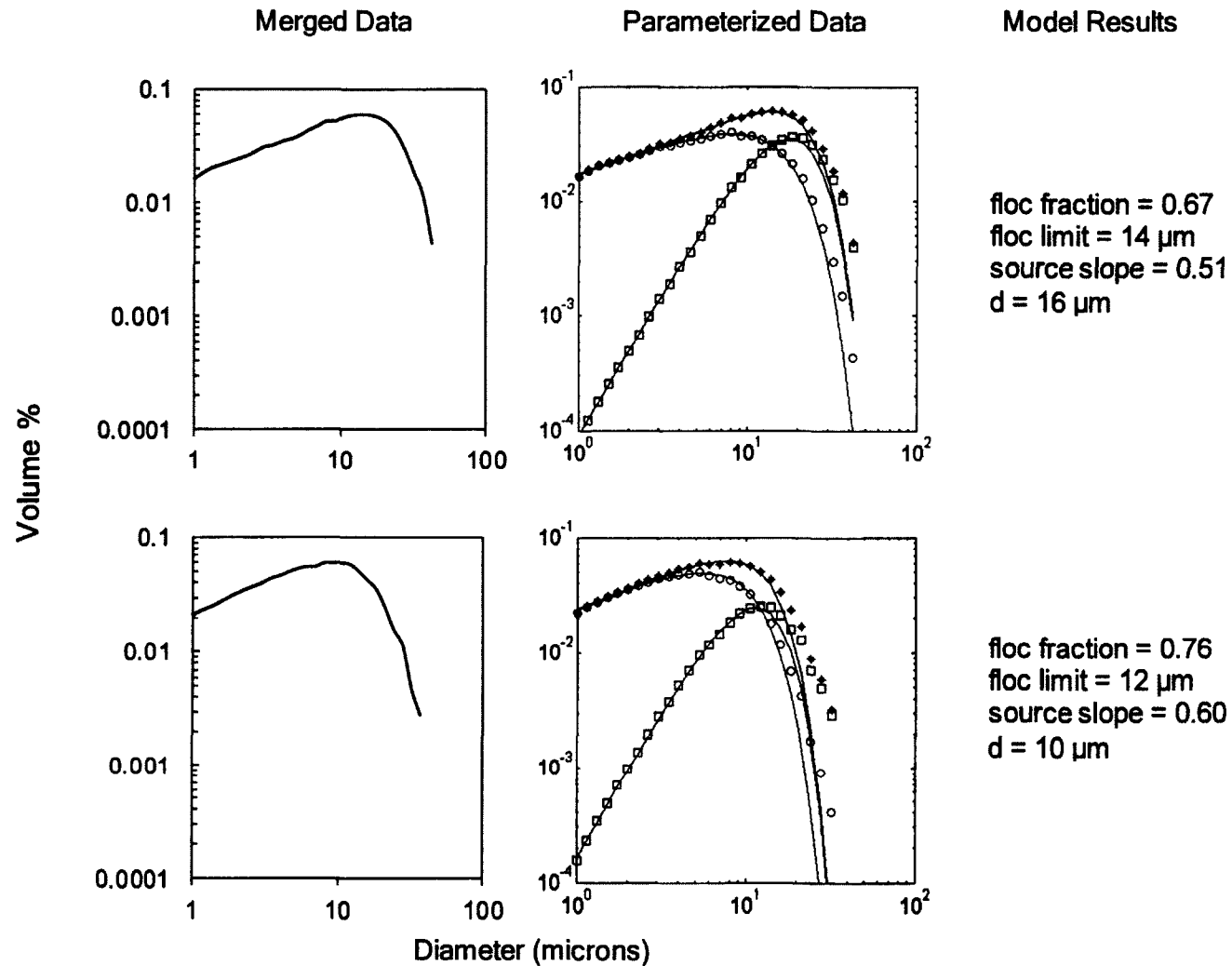
Figure 3.4: Examples of DIGS distributions (merged data from 200 and 30 μm aperture tubes), parameterized data and model results. Blue squares in parameterized data represent modelled single-grain settling, and red circles indicate floc-settled material; black stars show actual grain-size results; and the black line shows the modeled distribution.

3.5   Results

Data were collected during 15 individual tidal cycles over a range of spring and neap conditions, where maximum depth in the tidal creek varied between 2.3 and 5.2 metres. Time-series of current velocity and parameters derived from ADV data for five tidal cycles are shown, relative to high tide, in Figure 3.5. These results show that tides which inundate the marsh surface generate faster and more turbulent ebb phases in response to a greater tidal prism, compared with those that remain restricted to channels. Near-bed velocity and turbulence in the tidal creek tends to be greatest with water depth in the creek near the bankfull level, associated with flooding and drainage of high marsh surfaces in close proximity to high water, reflecting the results of other studies (e.g. Blanton *et al.*, 2002; Friedrichs and Perry, 2001; Dronkers, 1986).

Variations in near-bed current velocity measured by thalweg- and bank-mounted ADVs are also evident in ADCP measurements throughout the lower water column (0.15 - 2.97 m). Prominent flow accelerations (< 50 cm·s^{-1}) are noted with water depth in the creek at and above the mean bankfull level (4.5 m), most notably during ebb stages of over-marsh tides. This, like near-bed accelerations noted in ADV records, is associated with flooding and drainage of the high marsh surface in close proximity to high tide. Flow velocity showed more variability during channel-restricted compared with over-marsh cycles, up to the profiling limit of the ADCP (2.97 m). ADCP profiles show isolated regions of acceleration (up to 15 cm·s^{-1}) near the bed during channel-restricted
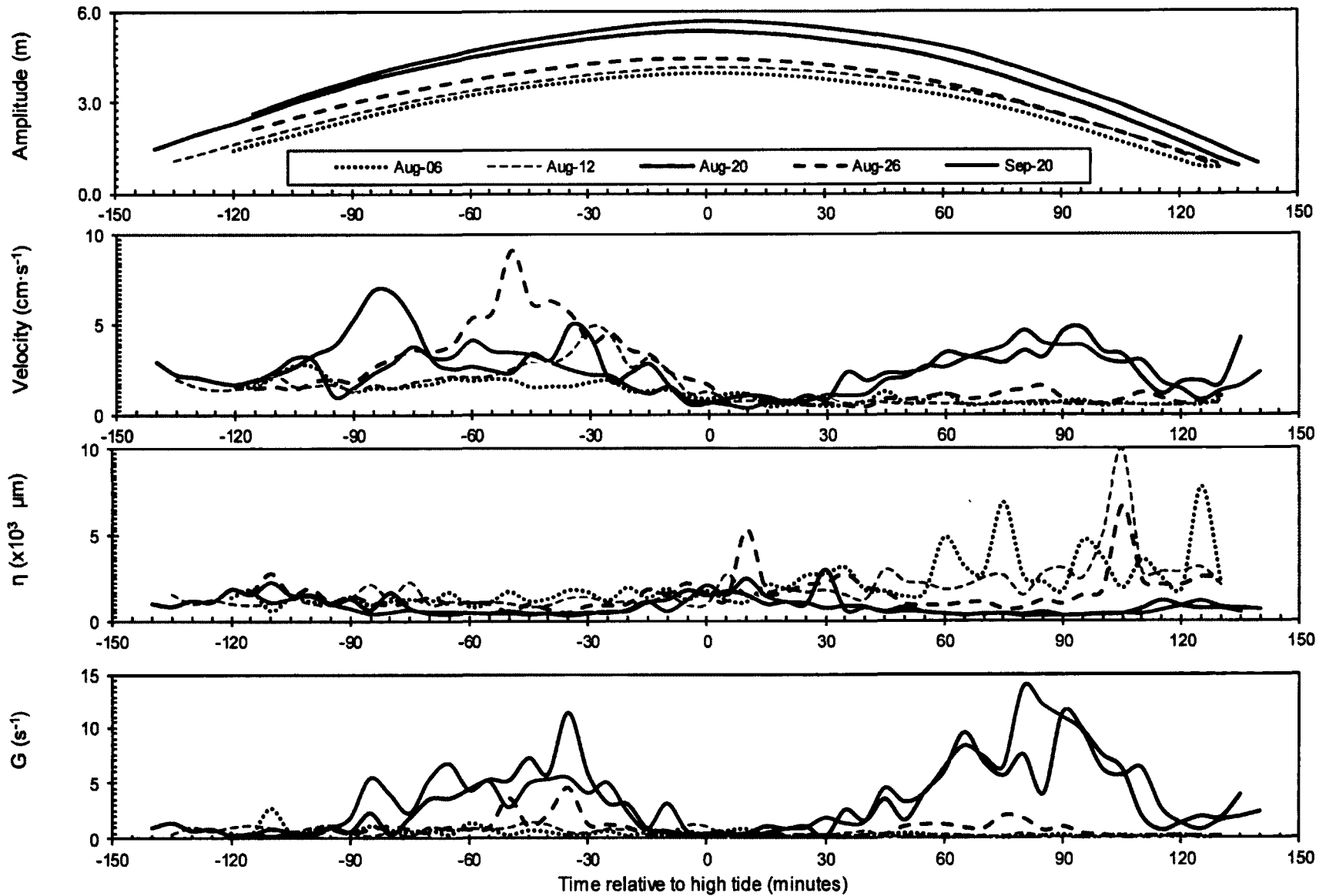
Figure 3.5: 5-minute mean values of tidal elevation, velocity, Kolmogorov microscale (η) and dissipation parameter (G), over 5 individual tidal cycles.

flood tides, and higher in the water column (2 - 3 meters above the bed) during corresponding ebbs. In contrast, over-marsh tides develop ebb-phase accelerations that penetrate through the water column to the bed. This is emphasized by ADV-derived estimates of bed shear stress, which achieves maximum during ebb phases of over-marsh tides.

Velocity-derived Kolmogorov microscale (η), dissipation parameter (G) and bed shear stress (τ_0) values are shown in Figures 3.5 & 3.6. The Kolmogorov microscale (η) describes the maximum allowable size for potential floc formation, as estimated from turbulence levels. Results demonstrate that values of η were routinely higher and showed more variability during channel-restricted tidal cycles than during over-marsh tides. In general, peak values on channel-restricted cycles ranged from 4-10 x 10^3 μm, while that of over-marsh tides ranged from 3-6 x 10^3 μm. This suggests that the moderate turbulence level associated with typical channel-restricted tides allows for formation of flocs up to 50% larger than more turbulent over-marsh tides. Turbulence levels were especially low (0.01 - 0.1 J·m^{-3}) for the duration of ebb phases of channel-restricted tides, which resulted in peaks to very high η (20-38 x 10^3 μm) at both thalweg and bank sampling locations, suggesting that floc formation would be most efficient during ebb phases of channel-restricted tidal cycles. These peaks to high values promoted the aforementioned variability (indicated by standard-error bars in Figure 3.6) during channel-restricted cycles, contrasting relatively short periods of increased η during over-marsh cycles, with minimal variability.
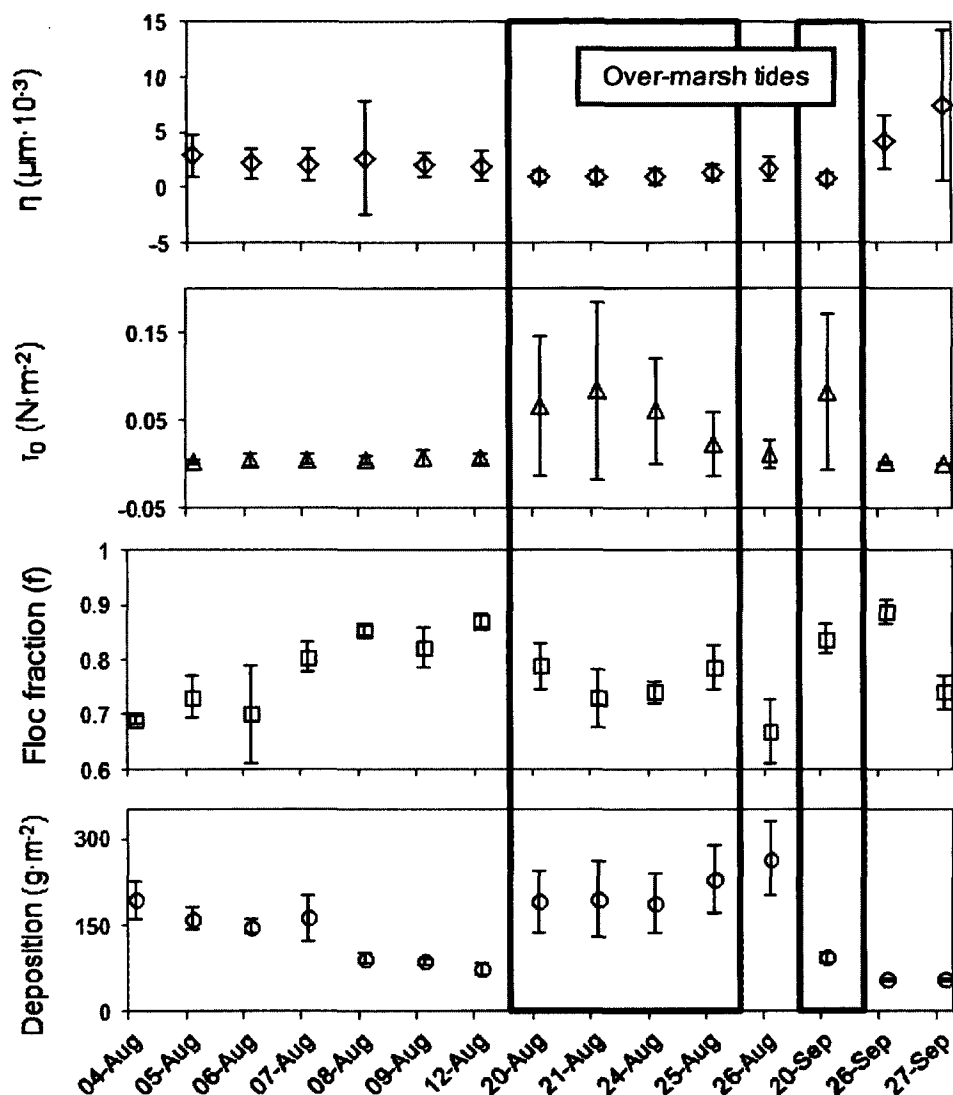
Figure 3.6: Full-deployment time-series, showing variation in 5-minute mean values of Kolmogorov microscale (η) and bed shear stress (τ₀), along with daily mean values of floc fraction (f) and deposition. Over-marsh tides are contained within the gray boxes (e.g. Aug 20, 21, 24, 25 and Sep 20). Hydrodynamic data (η and τ₀) were not collected on August 4. Error bars represent standard error, calculated over 5-minute averaging periods for hydrodynamic data, and across the four trap locations for sedimentary data.

113

Over-marsh tides demonstrate maximal η during high water, with submergence of the marsh surface, a stage which persists until ebb flow velocity increases (~40 minutes following high tide). Higher dissipation parameter (G) (2 - 15 s^{-1}) and bed shear stresses (τ_0) (0.1 - 0.5 N·m^{-2}) during initial and final stages of over-marsh tides are associated with turbulent flows, and are potentially periods of erosion or resuspension. However, lower values of G and τ_0 (0.1 - 2 s^{-1} and 0.001 - 0.05 N·m^{-2}, respectively) over the duration of slack tide (30 to 45 minutes) are associated with moderate potential for floc formation (η = ~2.5 x 10^3 μm). Overall, bed shear stresses peaked during flows that can be linked to flooding and drainage of low-marsh surfaces, independent of maximum tidal height (Figure 3.7). The general pattern of tidal energy over the study period follows this trend, and shows higher kinetic energy with submergence of high- and low-marsh surfaces (e.g. over-marsh tides). This is most notable during early ebb stages, associated with gravity-driven drainage of the marsh. Figure 3.8 shows that increasing channel cross-sectional area correlates well with increasing kinetic energy of in-channel flows.

A complete description of suspended sediment dynamics in the tidal creek as observed by OBS sensors is presented in O'Laughlin and van Proosdij (in review). Suspended sediment concentration generally demonstrated a continuously decreasing pattern throughout flood stages, at both bank and thalweg measurement locations, for both channel-restricted and over-marsh tidal cycles. Initial suspended sediment concentration at the thalweg ranged from 100
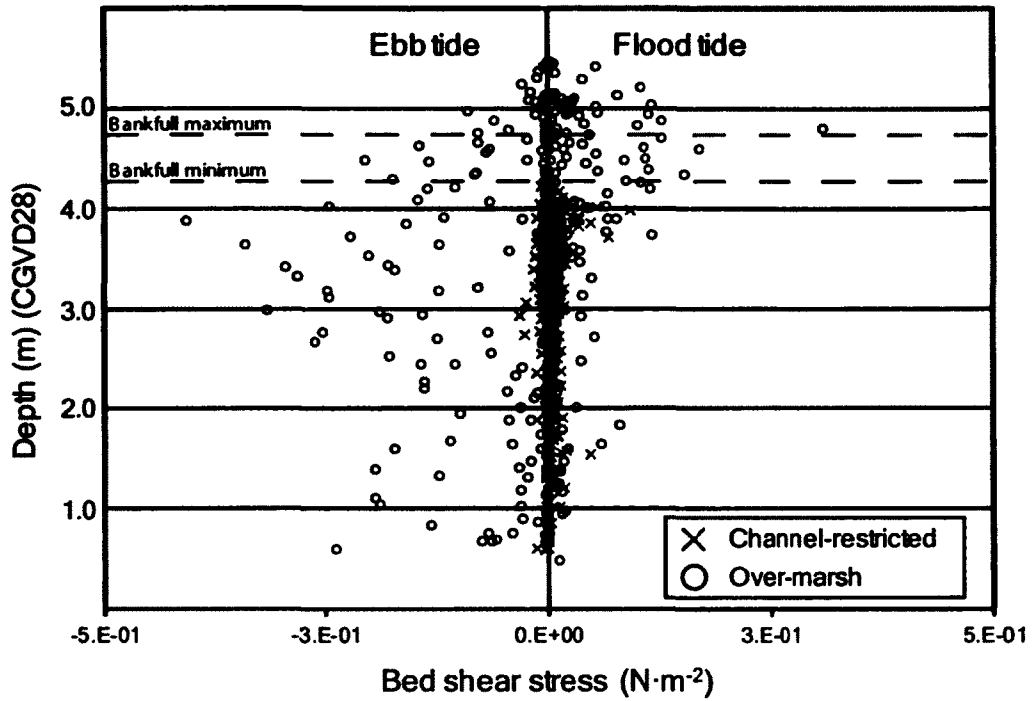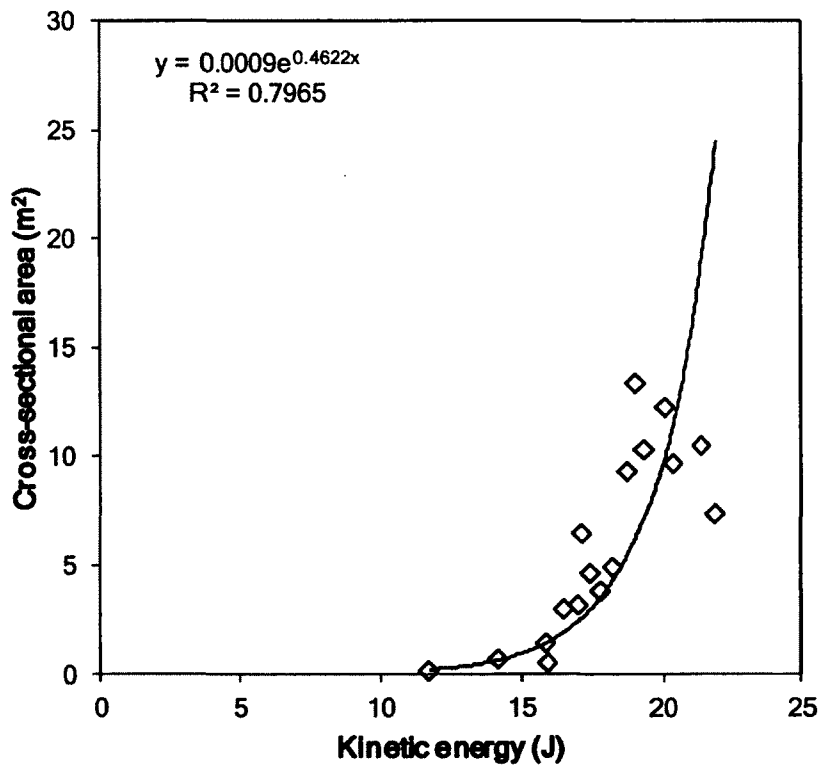
Figure 3.7 (above): Stage-height relationship showing variation in bed shear stress ($N \cdot m^{-2}$), relative to the bankfull region (4.2 - 4.8 metres).

Figure 3.8 (below): Cross-sectional area (m^2) versus kinetic energy (J).

$$y = 0.0009e^{0.4622x}$$
$$R^2 = 0.7965$$

115

- 300 mg·l^{-1}, although the tide on Aug 23rd showed an incoming concentration >3000 mg·l^{-1} in response to a rainfall event in the region. Ebb phases of over-marsh tides frequently show episodic increases to high concentration (up to 1000 mg·l^{-1}) at the thalweg location, initiating 20-40 minutes following high tide (Figure 3.9). Increases in SSC at 10 cm above the bed are thought to be associated with clearance of material from further up in the water column; however, these increases were limited to the thalweg sampling location and may represent the transport of material out of the creek through the thalweg.

Variability in suspended concentration measured through DIGS analysis of suspended samples (Figure 3.10) agrees with that monitored by OBS sensors. Peak concentrations generally occurred during initial flood and final ebb stages. Notable increases in concentration following high tide were associated with over-marsh tidal cycles. Suspended concentration regularly increased with flow accelerations at and above the bankfull level, as the marsh surface flooded and drained, resulting in alternating periods of resuspension and potential deposition occurring throughout over-marsh tides. Potential deposition is characterized by periods of decreasing suspended concentration, which are truncated by increases in concentration associated with velocity pulses and resuspension. Most prominent during over-marsh tides is rapid fluctuation in concentration that occurred in association with declining flow velocity during slack tide phases, evidenced by drastic reductions in concentration (Figure 3.10). In contrast, channel-restricted tides show a near-continuous decrease in suspended

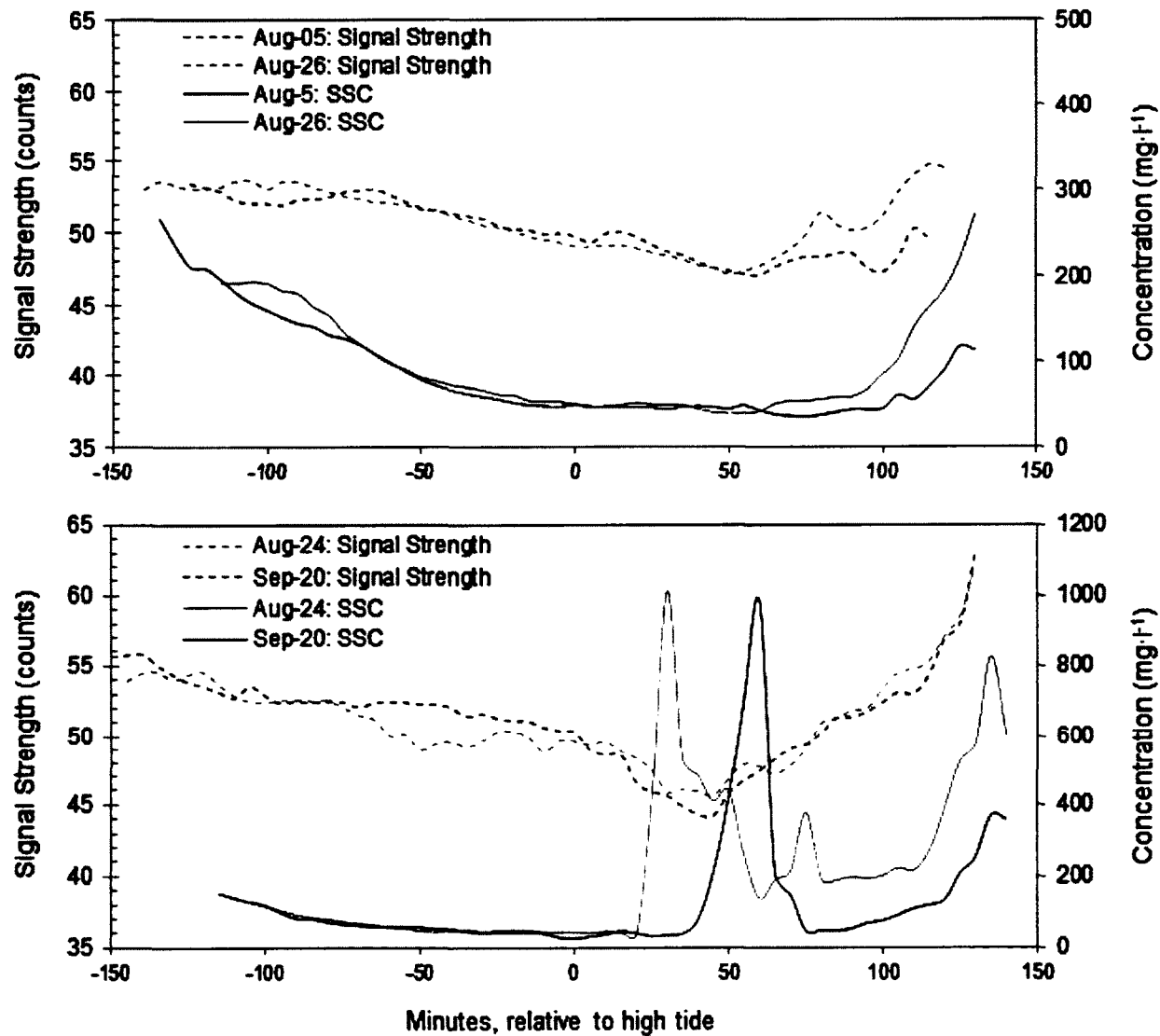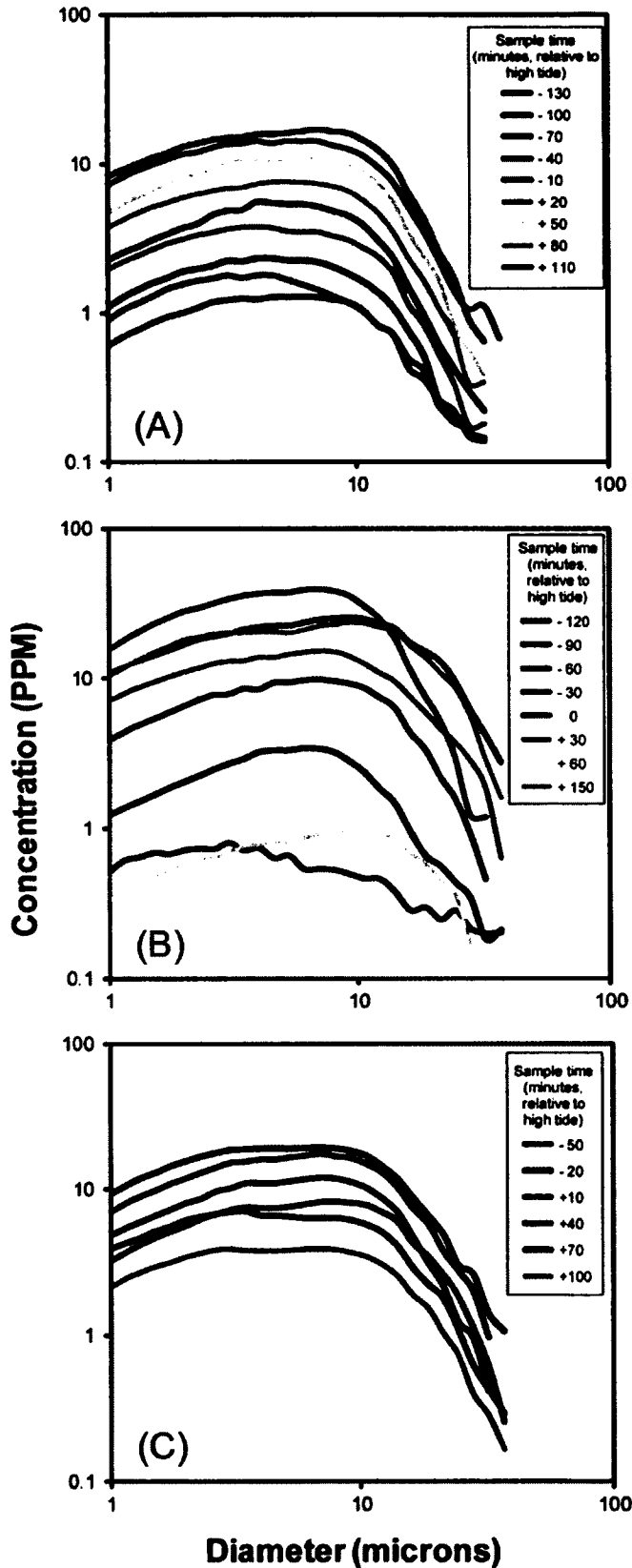Figure 3.9. OBS-derived time-series of suspended sediment concentration (mg·l⁻¹) shown with ADCP average signal strength at 50 cm above the bed, for channel-restricted (e.g. August 5, 26) (top) and over-marsh (e.g. August 24, September 20) (bottom) tidal cycles. Note variation in scale of secondary y-axes.

concentration throughout tidal cycles, reducing from a maximal concentration measured during the first 1 or 2 samples (Figures 3.9 & 3.10).

Under the assumption that suspended material was eroded from bottom deposits, suspended sediment DIGS were parameterized in a similar fashion to deposited samples. Initial flood-tide values of floc fraction (f), or the proportion of the total suspended mass held in flocs, followed fluctuations in suspended concentration, gradually decreasing throughout tidal cycles, before increasing slightly during late ebb stages. An increase in floc fraction (f) was also occasionally observed during slack tide periods, potentially increasing the flux of material to the bed. This is supported both by increased suspended concentration at 10 cm above the bed during these periods, as monitored by the thalweg OBS sensor, and samples of suspended sediment. Daily mean values of f and source slope (m) were relatively constant throughout the study period, varying between 0.78 and 0.83, and 0.31 and 0.54, respectively (Table 3.1). This limited variability suggests that the flocculated nature of suspended sediments, and their source, does not change drastically over the study period. These values closely reflect the range of variability in floc fraction and source slope, measured in samples of deposited sediments.

Similar to variability in current velocity, notable differences exist in the fluctuation of suspended sediment concentration in response to changing tidal amplitude and inundation time (Figure 3.10). Over-marsh tides show cyclic periods of increasing and decreasing concentration as current velocity is adjusted

118

100

10

1

0.1

Sample time
(minutes, relative to
high tide)
━━ - 130
━━ - 100
━━ - 70
━━ - 40
━━ - 10
━━ + 20
━━ + 50
━━ + 80
━━ + 110

(A)

1   10   100

Concentration (PPM)

100

10

1

0.1

Sample time
(minutes,
relative to
high tide)
━━ - 120
━━ - 90
━━ - 60
━━ - 30
━━ 0
━━ + 30
━━ + 60
━━ + 150

(B)

1   10   100

100

10

1

0.1

Sample time
(minutes,
relative to
high tide)
━━ - 50
━━ - 20
━━ +10
━━ +40
━━ +70
━━ +100

(C)

1   10   100

Diameter (microns)

Date	Daily means	
	f	m
04-Aug	0.78	0.40
05-Aug	0.79	0.45
07-Aug	0.80	0.43
08-Aug	0.79	0.42
09-Aug	0.80	0.39
10-Aug	0.81	0.34
11-Aug	0.80	0.45
24-Aug	0.80	0.31
25-Aug	0.80	0.44
26-Aug	0.82	0.50
20-Sep	0.80	0.54
26-Sep	0.83	0.46
27-Sep	0.83	0.48

Table 3.1 (above): Mean parameterized values of suspended sediments: floc fraction (f) and source slope (m).

Figure 3.10 (left): Suspended sediment concentration from water samples, following DIGS processing. The log of concentration is shown on the Y-axis, in parts per million (PPM), versus log of the diameter (microns). Three tidal cycles (A-C) are shown: August 26th, maximum depth near the bankfull level (A); September 20th, high over-marsh tide (B); and September 27th, a low channel-restricted tide. Sample times, relative to high tide (in minutes), are shown for each tidal cycle. Over-marsh tides show high variability in suspended sediment concentration throughout tidal cycles, linked to velocity pulses. Channel-restricted tides show gradual and constant clearance of the water column.

119

by topography during both flood and ebb stages. Flow accelerations linked to flood and ebb pulses represent periods of increased concentration, indicating potential resuspension of newly introduced materials. Channel-restricted tides show a contrastingly progressive decline in concentration following early flood tide stages, indicating that material is continuously removed from suspension. Tides that peak near the bankfull level show a pattern more similar to over-marsh tidal cycles, where flow accelerations linked to topographic forcing and drainage lead to increases in concentration that occur throughout tidal cycles.

The amplitude of the return signal measured by the ADCP shows variability in response to changing amounts of suspended material present in the water column, and is reported by the instrument as a signal strength (represented by 'counts'). As mentioned, amplitude data discussed here remains un-calibrated, and has been applied as an un-quantified, relative indicator of changing suspended sediment concentration. Examples of amplitude plots typical of over-marsh and channel-restricted tides are shown in Figure 3.11. Channel-restricted tides show a continuous and steady decrease in suspended content, evidenced by decreasing signal strength at a given depth. This pattern persists until mid-ebb, when signal strength increases in response to export of material that either remained in suspension for the duration of tidal cycles, or was re-mobilized by ebb flow (Figures 3.9 & 3.11). Over-marsh tides experience a similar gradual reduction in suspended matter following initial flood, prior to ebb-stage increases that are related to resuspension or advection (Reed, 1988).
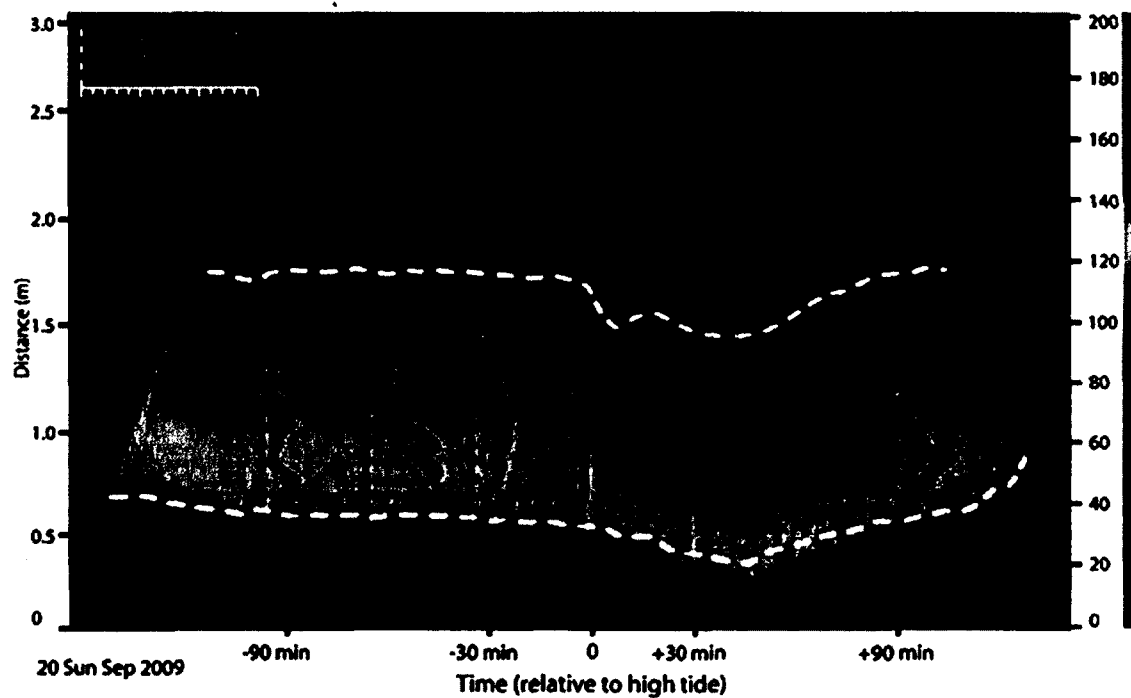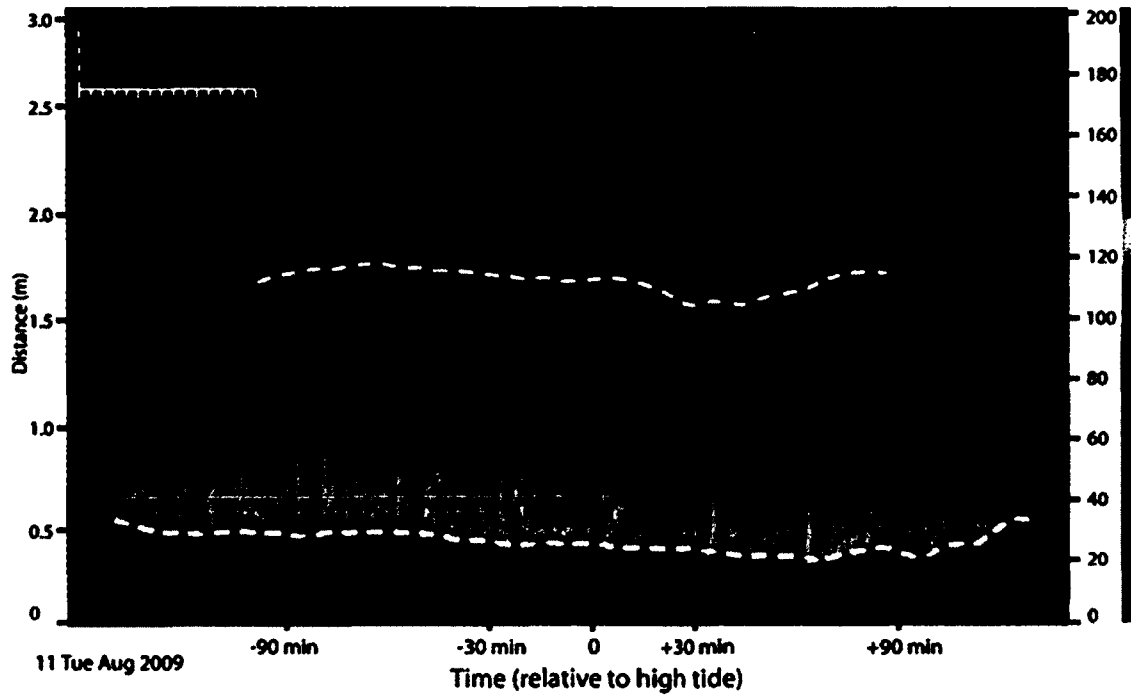
Figure 3.11. Plots of ADCP amplitude, or the strength of the return signal, are shown for two tidal cycles: August 11 (channel-restricted tide) and September 20 (Over-marsh tide). Vertical black lines are velocity profiles, showing variability relative to y-axes (vertical gray dashed line) in each case. The scale of the x-axis is shown in top left. Horizontal white lines indicate fluctuations in signal strength at two elevations: 50 and 170 cm above the bed.

121

Clearance rates describing decreasing signal strength at 170 cm above the bed during the 30-minute period following high tide varied by up to one magnitude (0.02 - 0.2 counts/minute), and achieved maximum in response to channel-restricted tidal cycles. However, at 50 cm above the bed, rates of change were higher during most over-marsh tidal cycles (~0.1 counts/minute) compared with that of channel-restricted cycles (~0.03 counts per minute).

Deposited sediment was primarily composed of medium silt, with a mean grain size of 6.2 μm and median of 6.7 μm. Over-marsh tides generally deposited more material, although a wide range of variability exists: the lowest deposition (55.02 $g \cdot m^{-2}$) was measured on a channel-restricted tide (Sept 26), and the highest (328.19 $g \cdot m^{-2}$) on a tide that peaked near the bankfull level (August 26) (Figure 3.6). Statistical analysis using nested ANOVA and standard two-sample T-tests showed that the difference in deposition for over-marsh and channel-restricted tidal cycles was not statistically significant; however, shifting the approximately bankfull tide on August 26th from the channel-restricted category to the over-marsh category produces a significant difference (0.05, 95%) in net deposition between the two groups. Parameterized DIGS of deposited sediment indicate that mean (per day) floc fraction (f), or the proportion of the total suspended mass held in flocs, ranged from 0.67 to 0.89, and was generally maximized on channel-restricted tides (Figure 3.6). Floc limit (d_f), which describes the grain size at which the flux of mass to the seabed via floc or single-grain deposition is equal, followed a similar pattern over a range of 8 to 32 μm

(Table 3.2). Mean source slope (m) showed minor variation over the study (approximately 0.4 to 0.6), suggesting limited variability in source material.

Entropy analysis was used to divide size distributions into groups such that similarity within each and dis-similarity between groups is maximized, to consider potential variations in forcing conditions. Entropy analysis was applied to deposited sediment DIGS, and determined a nominal separation into 4 unique groups (Figure 3.12 & Table 3.3). Groupings determined here show notable variation at the fine end of the curve, demonstrated by changing mean f across groups (0.7 to 0.82). Group 2 shows the highest mean tidal amplitude (4.73 m) and the highest mean f (0.82), coupled with relatively low net deposition (145 $g \cdot m^{-2}$). Group 1 shows the lowest f (0.70) and highest net deposition (195 $g \cdot m^{-2}$), associated with tides that generally peak near the bankfull level (4.5 m). Group 1 tides also demonstrated the greatest amount of suspended material in suspension at the thalweg location.
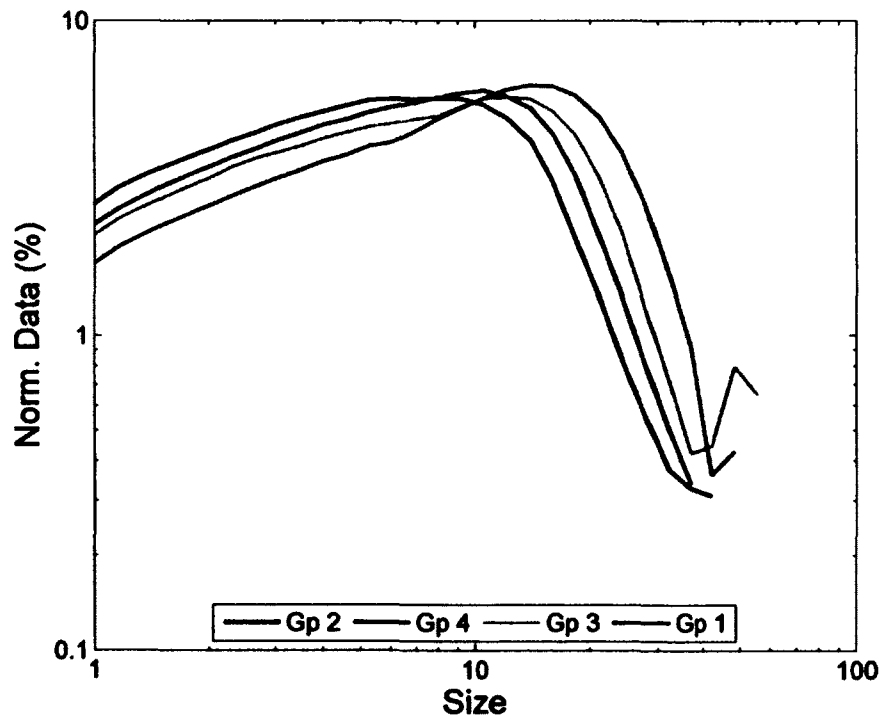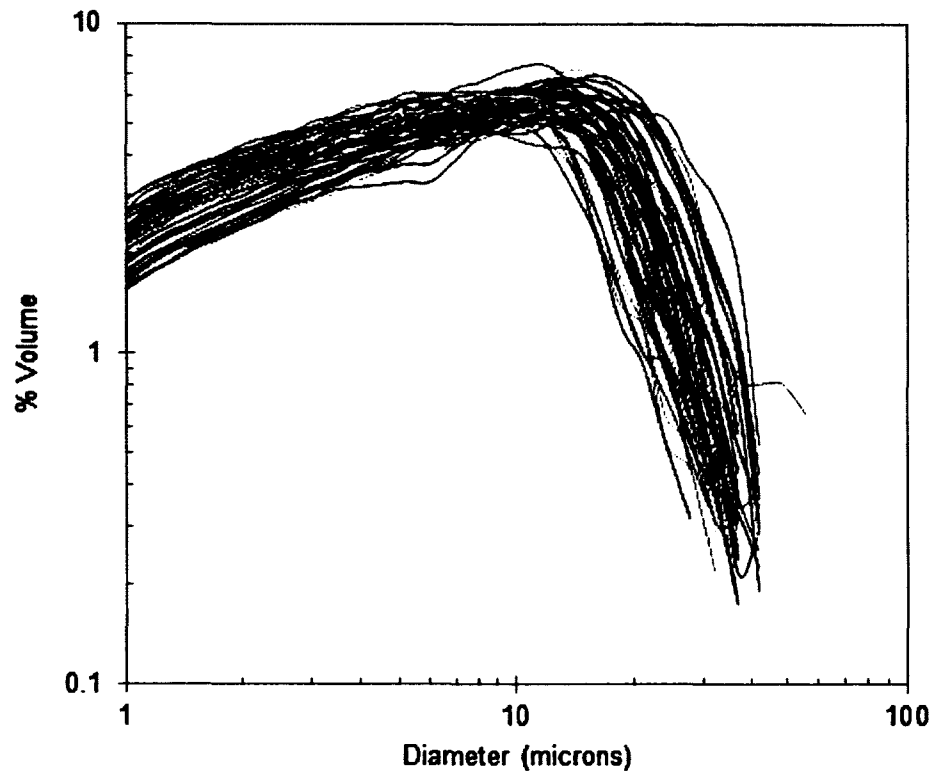
Figure 3.12: Top: DIGS distributions for all processed samples of deposited sediment. Bottom: Groupings of DIGS distributions as defined by entropy analysis.

124

Date	Elevation m, CGVD28	Deposition $g \cdot m^{-3}$	Organic content %	f	m	d_f µm
04-Aug-09	3.40	186.38	7.88	0.69	0.50	11.67
05-Aug-09	3.60	164.12	7.34	0.73	0.45	15.00
06-Aug-09	3.75	140.08	8.16	0.70	0.47	15.25
07-Aug-09	3.91	159.26	7.62	0.81	0.57	21.00
08-Aug-09	4.03	103.79	7.92	0.85	0.53	21.00
09-Aug-09	4.04	98.65	9.09	0.82	0.46	18.75
12-Aug-09	4.16	87.93	8.44	0.87	0.55	23.00
20-Aug-09	5.14	169.01	7.72	0.79	0.48	15.75
21-Aug-09	5.36	254.36	7.24	0.73	0.46	15.50
24-Aug-09	5.14	241.37	8.31	0.74	0.41	15.00
25-Aug-09	4.75	242.85	7.04	0.79	0.44	15.50
26-Aug-09	4.23	328.19	8.55	0.67	0.44	12.50
20-Sep-09	5.69	106.62	7.54	0.84	0.45	21.25
26-Sep-09	3.07	55.02	8.11	0.89	0.55	26.00
27-Sep-09	2.57	55.63	10.08	0.74	0.60	12.00

Table 3.2: Daily-mean values of tidal elevation, sediment deposition, organic content, and results of deposited DIGS, including floc fraction (f), source slope (m), and floc limit (d_f).

Potential Forcing Parameters	Entropy Groups			
	1	2	3	4
Tidal elevation (m, CGVD28)	4.47	**4.73**	4.39	4.24
Suspended sediment concentration ($mg \cdot l^{-1}$)	**127.3**	105.8	96.6	87.3
Velocity ($cm \cdot s^{-1}$)	1.89	**2.11**	1.65	1.64
Turbulent kinetic energy ($J \cdot m^{-3}$)	0.2	**0.26**	0.17	0.18
Bed shear stress ($N \cdot m^{-2}$)	0.021	**0.035**	0.024	0.024
Kolmogorov microscale ($\mu m \cdot 10^{-3}$)	1.74	1.91	1.95	**2.69**
Mean deposition ($g \cdot m^{-2}$)	**195.12**	145.67	164.63	103.12
Organic content (%)	7.97	7.71	7.82	**8.39**
Floc limit (µm)	17.4	16.5	17.5	**18.2**
Floc fraction (0 - 1)	0.70	**0.82**	0.77	0.80

Table 3.3: Mean values of various forcing condition variables measured at the thalweg location in the tidal creek, as grouped by entropy analysis. Maximum values for each parameter are indicated by bold text.
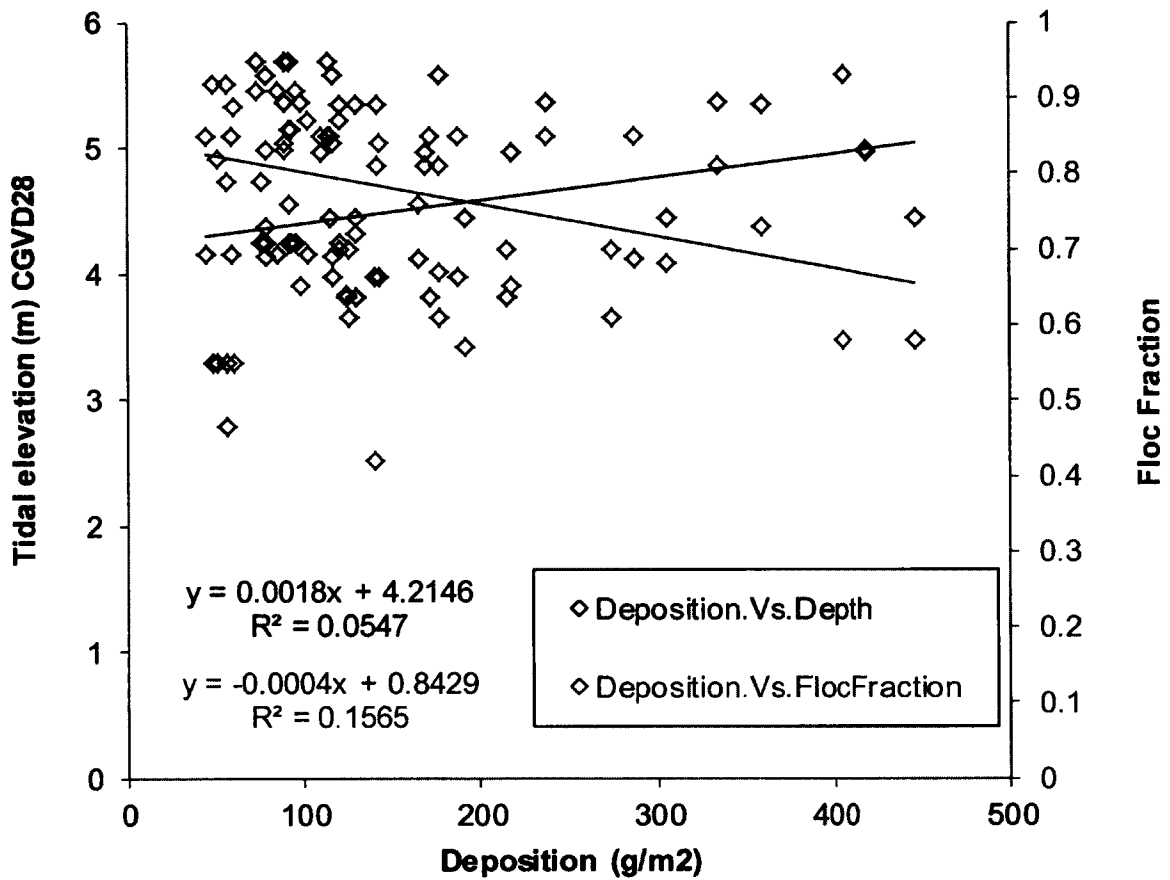
125

Figure 3.13: Scatterplot comparing sediment deposition versus depth, and changes in floc fraction versus depth. Despite low r^2 value, a slight tendency toward reduced deposition with increased floc fraction exists, with a very weak relationship between increased deposition and increasing tidal elevation.

3.6 Discussion

The studied location shows high variability in net deposition linked to topographic influences on flow dynamics in the tidal creek, reflecting the results of Torres and Styles (2007) and O'Laughlin and van Proosdij (in review), which identified topography as a first-order control on in-channel currents. Due to the large tidal range in the Bay of Fundy, complete submergence of high marsh surfaces (e.g. beyond the limits of the drainage basin) promotes ebb-dominance in tidal creeks, due to rapid drainage and the associated pressure gradient, the influence of wind over a large submerged area, and basin-scale influences. Over-marsh tides generally caused more sediment deposition, presumably due to longer inundation time, which can be up to 2 hours longer in the tidal creek than during channel-restricted cycles (Figure 3.6). Incoming suspended sediment concentrations were high, and generally comparable for over-marsh and channel-restricted cycles (> 100 - 200 $mg \cdot l^{-1}$). All tides show a continuous decrease in suspended content from initial concentrations over the duration of tidal cycles, which is most notable and consistent with channel-restricted tides. This reflects results of other tidal creek and salt marsh studies (e.g. Voulgaris and Meyers, 2004; Ralston and Stacey, 2007) as well as that of several Bay of Fundy studies, which indicate continuous deposition throughout tidal cycles (e.g. van Proosdij *et al.*, 2000; Davidson-Arnott *et al.*, 2002; van Proosdij *et al.*, 2006a). While suspended concentration certainly plays a role in the amount of material available for deposition, the relatively constant measurements of incoming concentration

over the sampled tides are not a suitable indicator of net deposition. This directly contrasts results presented by other similar studies (e.g. Voulgaris and Meyers, 2004). Given that incoming suspended sediment concentration is relatively constant at this site (standard deviation of ~40 mg·l^{-1}), excluding tides where suspended sediment concentration was influenced by Hurricane Bill (e.g. Aug 23 and 24), inundation time and surface reworking by energetic ebb flows are likely first-order controls on net deposition on creek banks (Reed, 1988; Torres and Styles, 2007).

Near-bed variations in flow velocity measured by ADVs are echoed by ADCP measurements, which show increased variability (over the profiling range) in response to over-marsh tidal cycles, compared with those that are confined to channels. This follows results presented by Torres and Styles (2007) where increased depth on the marsh surface was found to encourage higher in-channel flow velocity. Flow accelerations associated with channel-restricted tides are limited to lower sections (< 2 m) of the water column during flood tides, and the upper section of the sampling region during ebb phases (2 - 3 m). Conversely, over-marsh tides show flow accelerations that penetrate from the bed to the top of the sampling region (~0.2 - 3 m), most notably during ebb phases, which is supported by estimates of bed shear stress from thalweg- and bank-mounted ADVs (Figure 3.6), and measured variability in suspended concentration of water samples (Figure 3.10). This describes a situation of increased sediment mobility and potential deposition associated with over-marsh tides, similar to that

described by Voulgaris and Meyers (2004) in response to increased particle settling velocities.

Resuspension of newly deposited material by active ebb currents during over-marsh tidal cycles is supported by results from Reed (1988), Torres and Styles (2007) and Voulgaris and Meyers (2004). This is demonstrated here with samples of deposited and suspended sediment, which show evidence of resuspension and considerable variability in net deposition and resuspension effects over the ~2 m^2 sampling plot. Varying retention of material deposited during individual tidal cycles is identifiable through corresponding standard error estimates of mean deposition values, which are consistently greater for over-marsh tides (Figure 3.6). All traps theoretically should receive a similar amount of material during individual tidal cycles, assuming relatively uniform deposition over the ~2 m^2 sampling plot. This indicates increased variability in net deposition across the sampling area in response to increased water depth, associated with more turbulent flows that develop with drainage of high marsh surfaces.

A general threshold depth for total submergence of the marsh surface, as proposed by Temmerman *et al.*, (2005) for development of sheet flows above marsh vegetation and input of tidal water via marsh margins, and by Torres and Styles (2007) for development of flow reversals in creek flows, is supported by evidence of enhanced in-channel flows presented here. Tides that only partially submerge high marsh surfaces do not develop enhanced ebb flows, and thus

promote higher net deposition on creek banks (Figures 3.5 & 3.6). Spring tides measured early in the study did not inundate the marsh surface.

ADV-derived estimates of Kolmogorov microscale (η) and turbulent dissipation (G) suggest that floc formation is most efficient during ebb phases of channel-restricted tides, contrasting results presented in Voulgaris and Meyers (2004). However, over-marsh tides do reflect the general pattern discussed in Voulgaris and Meyers (2004), where increases in η were limited to periods of slack water. An increased efficiency for flocculation during slack tide on over-marsh tidal cycles can be associated with reduced near-bed current velocity measurements and bed shear stress estimates from ADV data, as well as clearance of the water column and reduced current velocity identified in ADCP records. Although it can be expected that values of net deposition will substantiate this with maximal deposition, this is not the case; over-marsh tides did supply generally more material for deposition, but the highest over-marsh tide resulted in deposition that is lower than most channel-restricted tides. This relationship supports the notion that energetic ebb-stage currents associated with increasing tidal amplitude reduce net-deposition through resuspension of newly deposited material. Also, while the efficiency for floc formation was increased during channel-restricted cycles, this did not appear to substantial increase the amount of material deposited to the surface, presumably due to a relatively shorter inundation period in the channel compared with over-marsh tides.

In general, parameterized results (e.g. floc fraction, source slope and floc limit) from DIGS of deposited sediment reflect similar data presented in Christiansen *et al.* (2000) from a microtidal system with similar grain size; those results were determined using a similar particle sizing protocol (Coulter Multisizer IIe). Data presented here show an increased efficiency for floc formation noted on channel-restricted tides, although this did not appear to impact the floc fraction of deposited sediment. Surprisingly, the observed variability in this parameter occurred seemingly independent of changes in maximum tidal amplitude (Table 3.2). In terms of net deposition, tides which contributed less material to the surface showed higher floc fractions (Figure 3.6). Conversely, the highest net deposition measured was in response to a tide showing the lowest mean floc fraction (Figure 3.13). This relationship is contrary to what is demonstrated by Law *et al.* (in press), which describes increased deposition from more flocculated suspensions (analysis with Coulter Multisizer IIe). Results of this study also contradict that of Voulgaris and Meyers (2004), who measured variations in floc density related to the spring-neap cycle with laser in-situ scattering and transmissometery instrumentation. Although data presented here are insufficient for a full investigation of this relationship, it would appear that variations in flocculated parameters noted at this site are also not related to either tidal amplitude or the spring-neap cycle. However, variables describing the flocculated nature of deposited material, including floc fraction (f) and floc limit (d_f), showed high variability within the sampling zone, which was not expected on such a limited spatial scale. This supports a situation of increasing variability in

deposition and resuspension processes with increased tidal energy, which is linked to tidal amplitude (Figure 3.8).

It is possible that floc density, which is known to decrease with floc growth and increasing particle size, due to increased interstitial space and increased incorporation of water (Hill et al., in press; Curran et al., 2007), may be responsible for variation in the settling and deposition patterns of over-marsh and channel-restricted tides. Larger, lower-density flocs that may develop with optimal formation conditions (e.g. high η and low G associated with channel-restricted tides) would have lower settling velocities, potentially retaining more particles in suspension throughout tidal cycles. This, coupled with limitations in the duration of slack tide and total inundation time, would support reduced deposition during channel-restricted tides, following results presented in Curran *et al.* 2007), Van der Lee (2000) and Hill *et al.* (in press).

It is notable that during over-marsh tides, clearance of the water column (at ~1.5 - 2.0 meters above the bed) routinely accelerates +/-10 minutes of high water, following results described by Christiansen et al. (2000) and Voulgaris and Meyers (2004). Ebb phases of over-marsh tides frequently show rapid pulses to high concentrations (up to 1000 mg·l^{-1}) in OBS signals measured at the thalweg location (Figure 3.7). Pulses initiate within 20 - 40 minutes after high tide, and may indicate material being transported to the bed, associated with clearance of material from further up in the water column. However, these increases were limited to the thalweg sampling location, and were typically associated with

increasing flow velocity, suggesting that these pulses may relate to mobilized material moving through the thalweg. To investigate this, an estimated floc still-water settling velocity of 1 $mm \cdot s^{-1}$ was applied, based on results of a variety of flocculation studies in different environments (e.g. Dyer *et al.*, 1996; Dyer and Manning, 1999; Manning *et al.*, 2010; Perjup and Edelvang, 1996; Hill *et al.*, 2000; Mikkelsen *et al.*, 2004), to determine an approximate time required for particles to reach the bed from heights where clearance is observed in ADCP records. Figure 3.9 shows the relationship between signal strength deterioration at 50 cm above the bed and suspended sediment concentration reported by the thalweg OBS sensor at 10 cm above the bed. The temporal sequence of clearance initiating at 1.7 - 2.0 meters above the bed ~10 minutes after high tide is in agreement with the arrival of material at 10 cm above the bed ~30 minutes later, as indicated by OBS measurements (Figure 3.9). Under the assumed settling velocity of 1 $mm \cdot s^{-1}$, particles should take ~30 minutes to reach the OBS measurement volume (at 10 cm above the bed), from 1.7 - 2.0 meters above. There is sufficient time for this sequence of events to elapse during over-marsh tides. However, the relatively shorter inundation period associated with channel-restricted tidal cycles is not as accommodating, and particles settling from ~2 meters above the bed are not allowed the time required to reach the bed.

While the 30-minute period following high tide on channel-restricted tidal cycles shows clearance of the mid to upper water column (e.g. 170 cm above the bed), settling is not initiated nearer the bed (e.g. 50 cm above the bed). The

opposite is true for over-marsh tides, where sustained reductions in current velocity and turbulence at slack tide allow for transfer of material from the mid to upper water column to the bed. This fundamental difference in depositional mechanisms is likely a simple response to increased inundation time associated with over-marsh tides, and is independent of variations in concentration or the flocculated nature of suspended materials.

Entropy analysis was performed on DIGS of deposited sediments to investigate the dominance of forcing conditions. Entropy analysis has been applied to DIGS distributions before, namely by Mikkelsen *et al.* (2007) for consideration of marine in-situ floc size spectra. The nominal number of groups determined here from entropy analysis of deposited sediment DIGS is four (Figure 3.12), which indicates potential control of four unique forcing conditions. Group 2 (blue line) contains tides with the greatest maximum depths, highest mean current velocities, and marginally higher mean floc fractions (Table 3.3). However, net deposition resulting from tides in group 2 was comparatively less than that of other groups. The response of creek banks to more energetic ebb phases associated with over-marsh tides is demonstrated by this variability, through re-working of newly deposited material by increased current velocities and the associated kinetic energy, turbulence and bed shear stresses which are largely responsible for reducing net deposition. While the mass held in flocs can be slightly higher during over-marsh tidal cycles, any existing relationship with increased deposition is obscured by re-working of creek banks during ebb

phases. By contrast, group 1 (red line) is composed of tides that show the smallest proportion of matter held in flocs, maximum depth nearest the bankfull level, and the highest amount of net deposition. Tides from this group also showed the highest suspended sediment concentration at the thalweg location, and had the highest occurrence of coarser material. Overall, this suggests that increased deposition is not directly linked to increases in floc fraction. The presence of larger grain sizes in group 1, demonstrated by the right side of the curve (Figure 3.12), as well as higher suspended sediment concentration, indicates potentially increased energy and carrying capacity associated with this group of tides. However, as the mean maximum depth for this group is near the bankfull level, it is most likely that exposed creek surfaces were not subjected to the enhanced ebb flows of deeper, over-marsh tides, which remove newly deposited material and reduce net deposition.

Entropy analysis also showed that of the four daily sediment samples processed for grain size analysis, each typically falls into a different entropy group. The anticipated division, where samples of deposited sediment collected on one particular day would be similar to one another and fall into one entropy group, was only realized twice, in response to channel-restricted tides (Aug 7 and Sept 26). This suggests that entropy analysis would be most informative when performed on DIGS datasets yielded from each trap location, rather than a comparison of all samples together. This reiterates the degree of variability measured over the 2 m² sampling area, and suggests that mean values per day

may be the best way to characterize a generalized value of net deposition on creek banks.

Regression analysis (Figure 3.13) demonstrates that increased deposition on creek banks is associated with increased water depth, although this relationship is not statistically significant. This relation is likely a response to increased inundation time associated with higher maximum tidal elevation. It is also shown that the mass of sediments held in flocculated form decreases with increasing tidal amplitude. While r^2 values are low, this can largely be accounted for by the high variability encountered daily over the sampling zone. Although suspended sediments show variability in concentration and their flocculated nature, both concentration and the degree of flocculation can ultimately be considered as consistently high in sheltered hypertidal creeks. This implies that higher net deposition is likely not associated with an increase in the mass of suspended sediment held in flocculated form.

3.7 Conclusions

Samples of deposited and suspended sediments were collected in a hypertidal creek in the Bay of Fundy, over 15 individual tidal cycles and across various stages of the spring-neap cycle. Samples were analysed for grain size, organic content and the flocculated nature of constituent particles. Disaggregated inorganic grain size analysis performed with a Coulter Multisizer III indicates that variations in the proportion of suspended matter held in flocs,

while high, is not directly linked to deposition processes on creek banks (Figure 3.11). The high floc fraction in the tidal creek is likely driven by routinely high suspended sediment concentration, as well as energy levels that are frequently favourable for floc formation. Turbulence levels estimated from ADV records suggest that channel-restricted tidal cycles show the greatest potential for the formation of large flocs, along with calm flow conditions that are ideal for particle settling. However, presumably due to limitations in inundation time, deposition was comparatively less with channel-restricted tides. The influence of inundation time is further suggested by a relatively consistent incoming suspended sediment concentration, excluding high concentration motivated by rainfall. Concentration at the thalweg is routinely 100 – 200 mg·l^{-1} at the initial stages of flood tides under non-storm conditions, and does not appear to vary substantially with changes in maximum tidal elevation. The magnitude of ebb-phase flow velocity is directly linked to tidal elevation through topographically-influenced flow patterns in the creek, and on over-marsh cycles where the marsh is well submerged (> 30 cm depth), ebb flows appear to regularly modify newly deposited materials and exert a large degree of control on net deposition on creek banks. This equilibrium relationship is necessary to ensure that tidal creeks are not completely infilled.

Variability in depositional characteristics (e.g. total amount, floc fraction) was identified over the ~2 m^2 sampling area where deposited sediments were obtained. Entropy analysis performed on DIGS of deposited sediments indicates that independent samples collected during individual tidal cycles frequently fall

into different groups. This highlights the differential effects of ebb-phase flows and resuspension on creek banks, and suggests that variability in net deposition can occur over limited spatial scales. It also demonstrates the necessity of considering each trap independently, owing to these differential effects of ebb flows and varied resuspension over the sampling plot. It would perhaps be helpful in future work to place traps at discrete locations rather than develop mean values to characterize deposition over a larger plot.

In the context of tidal power generation, results of this study suggest that Bay of Fundy salt marshes exist under a range of highly variable depositional conditions, which are not clearly linked to changing suspended sediment concentration or the nature of suspended materials, tidal elevation or the spring-neap cycle. Suspended concentration and the degree of flocculation can ultimately be considered to be consistently high in sheltered hypertidal creeks due to the consistent abundance of fine-grained materials. Variability in net deposition in these areas may be most sensitive to topographically-influenced flow dynamics and resuspension of newly introduced material, compared with changes in the flocculated nature of incoming suspended sediments. This suggests that moderate changes in tidal amplitude caused by energy extraction via tidal power generation may impact the distribution of creek-deposited material to the marsh surface, but will not have a marked effect on the flocculated nature of suspended sediments in confined, sheltered tidal creeks. This is an important step in a thorough understanding the vulnerability, and more importantly the

resilience, of salt marsh environments in the Bay of Fundy and their potential response to energy extraction.

Acknowledgements

References

Allen JRL. 2000. Morphodynamics of Holocene salt marshes: a review sketch from the Atlantic and Southern North Sea Coasts of Europe. *Quartemary Science Reviews* **19**: 1155-1231.

Amos C. 1987. Fine-grained sediment transport in Chignecto Bay, Bay of Fundy, Canada. *Continental Shelf Research* 7 (11/12): 1295-1300.

Amos CL, Mosher DC. 1985. Erosion and deposition of fine-grained sediments from the Bay of Fundy. *Sedimentology* 32: 815-832.

Barnes MP, O'Donoghue T, Alsina JM, Baldock TE. 2009. Direct bed shear stress measurements in a bore-driven swash. *Coastal Engineering* 56: 853-867. DOI: 10.1016/j.coastaleng.2009.04.004

Bartholomä A, Kubicki A, Badewien TH, Flemming BW. 2009. Suspended sediment transport in the German Wadden Sea—seasonal variations and extreme events. *Ocean Dynamics* 59: 213-255.

Biron PM, Robson C, Lapointe MF, Gaskin SJ. 2004. Comparing different methods of bed shear stress estimates in simple and complex flow fields. *Earth Surface Processes and Landforms* 29: 1403-1415. DOI: 10.1002/esp.1111

Blanton JO, Lin G, Elston SA. 2002. Tidal current asymmetry in shallow estuaries and tidal creeks. *Continental Shelf Research* 22: 1731-1743.

Blott S. 2010. GRADISTAT (version 8.0): A grain size distribution and statistics package for the analysis of unconsolidated sediments by sieving or laser granulometer. Kenneth Pye Associates Ltd., Berkshire, UK.

Boorman LA. 2003. Saltmarsh Review. An overview of coastal saltmarshes, their dynamic and sensitivity characteristics for conservation and management. *JNCC Report, No. 334.*

Boorman, 1999. Salt marshes - present functioning and future change. *Mangroves and Salt Marshes* 3: 227-241.

Bowron T, Neatt N, van Proosdij D, Lundholm J, Graham J. 2009. Macro-tidal salt marsh ecosystem response to culvert expansion. *Restoration Ecology* 19 (3): 307-322. DOI: 10.1111/j.1526-100X.2009.00602.x

Bryden IG, Grinsted T, Melville GT. 2004. Assessing the potential of a simple channel to deliver useful energy. *Applied Ocean Research* 26: 198-204. doi:10.1016/j.apor. 2005.04.001

Christiansen T, Wilberg PL, Milligan TG. 2000. Flow and sediment transport on a tidal salt marsh surface. *Estuarine, Coastal and Shelf Science* 50: 315-331. DOI: 10.1006/ecss.2000.0548

Charlier, RH. 2003. A "sleeper" awakes: tidal current power. *Renewable and Sustainable Energy Reviews* 7: 515-529.

Craft C, Clough J, Ehman J, Joye S, Park R, Pennsings S, Guo H, Machmuller M. 2009. Forecasting the effects of accelerated sea-level rise on tidal marsh ecosystem services. *Frontiers in Ecology and the Environment* 7(2): 73-78. DOI: 10.1890/070219.

Curran KJ, Hill PS, Schnell TM, Milligan TG, Piper DJW. 2004. Inferring the mass fraction of floc-deposited mud: application to fine-grained turbidites. *Sedimentology* 51: 927-944. DOI: 10.1111/j.1365-3091.2004.00647.x

Davidson-Arnott RGD, van Proosdij D, Ollerhead J, Schostak L. 2002. Hydrodynamics and sedimentation in salt marshes: examples from a macrotidal marsh, Bay of Fundy. *Geomorphology* 48: 209-231

deGelleke, L. 2011. Sediment dynamics during Heinrich event H1 inferred from grain size. M.Sc. Thesis, Dalhousie University. 78 pp.

Desplanque C, Mossman DJ. 2001. Bay of Fundy tides. *Geoscience Canada* 28 (1): 1-11.

DFO. 2009. Department of Fisheries and Oceans Assessment of Tidal and Wave Energy Conversion Technologies in Canada. DFO Canadian Science Advisory Secretariat Science Advisory Report, 2009/064.

Dronkers J. 1986. Tidal asymmetry and estuarine morphology. *Netherlands Journal of Sea Research* 20 (2/3): 117-131

Donnelly JP, Bertness MD. 2001. Rapid shoreward encroachment of salt marsh cordgrass in response to accelerated sea-level rise. *Proceedings of the National Academy of Sciences of the United States of America* 98 (25):14218-14223

Dupont F, Hannah C, Greenberg D. 2005. Modelling the Sea Level in the Upper Bay of Fundy. *Atmosphere-Ocean* 43 (1): 33-47

Dyer KR, Manning AJ. 1999. Observation of the size, settling velocity and effective density of flocs and their fractal dimensions. *Journal of Sea Research* 41: 87-95.

Dyer KR, Cornelisse J, Dearnaley MP, Fennessy MJ, Jones SE, Kappenberg J, McCave IN, Pejrup M, Puls W, van Leussen W, Wolfstien K. 1996. A comparison of *in situ* techniques for estuarine floc settling measurements. *Journal of Sea Research* 36 (1): 15-29.

Eisma D. 1986. Flocculation and de-flocculation of suspended matter in estuaries. *Netherlands Journal of Sea Research* 20 (2/3): 183-199.

Friedrichs CT, Perry JE. 2001. Tidal salt marsh morphodynamics: a synthesis. *Journal of Coastal Research* 27: 7-37

French JR, Stoddart DR. 1992. Hydrodynamics of Salt Marsh Creek Systems: Implications for Marsh Morphological Development and Material Exchange. *Earth Surface Processes and Landforms* 17: 235-252

Forrest J, Clark NR. 1989. Characterizing grain-size distributions: evaluation of a new approach using a multivariate extension of entropy analysis. *Sedimentology* 36: 711-722.

Fugate DC, Friedrichs CT. 2002. Determining concentration and fall velocity of estuarine particle populations using ADV, OBS and LISST. *Continental Shelf Research* 22:1867-1886.

Gordon DC. 1994. Intertidal ecology and potential power impacts, Bay of Fundy, Canada. *Biological Journal of the Linnean Society* 51: 17-23.

Hill DC, Jones SE, Prandle D. 2003. Derivation of sediment resuspension rates from acoustic backscatter time-series in tidal waters. *Continental Shelf Research* 23: 19-40.

Hill PS, Milligan TG, Geyer WR. 2000. Controls on the effective settling velocity of suspended sediment in the Eel River flood plume. *Continental Shelf Research* 20: 2095-2111.

Hill PS, Newgard JP, Milligan TG. In press. Flocculation on a muddy intertidal flat in Willapa Bay, Washington, Part II: Observations of suspended particle size in a secondary channel and adjacent flat. *Continental Shelf Research.* 44 pp.

Hoitink AJF, Hoekstra P. 2005. Observations of suspended sediment from ADCP and OBS measurements in a mud-dominated environment. *Coastal Engineering* 52: 103-118. DOI: 10.1016/j.coastaleng.2004.09.005

Holdaway GP, Thorne PD, Flatt D, Jones SE, Prandle D. 1999. Comparison between ADCP and transmissometer measurements of suspended sediment concentration. Continental Shelf Research 19: 421-441.

Johnston R J, Semple RK. 1983. Classification using information statistics. Geo-Books, Norwich. 43 pp.

Karas AN. 1978. System planning for Bay of Fundy tidal power development. *IEEE Transactions on Power Apparatus and Systems* PAS-97 (5): 1600-1606.

Karsten RH, McMillan JM, Lickley MJ, Haynes RD. 2008. Assessment of tidal current energy in the Minas Passage, Bay of Fundy. *Proceedings of the Institution of Mechanical Engineers* 222 (A-J): 493-507.

Kim SC, Friedrichs CT, Maa JP-Y, Wright LD. 2000. Estimating bottom stress in tidal boundary layer from acoustic Doppler velocimeter data. *Journal of Hydraulic Engineering, ASCE* **126** (6): 399-406

Kim SC, Voulgaris G. 2003. Estimation of suspended sediment concentration in estuarine environments using acoustic backscatter from an ADCP. *Proceedings of the Fifth International Conference on Coastal Sediments*, 2003. 10pp.

Kranck K. 1980. Experiments on the significance of flocculation in the settling of fine-grained sediment in still water. *Canadian Journal of Earth Sciences* **17**: 1517-1526.

Kranck K. 1981. Particulate matter grain-size characteristic and flocculation in a partially mixed estuary. *Sedimentology* **28**: 107-114.

Kranck K, Milligan TG. 1991. Grain size in oceanography. In: Syvitski, JPM [ed]. *Principles, Methods, and Applications of Particle Size Analysis.* Cambridge University Press: 368 pp.

Kranck K, Milligan TG. 1985. Origin of grain size spectra of suspension deposited sediment. *Geo-Marine Letters* **5**: 61-66.

Kranck K, Smith P, Milligan TG. 1996a. Grain-size characteristics of fine-grained unflocculated sediments I: 'one-round' distributions. *Sedimentology* **43**: 589-596.

Kranck K, Smith P, Milligan TG. 1996b. Grain-size characteristics of fine-grained unflocculated sediments II: 'multi-round' distributions. *Sedimentology* **43**: 597-606.

Kranck, K., and T. G. Milligan (1992), Characteristics of Suspended Particles at an 11-Hour Anchor Station in San Francisco Bay, California, *J. Geophys. Res.*, 97(C7), 11,373-11,382, doi:10.1029/92JC00950

Law BA, Hill PS, Milligan TG, Curran KJ, Wiberg PL, Wheatcroft RA. 2008. Size sorting of fine-grained sediments during erosion: Results from the western Gulf of Lions. *Continental Shelf Research* **28**: 1935-1946.

Law BA, Milligan TG, Hill PS, Newgard JP, Wheatcroft RA, Wilberg PL. In press. Flocculation on a muddy intertidal flat in Willapa Bay, Washington, Part I: A regional survey of the grain size of surficial sediments. *Continental Shelf Research.* 44 pp.

Lawrence DSL, Allen JRL, Havelock GM. 2004. Salt marsh morphodynamics: An investigation of tidal flows and marsh channel equilibrium. *Journal of Coastal Research* **20**: 301-316.

Lee STY, Deschamps C. 1978. Mathematical model for economic evaluation of tidal power in the Bay of Fundy. *IEEE Transactions on Power Apparatus and Systems* PAS-97 (5): 1769-1778.

Lynch JF, Gross TF, Brumley BH, Filyo RA. 1991. Sediment concentration profiling in HEBBLE using a 1-Mhz acoustic backscatter system. *Marine Geology* 99: 361-385.

MacDonald GK, Noel EN, van Proosdij D, Chumra GL. 2010. The legacy of agricultural reclamation on channel and pool networks of Bay of Fundy salt marshes. *Estuaries and Coasts* 33: 151-160. DOI 10.1007/s12237-009-9222-4

Manning AJ, Bass SJ. 2006. Variability in cohesive sediment settling fluxes: Observations under different estuarine tidal conditions. *Marine Geology* 235: 177-192. DOI: 10.1016/j.margeo.2006.10.013

Manning AJ, Dyer KR. 2002. A comparison of floc properties observed during neap and spring tidal conditions. In: *Fine Sediment Dynamics in the Marine Environment*, Winterwerp JC, Kranenburg C (eds). Elsevier: Amsterdam; 233-250.

Manning AJ, Langston WJ, Jonas PJC. 2010. A review of sediment dynamics in the Severn Estuary: Influence of flocculation. *Marine Pollution Bulletin* 61: 37-61.

Mikkelsen OA, Curran KJ, Hill PS, Milligan TG. 2007. Entropy analysis of in situ particle size spectra. *Estuarine, Coastal and Shelf Science* 72: 615-625.

Mikkelsen OA, Milligan TG, Hill PS, Moffatt D. 2004. INSSECT— an instrumented platform for investigating floc properties close to the seabed. *Limnology and Oceanography: Methods* 2: 226-236.

Milligan TG, Law BA. 2005. The effect of marine agriculture on fine sediment dynamics in coastal inlets. In: Hargrave, B. [ed]. Environmental Effects of Marine Finfish Aquaculture. *The Handbook of Environmental Chemistry* 5: Water Pollution. Springer, Berlin Heidelbrg New York, 467 pp.

Milligan TG, Loring DH. 1997. The effect of flocculation on the size distributions of bottom sediment in coastal inlets: implications for contaminant transport. *Water, Air and Soil Pollution* 99: 33-42.

Milligan TG, Kineke GC, Blake AC, Alexander CR, Hill PS. 2001. Flocculation and Sedimentation in the ACE Basin, South Carolina. *Estuaries* 24 (5) Dedicated Issue: Processes and Products of the Estuarine Turbidity Maximum: Symposium Papers from the 15th Biennial Estuarine Research Federation Conference: 734-744.

Milligan TG, Kranck K. 1991. Electroresistance particle size analyzers. In: Syvitski, JPM. [ed]. *Principles, methods and applications of particle size analysis.* Cambridge University Press, New York, 368 pp.

Milligan TG, Hill PS. 1998. A laboratory assessment of the relative importance of turbulence, particle composition, and concentration in limiting maximal floc size and settling behaviour. *Journal of Sea Research* **39**: 227-241.

Neumeier U, Amos CL. 2006. The influence of vegetation on turbulence and flow velocity in European salt-marshes. *Sedimentology* **53**: 259-277. DOI: 10.1111/j.1365-3091.2006.00772x

OEER. 2008b. Final Report: Background Report for the Fundy Tidal Energy Strategic Environmental Assessment. Prepared by Jacques Whitford Consultants for the OEER Association. Project No. 1028476. 291 pp.

O'Laughlin C, van Proosdij D. In review. Influence of varying tidal prism on hydrodynamics and sedimentary processes in a hypertidal salt marsh creek. Submitted to *Earth Surface Processes and Landforms*, March 2012.

Orpin AR, Kostylev VE. 2006. Towards a statistically valid method of textual seafloor characterization of benthic habitats. *Marine Geology* **225**: 209-222.

Pejrup M, Mikkelsen OA. 2010. Factors controlling the field settling velocity of cohesive sediment in estuaries. *Estuarine,Coastal and Shelf Science* **87**: 177-185.

Perjup M, Edelvang K. 1996. Measurements of *in situ* settling velocities in the Elbe estuary. *Journal of Sea Research* **36**: 109-113.

Polagye BL, Malte PC. 2010. Far-field dynamics of tidal energy extraction in channel networks. *Renewable Energy* **36**: 222-234. DOI:10.1016/j.renene.2010.06.025

Polagye B, Van Cleve B, Copping A, Kirkendall K (eds). 2011. Environmental effects of tidal energy development. *U.S. Dept. Commerce, NOAA Tech. Memo.* 181 pp.

Puleo AJ, Johnson RV, Butt T, Kooney TN, Holland KT. 2007. The effect of air bubbles on optical backscatter sensors. *Marine Geology* **230**: 87-97. DOI:10.1016/j.margeo. 2006.04.008

Ralston DK, Stacey MT. 2007. Tidal and meteorological forcing of sediment transport in tributary mudflat channels. *Continental Shelf Research* **27**: 1510-1527.

Reed D, Spencer T, Murray AL, French JR, Leonard L. 1999. Marsh surface sediment deposition and the role of tidal creeks: implications for created and managed coastal marshes. *Journal of Coastal Conservation* 5: 81-90.

Sanders RE, Baddour E. 2008. Engineering issues in the harvest of tidal energy in the Bay of Fundy, Canada. *Report to the Engineering Committee on Oceanic Resources Symposium.* 10 pp.

Seoni RM. 1979. Major electrical equipment proposed for tidal power plants in the Bay of Fundy. *IEEE Transactions on Power Apparatus and Systems* PAS-89 (5): 1750-1760.

Sheldon RW. 1972. Size separation of marine seston by membrane and glass-fiber filters. *Limnology and Oceanography* 17 (3): 494-498.

Sheldon RW, Sutcliffe WH. 1969. Retention of marine particles by screens and filters. *Limnology and Oceanography* 14 (3): 441-444.

Smith SJ, Friedrichs CT. 2011. Size and settling velocities of cohesive flocs and suspended sediment aggregates in a trailing suction hopper dredge plume. *Continental Shelf Research* 31: 550 - 563.

Soulsby RL. 1983. The bottom boundary layer of shelf seas. *Elsevier Oceanography Series* 35: 189-266.

Sun X, Chick JP, Bryden IG. 2008. Laboratory-scale simulation of energy extraction from tidal currents. *Renewable Energy* 23: 1267-1274.

Temmerman S, Bouma TJ, Govers G, Lauwaet D. 2005. Flow paths of water and sediment in a tidal marsh: relations with marsh development stage and tidal inundation height. *Estuaries* 28 (3): 338-352.

Thorne PD, Hardcastle PJ, Soulsby RL. 1993. Analysis of acoustic measurements of suspended sediment. *Journal of Geophysical Research* 98 (C1): 899- 910.

Thorne PD, Hanes DM. 2002. A review of acoustic measurements of small-scale sediment processes. *Continental Shelf Research* 22: 603-632.

Torres R, Styles R. 2007. Effects of topographic structure on salt marsh currents. *Journal of Geophysical Research* 112: 1-14. DOI: 10.1029/2006JF000508

Turk TR, Risk MJ, Hirtle RWM, Yeo RK. 1980. Sedimentological and biological changes in the Windsor mudflat, and area of induced siltation. *Canadian Journal of Fisheries and Aquatic Sciences* **37**: 1387-1397.

van Der Lee WTB. 2000. Temporal variation of floc size and settling velocity in the Dollard estuary. *Continental Shelf Research* **20**: 1495-1511.

van Proosdij D. 2001. Spatial and temporal controls on the sediment budget of a macro-tidal saltmarsh. Ph.D. Diss., University of Guelph, 2001.

van Proosdij D, Lundholm J, Neatt N, Bowron T, Graham J. 2010. Ecological re-engineering of a freshwater impoundment for salt marsh restoration in a hypertidal system. *Ecological Engineering* **36**: 1314-1332. DOI: 10.1016/j.ecoleng.2010.06.008

van Proosdij D, Milligan T, Bugden G, Butler K. 2009. A tale of two macro-tidal estuaries: Differential morphodynamic response of the intertidal zone to causeway construction. *Journal of Coastal Research*, Special Issue **56**: 772-776.

van Proosdij D, Ollerhead J, Davidson-Arnott RGD. 2000. Controls on suspended sediment deposition over single tidal cycles in a macrotidal saltmarsh, Bay of Fundy, Canada. *Journal of the Geological Society*, Special Publications **175**: 43-57

van Proosdij D, Ollerhead J, Davidson-Arnott RGD. 2006. Seasonal and annual variations in the volumetric sediment balance of a macro-tidal salt marsh. *Marine Geology* **225**: 103-127. DOI: 10.1016/j.margeo.2005.07.009

Voulgaris G, Meyers ST. 2004. Temporal variability of hydrodynamics, sediment concentration and sediment settling velocity in a tidal creek. *Continental Shelf Research* **24**: 1659-1683. DOI: 10.1016/j.csr.2004.05.006

Whitehouse, R., Soulsby, R., Roberts, W. and Mitchener, H. (2000). *Dynamics of estuarine muds*. Thomas Telford Publishing, London, 210 pp.

Williams ND, Walling DE, Leeks GTL. 2006. High temporal resolution in situ measurement of the effective particle size characteristics of fluvial suspended sediment. *Water Research* **41** (**5**): 1081-1093.

Winterwerp JC. 2002. On the flocculation and settling velocity of estuarine mud. *Continental Shelf Research* **22**: 1339-1360.

Winterwerp JC, van Kesteren WGM. 2004. Introduction to the physics of cohesive sediment in the marine environment. *Developments in Sedimentology* **56**: 466 pp.

Woolfe KJ, Michibayashi K. 1995. "Basic" entropy grouping of laser-derived grain-size data: An example from the Great Barrier Reef. *Computers and Geosciences* 21 (4): 447-462.

Yeo RK, Risk MJ. 1979. Fundy tidal power: Environmental sedimentology. *Geoscience Canada* 6 (3): 115-121.

CHAPTER 4: HYDRODYANAMICS AND SEDIMENTATION IN A HYPERTIDAL CREEK: A SYNTHESIS

As discussed in the previous chapters, the capacity of salt marshes to perform various ecosystem and storm protection services is directly dependent on the continued import and retention of sedimentary material, necessary to maintain equilibrium with rising sea level (Donnelly and Bertness, 2001; Reed *et al.*, 1999; Morris *et al.*, 2002). In order for minerogenic marshes to continually function as critical habitat in biological production, and as sites capable of energy absorption, the current state of equilibrium with sea level should be at best modestly disturbed (Whitford, 2008). It has been demonstrated that powerful estuarine systems in the Bay of Fundy region become large-scale depositional sinks following modification and disruption of natural hydrodynamics and energy (e.g. van Proosdij et al., 2009; van Proosdij et al., 2006; Amos and Mosher, 1985; Turk *et al.*, 1980). A tidal creek is the subject of study here, because creeks are the main conduits for sediment transport into marshes, to be spread over high marsh surfaces and trapped by vegetation, contributing to the vertical growth of the marsh platform (Allen, 2000; Friedrichs and Perry, 2001; van Proosdij 2006b; Voulgaris and Meyers 2004).

Deposition in the intertidal zone is a complex function of variables controlling sediment availability and the opportunity for deposition (van Proosdij *et al.*, 2006a). Intrinsic controls that influence salt marsh and tidal creek processes (e.g. topography, tidal prism), and others which are externally-driven (e.g. suspended sediment concentration, the flocculated nature of materials, changing tidal amplitude and current velocity) were investigated as to their

influence on sediment deposition patterns in a hypertidal creek. It has been shown through research presented here that tides which inundate the marsh surface show very different velocity patterns compared with those that remain restricted to channels, following the conclusions of similar studies (e.g. Torres and Styles, 2007; Lawrence *et al.*, 2004; French and Stoddart, 1992). Results presented in this study emphasize this (e.g. Figures 2.6 & 2.7), and reinforce the idea of a threshold depth on marsh surfaces, associated with the development of flow reversals in tidal creeks (Torres and Styles, 2007), as well as sheet flows above marsh vegetation (Temmerman *et al.*, 2005). Data from this study show that the development of early ebb-stage flow accelerations were limited to tides that surpassed this general threshold (~0.5 meters above high marsh). Also, the degree to which ebb flows are accelerated as water depth falls below the bankfull level is linked to the maximum inundation depth on the marsh surface. This is seen here to be a primary control on net deposition on creek banks.

Research by Karsten *et al.* (2008) shows that proposed tidal power installations in the Minas Passage will result in an overall lowering of tidal amplitude in the Minas Basin. An extraction of 2.5 gigawatts of tidal energy would result in a moderate 5% decrease in tidal amplitude in the Minas Basin. Such a decrease in tidal amplitude would reduce the number of over-marsh tidal events by a similar figure. It of course follows that the occurrence of channel-restricted tides will increase, at the expense of over-marsh cycles. The frequency of bankfull (or 'marshfull') tides, such as those identified by Bayliss-Smith *et al.*

151

(1979) and discussed by French and Stoddart (1992), can potentially increase as well. In this case, amplified erosion of creek banks driven by prolonged wave access to marsh edges may create an additional sediment source for deposition in creeks, and could act to destabilize salt marsh platforms over time (Friedrichs and Perry, 2001; Allen, 2000). Accordingly, a decrease in inundation frequency of high marsh surfaces may impose a sediment deficit in these areas, with less material being distributed to the marsh surface from tidal creeks. This can impact marsh and channel equilibrium, vegetation community structure, ecological productivity, and the transfer of energy through marsh systems (Smith and Friedrichs, 2011; Craft *et al.*, 2009; Bertness, 1991).

The relative availability of sediment in tidal creeks can be viewed as a controlling factor for deposition on the marsh surface, which can be applied to infer the relative depositional capacity of both channel-restricted and over-marsh tides. Incoming suspended sediment concentration (> 100 $mg \cdot l^{-1}$), and the flocculated nature of deposited materials (0.67 - 0.89), were both relatively high for all tidal conditions sampled at Starrs Point. The measured tide that peaked near the bankfull level (August 26th) maximized the potential inundation time for a tide that did not flood the marsh surface, which allowed reduction in early ebb stage turbulence and flow velocity, and in turn encouraged an extended depositional period. Combined with a high incoming suspended concentration, large amounts of deposition were seen to occur in response to this particular tidal cycle.

In a hypertidal environment such as the Bay of Fundy, where the maximum tidal range is 16 metres, bankfull tides like the one on August 26th may be responsible for peak sediment import and deposition in tidal creeks, providing large amounts of material that is eventually distributed to and deposited on marsh surfaces by over-marsh cycles. As a result, the geomorphic 'importation' workload may be skewed towards bankfull tides for net sediment import, leaving over-marsh tides for distribution of materials from creek banks onto the marsh surface. With change to this relationship (e.g. the frequency of occurrence of any of the three types of tidal cycles), the current balance of sediment import, distribution and export will be forced to adapt. It is possible that an increase in channel-restricted tides will promote increasingly rapid deposition in tidal creeks, as less material that is imported is either distributed to the marsh surface, or removed by ebb-stage flow in response to over-marsh tidal cycles. The importance of those over-marsh cycles that do occur will be increased, as fewer will be available to mobilize and distribute sediments to the marsh surface with an overall reduction in tidal amplitude.

It is possible that variations in deposition are associated with changing floc dynamics in the creek, impacted by variable flow characteristics and turbulent conditions (Curran *et al.*, 2004; Dyer and Manning, 1999; Kranck and Milligan, 1992). The size distribution suspended materials can be applied to deduce sedimentary origin and provide insight into conditions of the depositional environment (Milligan and Loring, 1997; Curran *et al.*, 2004). Velocity-derived

estimates of Kolmogorov microscale (η) and dissipation parameter (G) from the tidal creek suggest that floc formation was most efficient during ebb phases of channel-restricted tides. Turbulence levels associated with typical channel-restricted tidal cycles were sufficient for formation of flocs up to 50% larger than more turbulent over-marsh tides. However, this did not appear to impact the mass fraction of sediments held in flocs, as determined through DIGS analysis of deposited sediment samples. While some variability was observed in mean floc fraction over the study period, this occurred seemingly independent of changes in maximum tidal amplitude. In regard to net deposition, tides that showed higher floc fractions contributed less material to the surface overall. In contrast, the maximum net deposition measured was in response to a tide showing the lowest mean floc fraction.

Kinetic energy was found to be higher with over-marsh tidal cycles, although this has been attributed to variable influences of topography on ebb-stage flows at this site. Incoming tidal energy was relatively similar for over-marsh and channel-restricted tides (Figure 3.8), and while flocculation was routinely high (Figure 3.6), a causative link between these two processes was not developed through this study. Therefore, it cannot be said for certain whether reduced tidal energy in the Minas Basin due to tidal power installations will alter the flocculated nature of suspended sediment in intertidal zones, based on the results of this study. A decrease in tidal energy may result in an overall reduction of material in suspension in the larger Minas Basin, which would have obvious

154

impacts for intertidal sediment supply. However, while reduced tidal amplitude has been shown to potentially be a source of increased sensitivity for marsh environments, the dominance of salt marshes in the Bay of Fundy, under such highly variable conditions in their current equilibrium, suggests that systems will adapt to moderate changes in tidal energy.

Net deposition, floc fraction (f) and floc limit (d_f) showed variability within the ~2 m^2 sampling zone that was not expected on such a limited spatial scale. This suggests high variability in net deposition over small spatial scales on creek banks in response to ebb-stage resuspension processes. It is possible that upstream sediment traps were preferentially exposed to enhanced ebb-stage currents, allowing more ebb-stage resuspension to occur at that location. This would suggest that variation in per-tide sediment weight and volume may be an artifact of the sampling method, such as the placement of the traps over the sampling area.

Figure 4.1 demonstrates variability in net deposition and the flocculated nature of samples, in response to one over-marsh tidal cycle. Figure 4.2 shows variability in d90 (diameter of the 90th percentile, in μm) over the study period. Entropy analysis revealed that of the four sediment trap locations sampled daily, the DIGS distribution of each typically fell into a different entropy group. This suggests that entropy analysis would be most informative when performed on DIGS datasets representative of each trap location, rather than completing a comparison of all samples together. This reiterates the degree of variability

measured over the ~2 m² sampling area, but does not provide further explanation of why this variation occurred. This does suggest that mean per-day values may be the best way to generalize daily net deposition on creek banks. In addition, such variability could advocate a small-scale investigation to consider the spatial unevenness of erosion and resuspension across creek banks, presuming these affects are overprinted on relatively homogenous deposition. In addition, the development of an in-situ instrument to accurately measure the contributions of individual tidal cycles while excluding ebb-phase modifications of sediment surfaces would be an ideal approach to this problem. A one-way, closing sediment trap should be considered, with the ability to restrict access by ebb tide flows to captured deposited material. A small chamber or column would trap material descending through the water column onto a standard filter paper, then close to retain the sampled sediment until ebb tides have elapsed and samples are available for collection by field personnel. Closing of the trap could be triggered by a pressure sensor, which would allow samples to be sealed when the water level stops rising, or as soon as it begins to drop. Such an approach should be considered for future work, and could be applied to investigate both sediment deposition and differential erosion and resuspension.

While suspended concentration certainly plays a role in the amount of material available to creek banks and the marsh surface, the relatively consistent measurements of incoming suspended sediment concentration over the sampled tides are not an optimal indicator of net deposition. This directly contrasts results
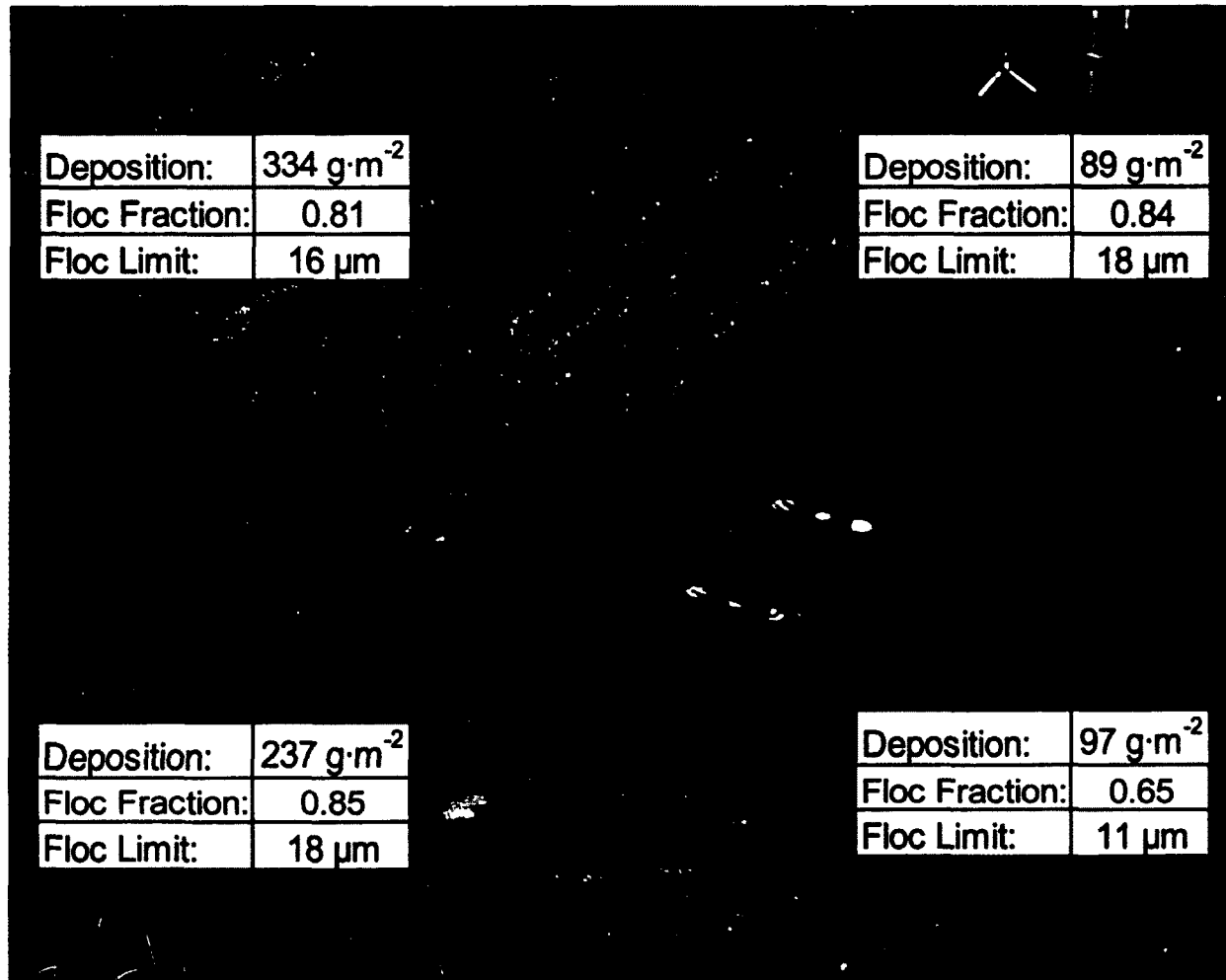
Deposition:	334 g·m^{-2}
Floc Fraction:	0.81
Floc Limit:	16 μm

Deposition:	89 g·m^{-2}
Floc Fraction:	0.84
Floc Limit:	18 μm

Deposition:	237 g·m^{-2}
Floc Fraction:	0.85
Floc Limit:	18 μm

Deposition:	97 g·m^{-2}
Floc Fraction:	0.65
Floc Limit:	11 μm

Figure 4.1: Variability in net deposition and the flocculated nature of deposited materials in response to an over-marsh tidal cycle (5.5 m CGVD28), August 21st 2009. Note the apparent effects of differential erosion/resuspension of trapped materials, where samples facing the ebb-current direction visually appear to have incurred the greatest impacts.
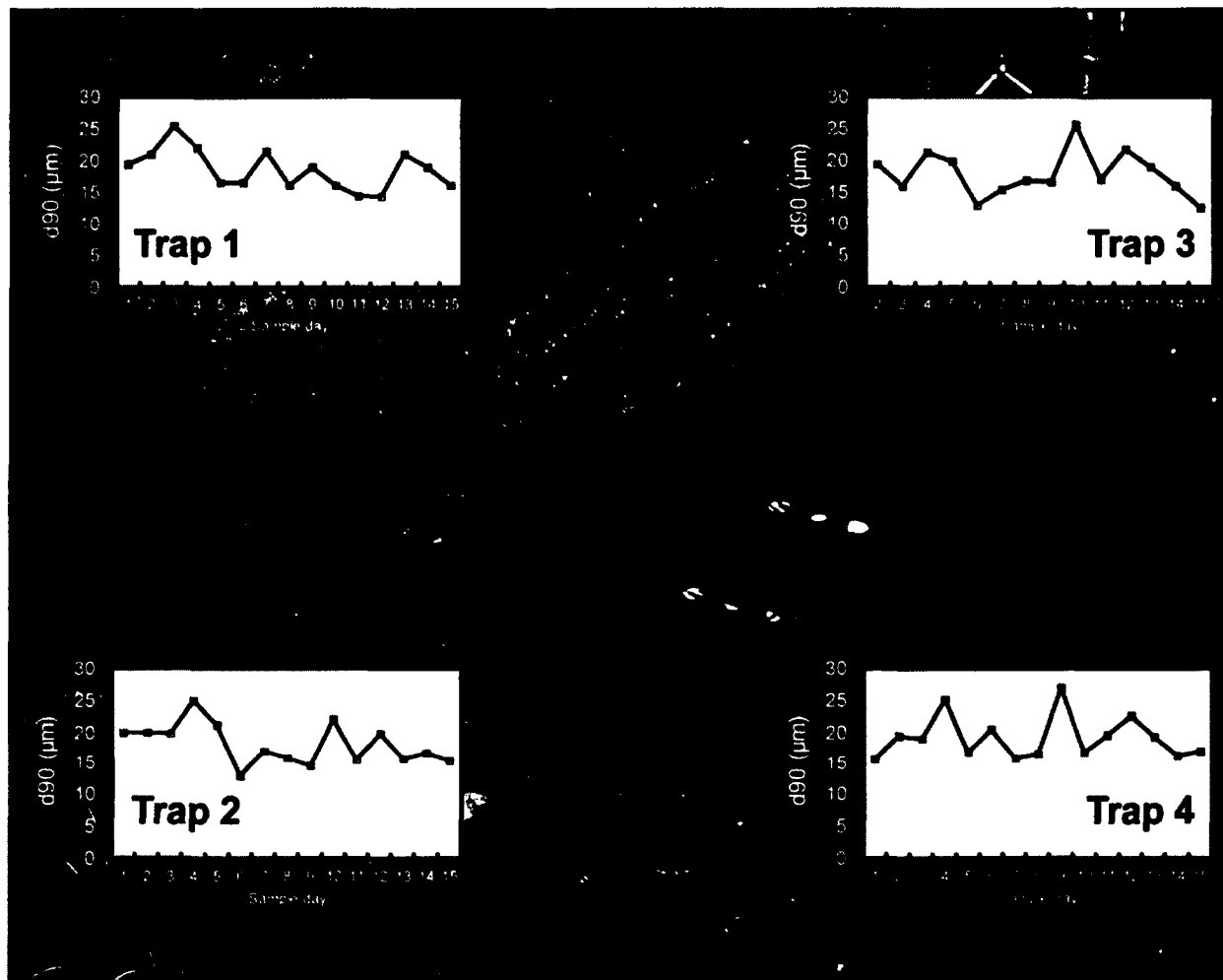
Figure 4.2: Variability in d90 (diameter of the 90th percentile) in deposited material over the study period (August – September, 2009). In general, patterns of change on the left traps (1 & 2) are similar, as are those for the traps on the right (3 & 4).

presented by similar studies (e.g. Voulgaris and Meyers, 2004). Given that incoming suspended sediment concentration is relatively constant, inundation time and surface reworking by energetic ebb flows are first-order controls on net deposition on creek banks (Reed, 1988; Torres and Styles, 2007). This suggests that reductions in overall tidal energy may reduce the amount of sediment introduced to the marsh surface, related to a reduced frequency of inundation of high marsh surfaces. This represents an important step in fully understanding the dynamic behavior of fine-grained materials in an intertidal portion of a hypertidal environment.

Recent initiatives driving tidal power development in the Bay of Fundy have raised questions about far-field environmental impacts. The magnitude of potential change in response to energy extraction still remains to be fully understood, and requires more work to quantify baseline conditions prior to installation of a commercial field of generating devices (Polagye *et al.*, 2011). Simple numerical models of energy extraction from various channel networks show a general decrease in kinetic power density of tidal flows with increasing dissipation by turbines (Polagye and Malte, 2010; Sun *et al.*, 2008; Bryden *et al.*, 2004). It is possible that such energy reductions will reduce the total amount of material in suspension in the Minas Basin, which would have impacts for intertidal sediment supply. However, data presented in this study support a continually high intertidal sediment supply over a range of tidal conditions, at least in sheltered salt marsh environments. Further work of this nature should be

completed at more exposed locations, where exposure and the potential for variability are increased. Seasonal variations (e.g. above- and below-ground biomass, bacterial and nutrient production, benthos activity) should also be investigated to consider the effects of these processes on sediment erodability and cohesion of suspended particles.

The forecast reduction in tidal amplitude associated with tidal power development and extraction will ultimately reduce the overall inundation time of regional salt marshes, although the current distribution of work between tidal cycles can potentially compensate for this. Over-marsh tides will continue to control the distribution of material to marsh surfaces from tidal creeks following energy extraction, although with a reduced frequency, individual tidal cycles may become more important. This may become a critical factor in the survival of high marsh surfaces as sea level continues to rise. The occurrence of channel-restricted tides will increase, but due to limitations in inundation time it is unlikely that this range of tidal cycles will introduce enough material to completely infill tidal creeks. Finally, a more frequent occurrence of bankfull tides is a possible response to reduction in tidal amplitude, which may increase active erosion of marsh edges along tidal creeks, reducing bank steepness and further increasing sediment supply in tidal creeks.

Due to the hypertidal nature of the Bay of Fundy environment, the margin of error for optimal tidal elevation appears to be fairly large. Modelled and corrected results from Webtide suggest that over 80% of tidal cycles inundate

high marsh surfaces, to some degree. Reducing this figure to 75% will moderately modify the current equilibrium between high marsh surfaces and regional sea level. Currently, sediment dynamics in sheltered tidal creeks are dependent on tidal amplitude and surface re-working by ebb-stage currents, and are relatively independent of suspended concentration and flocculated nature of suspended materials, which are routinely high. This study provides important baseline data from the intertidal zone for hydrodynamic and sediment transport modelling efforts currently underway for the Minas Basin region. This work will continue with investigation into the effects of entropy analysis of deposited sediment DIGS over discrete locations, to better characterize variability in net deposition over limited spatial scales. Further data collection and continued work of this nature are required to fully understand how the form and function of salt marsh environments in the Minas Basin will be impacted by a reduction in tidal amplitude.

References

Allen JRL. 2000. Morphodynamics of Holocene salt marshes: a review sketch from the Atlantic and Southern North Sea Coasts of Europe. *Quarternary Science Reviews* **19**: 1155-1231.

T. P. Bayliss-Smith, R. Healey, R. Lailey, T. Spencer, D. R. Stoddart, Tidal flows in salt marsh creeks, Estuarine and Coastal Marine Science **9 (3)**: 235-255. DOI: 10.1016/0302-3524(79)90038-0.

Bertness MD. 1991. Zonation of Spartina Patens and Spartina Alterniflora in a New England salt marsh. *Ecology* **72** (1): 138-148.

Bryden IG, Grinsted T, Melville GT. 2004. Assessing the potential of a simple channel to deliver useful energy. *Applied Ocean Research* **26**: 198-204. doi:10.1016/j.apor. 2005.04.001

Craft C, Clough J, Ehman J, Joye S, Park R, Pennsings S, Guo H, Machmuller M. 2009. Forecasting the effects of accelerated sea-level rise on tidal marsh ecosystem services. *Frontiers in Ecology and the Environment* **7**(2): 73-78. DOI: 10.1890/070219.

Curran KJ, Hill PS, Schnell TM, Milligan TG, Piper DJW. 2004. Inferring the mass fraction of floc-deposited mud: application to fine-grained turbidites. *Sedimentology* **51**: 927-944. DOI: 10.1111/j.1365-3091.2004.00647.x

Donnelly JP, Bertness MD. 2001. Rapid shoreward encroachment of salt marsh cordgrass in response to accelerated sea-level rise. *Proceedings of the National Academy of Sciences of the United States of America* **98** (25):14218-14223

Dyer KR, Manning AJ. 1999. Observation of the size, settling velocity and effective density of flocs and their fractal dimensions. *Journal of Sea Research* **41**: 87-95.

French JR, Stoddart DR. 1992. Hydrodynamics of Salt Marsh Creek Systems: Implications for Marsh Morphological Development and Material Exchange. *Earth Surface Processes and Landforms* **17**: 235-252

Friedrichs CT, Perry JE. 2001. Tidal salt marsh morphodynamics: a synthesis. *Journal of Coastal Research* **27**: 7-37

Karsten RH, McMillan JM, Lickley MJ, Haynes RD. 2008. Assessment of tidal current energy in the Minas Passage, Bay of Fundy. *Proceedings of the Institution of Mechanical Engineers* **222** (A-J): 493-507.

Kranck K, Milligan TG. 1991. Grain size in oceanography. In: Syvitski, JPM [ed]. *Principles, Methods, and Applications of Particle Size Analysis.* Cambridge University Press: 368 pp.

Kranck, K., and T. G. Milligan (1992), Characteristics of Suspended Particles at an 11-Hour Anchor Station in San Francisco Bay, California, *J. Geophys. Res.,* **97(C7)**, 11, 373 - 382, doi:10.1029/92JC00950

Law BA, Milligan TG, Hill PS, Newgard JP, Wheatcroft RA, Wilberg PL. In press. Flocculation on a muddy intertidal flat in Willapa Bay, Washington, Part I: A regional survey of the grain size of surficial sediments. *Continental Shelf Research.* 44 pp.

Lawrence DSL, Allen JRL, Havelock GM. 2004. Salt marsh morphodynamics: An investigation of tidal flows and marsh channel equilibrium. *Journal of Coastal Research* **20**: 301-316.

Milligan TG, Loring DH. 1997. The effect of flocculation on the size distributions of bottom sediment in coastal inlets: implications for contaminant transport. *Water, Air and Soil Pollution* **99**: 33-42

Morris JT, Sundareshwar PV, Nietch CT, Kjerfve B, Cahoon DR. 2002. Responses of coastal wetlands to rising sea level. Ecology **83 (10)**: 2869-2877.

Polagye BL, Malte PC. 2010. Far-field dynamics of tidal energy extraction in channel networks. *Renewable Energy* **36**: 222-234. DOI:10.1016/j.renene.2010.06.025

Polagye B, Van Cleve B, Copping A, Kirkendall K (eds). 2011. Environmental effects of tidal energy development. *U.S. Dept. Commerce, NOAA Tech. Memo.* 181 pp.

Reed D. 1988. Sediment dynamics and deposition in a retreating coastal salt marsh. *Estuarine, Coastal and Shelf Science* **26**: 67-79.

Reed D, Spencer T, Murray AL, French JR, Leonard L. 1999. Marsh surface sediment deposition and the role of tidal creeks: implications for created and managed coastal marshes. *Journal of Coastal Conservation* **5**: 81-90.

Smith SJ, Friedrichs CT. 2011. Size and settling velocities of cohesive flocs and suspended sediment aggregates in a trailing suction hopper dredge plume. *Continental Shelf Research* **31**: 550 - 563.

Sun X, Chick JP, Bryden IG. 2008. Laboratory-scale simulation of energy extraction from tidal currents. *Renewable Energy* **23**: 1267-1274.

Torres R, Styles R. 2007. Effects of topographic structure on salt marsh currents. *Journal of Geophysical Research* **112**: 1-14. DOI: 10.1029/2006JF000508

van Proosdij D, Davidson-Arnott RGD, Ollerhead J. 2006a. Controls on spatial patterns of sediment deposition across a macro-tidal salt marsh surface over single tidal cycles. *Estuarine, Coastal and Shelf Science* **69**: 64-86. DOI: 10.1016/j.ecss.2006.04.022

van Proosdij D, Ollerhead J, Davidson-Arnott RGD. 2006b. Seasonal and annual variations in the volumetric sediment balance of a macro-tidal salt marsh. *Marine Geology* **225**: 103-127. DOI: 10.1016/j.margeo.2005.07.009

Voulgaris G, Meyers ST. 2004. Temporal variability of hydrodynamics, sediment concentration and sediment settling velocity in a tidal creek. *Continental Shelf Research* 24: 1659-1683. DOI: 10.1016/j.csr.2004.05.006

Whitford J. 2008. Final Report: Background Report for the Fundy Tidal Energy Strategic Environmental Assessment. Prepared by Jacques Whitford Consultants for the OEER Association. Project No. 1028476. 291 pp.

APPENDIX A: Metadata

This document is available in digital format in the In_CoaST lab.

Near-bed velocity and suspended sediment concentration

In total, near-bed velocity and suspended sediment concentration data have been collected for a total of 17 tides during the summer of 2009 (August and September) using ADV and OBS arrays. These data characterize two discrete elevations in the tidal creek (0.5 and 1.25 m CGVD28) at Starrs Point over a range of maximum water depths. Data were collected at a rate of 16 Hz at the thalweg, and at a rate of 4 Hz over the creek bank. Data quality is good.

Vertical velocity profiles

An ADCP was deployed at the thalweg (upward oriented) for the same range of tides mentioned above. The ADCP recorded at a rate of 1 Hz, and profiled up to 2.97 metres of the water column, measuring 97 3-cm cells (high-resolution mode). Blanking distance above the instrument was 5 cm. Pulse distance was set to 3 meters to match the anticipated profile height and to minimize double-pings. The horizontal velocity range measured was 0.30 m/s, and the vertical velocity range measured was 0.13 m/s. Quality of this dataset is reasonably good, although there are suspicious events listed in the .ssl file, of unknown cause.

Suspended sediment concentration

Approximately 120 samples of suspended sediment were collected with the ISCO automated water sampler, drawn from the creek near the thalweg measurement location. These samples were filtered using standard gravimetric methods in the In_CoaST lab by A. Silver (2009). Portions of samples were processed for organic content (2009) in a muffle furnace (550°C). Samples of suspended sediment used in DIGS processing were ashed at BIO. These samples were processed using In_CoaST DIGS protocol for grain-size measurement (Coulter Multisizer III) by C. Wrathall and B. Blotnicky (2012) in the In_CoaST lab. Additional portions of these samples have been retained for future use.

Deposited sediment

Approximately 180 samples of deposited sediment were collected during this field campaign. Four traps were deployed over 15 tidal cycles (traps were not deployed in rainy weather), with three filter papers in each. These were processed for water content, organic content by A. Silver (2009), and grain size using DIGS methods (Coulter Multisizer III) in the In_CoaST lab by E. Poirier and C. Skinner (2011). One filter paper from each trap remains for future analysis.

Surface elevations

A high-resolution digital elevation model (DEM) was produced from a detailed reflectorless survey of the creek and surrounding area, using standard total station methods during June of 2009. This survey was completed by Greg Baker (MP_SpARC) and data are available through In_CoaST. These data have been used in calculation of bankfull elevations, creek volume and cross-sectional area.

Surface elevation on the creek bank was also tracked using a rod-surface interface method, where the base of each of a network of aluminum pins, placed on the creek bank in a grid arrangement, was surveyed using the total station in reflectorless mode. Measuring against the 20 centimeters of pin that was protruding from the surface, attempts to track changes in surface elevation were made on the scale of individual tidal cycles. However this data was not applied in this study, primarily due to the impacts of vegetation wrapping around the base of the pins, creating a tent of sediment-trapping material that obscured the interface of the pin with the surface.

Placing the pins farther apart may improve issues noted here. Also, ensure a stable construction of the fixed total station stand, as instability will cause the unit to sawy and generate further inaccuracy.
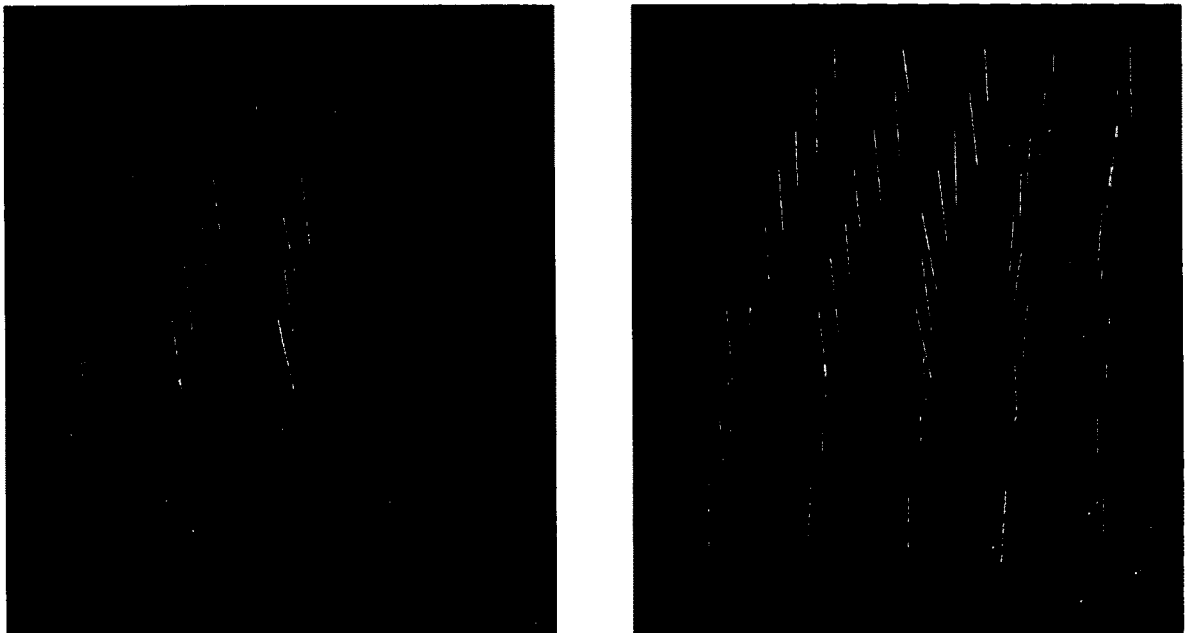

Figure 1A: The pin network in early August (left), at the initiation of the study, and in late September (right), near the end of the sampling period. The bases of most pins have been wrapped by loose vegetation, which trapped sediment, which obscured the base of the pin and impacted the accuracy of surveys.

Weather conditions

Hourly means of wind speed and direction, rainfall, humidity and atmospheric pressure were recorded on site using a portable weather station and tipping rain gauge. This dataset includes the passage of Hurricane Bill on August 23rd, 2009, which passed just south of Nova Scotia.

Analyses presented within this document have been performed by C. O'Laughlin.

Protocols describing analytical methods applied here are available in the In_CoaST Research Unit.

Data collection and sample processing was completed by C. O'Laughlin, A. Silver, E. Poirier, C. Skinner, C. Wrathall and B. Blotnicky.

All data associated with this research project are stored in the Intertidal Sediment Transport Research Unit (In_CoaST) at Saint Mary's University (4th floor Science Building, room s404).

To access these data, contact the Lab Director, Dr. Danika van Proosdij, at dvanproo@smu.ca or (902) 420-5738.
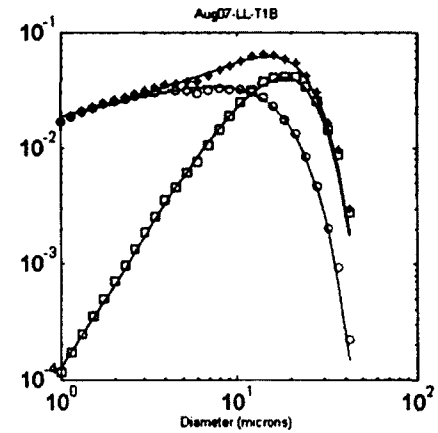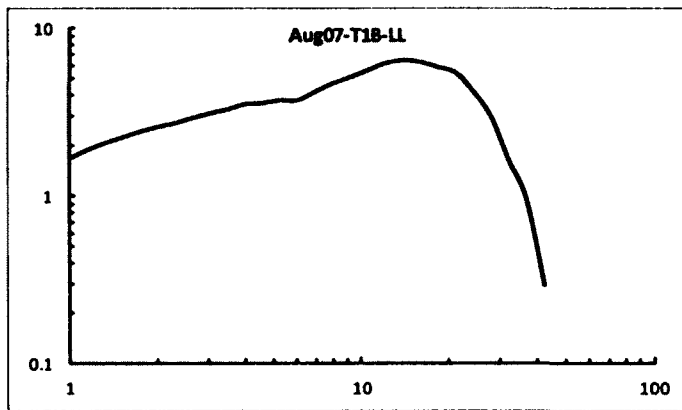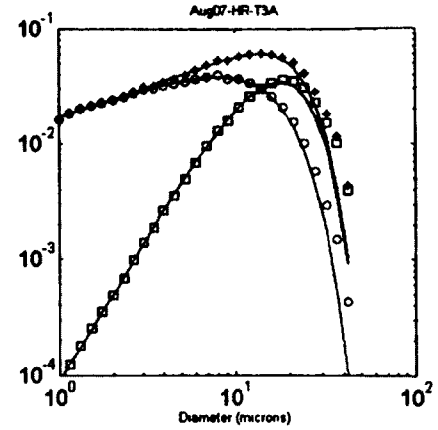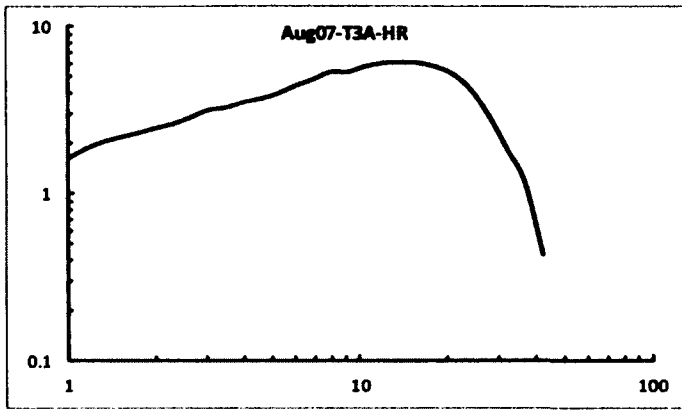
APPENDIX B: Example merged and parameterized DIGS distributions.

These samples have been included to show methodological approach and do not illustrate the full range of this dataset.

Sep27.   Neap tide (channel-restricted)
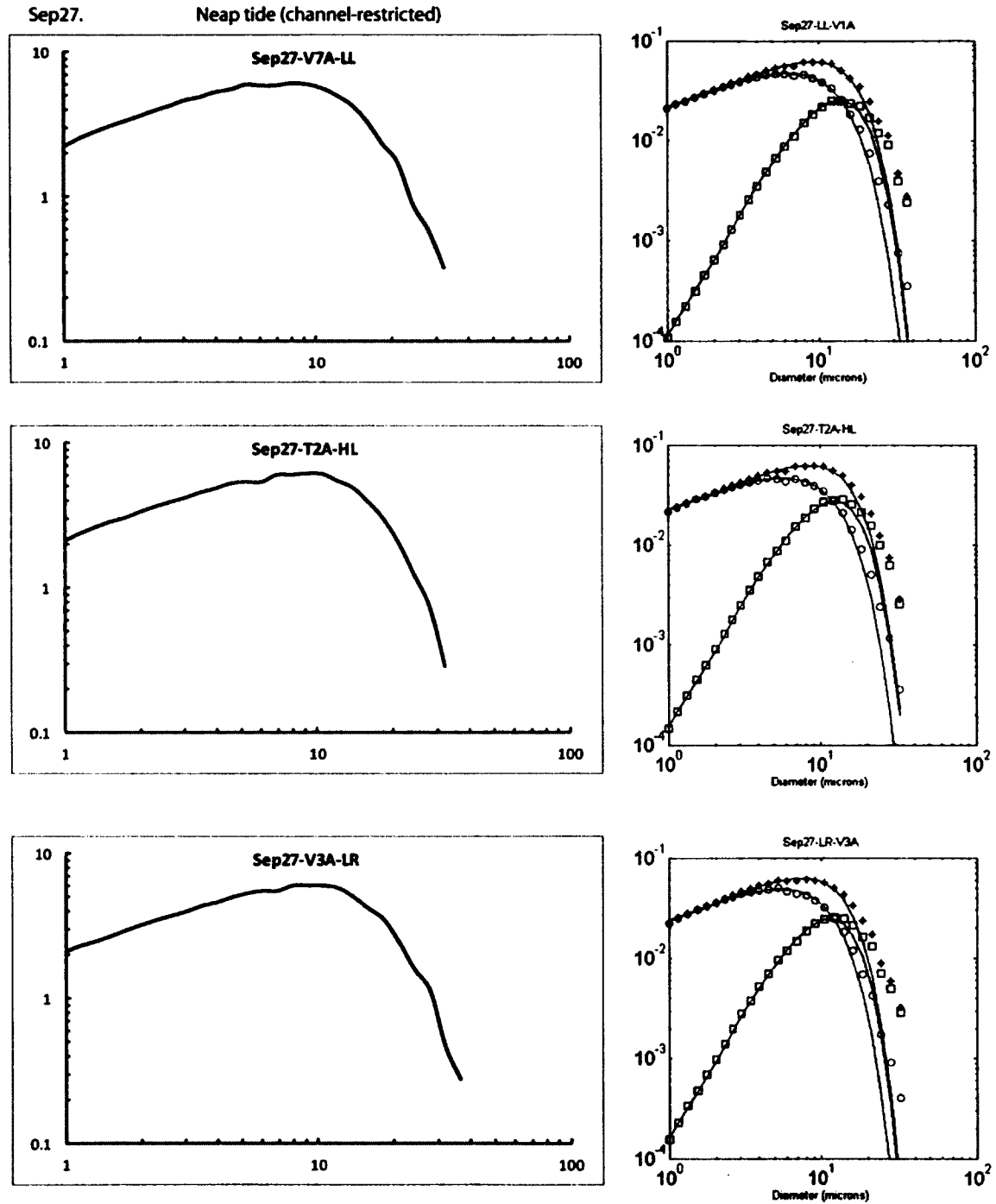
Aug07.   Transitional tide (channel-restricted)

Sample ID	Cut-off	Floc fraction	Floc limit	Source slope	Roll-off dia.
Sep27-V7A-LL	14	0.76	14	0.58	12
Sep27-T2A-HL	13.5	0.74	12	0.58	11
Sep27-LR-V3A	12.8	0.76	12	0.6	10
Aug7-HR-T3A	14.4	0.67	14	0.51	16
Aug7-T1B-LL	12.3	0.62	12	0.4	17

Table 1A: Manual cut-off values and model results for DIGS examples.